"A physiological proteomic approach to address infection-related issues of Gram-positive bacteria"

Inauguraldissertation

zur

Erlangung des akademischen Grades
eines Doktors der Naturwissenschaften der
Mathematisch-Naturwissenschaftlichen Fakultät

der

ERNST-MORITZ-ARNDT-UNIVERSITÄT GREIFSWALD

vorgelegt von

Theresa Winter

geboren am 20.Dezember 1979

in Bad Muskau

Greifswald, den 22.11.2011

Dekan : Prof. Dr.rer.nat. Klaus Fesser

1. Gutachter: Prof. Dr. Michael Hecker

2. Gutachter: Prof. Dr. Dieter Jahn

Tag der Promotion: 29.02.2012

Es gibt kein Problem, hinter dem nicht eine Goldgrube verborgen wäre.
Aber es gibt viele Menschen, die nur auf das Problem starren
und so die Goldgrube nie entdecken.

Bodo Schäfer

Table of content

List of all publications

➢ Thiol-disulphide oxidoreductase modules in the low-GC Gram-positive bacteria
   Kouwen, T. R., van der Goot, A., Dorenbos, R., Winter, T., Antelmann, H., Plaisier, M. C.,
   Quax, W. J., van Dijl, J. M., Dubois, J. Y. (2007)
   Molecular Microbiology May;64(4):984-99.

➢ Synthetic effects of *secG* and *secY2* mutations on exoproteome biogenesis in
   Staphylococcus aureus
   Sibbald, M.J*., Winter, T*, van der Kooi-Pol, M. M., Buist, G., Tsompanidou, E., Bosma,
   T., Schäfer, T., Ohlsen, K., Hecker, M., Antelmann, H., Engelmann, S., van Dijl, J.M.
   (2010)
   Journal of Bacteriology, *192*, 3788-3800
   * both author contributed equally to this work

➢ Environmental Salinity Determines the Specificity and Need for Tat-Dependent Secretion of
   the YwbN Protein in Bacillus subtilis
   van der Ploeg, R., Mader, U., Homuth, G., Schaffer, M., Denham, E. L., Monteferrante,
   C. G., Miethke, M., Marahiel, M. A., Harwood, C. R., Winter, T., Hecker, M., Antelmann,
   H., van Dijl, J. M. (2011)
   PLoS ONE 6(3): e18140.

➢ Characterization of the global impact of low temperature gas plasma on vegetative
   microorganisms
   Winter, T., Winter, J., Polak, M., Kusch, K., Mader, U., Sietmann, R., Ehlbeck, J., van
   Hijum, S., Weltmann, K. D., Hecker, M., Kusch, H. (2011)
   Proteomics 11(17): 3518-3530

➢ Comprehensive characterization of atmospheric pressure plasma impact on vegetative
   microorganisms in argon and air
   Winter, T, Winter, J., Polak, M., Mäder, U., Bernhardt, J., Sietmann, R., Ehlbeck, J.,
   Weltmann, K.D., Hecker, M., Kusch, H. (2011)
   Proceedings of 20th International Symposium on Plasma Chemistry (ISPC 20),
   Philadelphia, July 2011

➢ Common versus noble- *Bacillus subtilis* differentially responds to air and argon gas plasma
   Winter, T., Bernhardt, J., Winter, J., Mäder, U., Schlüter, R., Weltmann, K. D., Hecker,
   M., Kusch, H. (2011)
   Submitted to *PLoS ONE*

Summary

Against the opinion of earlier years, infectious diseases are the most dangerous cause of death worldwide. Their epidemiologic importance is present today and will be present in the future [1]. The complex topic of "infections" should be examined under two aspects: prevention and treatment. The prevention of infections covers the fields of decontamination and sterilization, hygiene, vaccination and health education. The treatment of infections is commonly associated with antibiotic treatment, as well as with the immunological side in terms of understanding the human immune response.

From 1969 to 2000 no new major class of antibiotics have been introduced and, to make matters worse, the decreasing interest and investment in antibiotic research by the pharmaceutical industry and the consequent decline in antibiotic discovery has been paralleled by a rapid spread of nosocomial acquired infections and cases of community-acquired, antibiotic (methicillin)-resistant infections [2, 3].

Fundamental research on infection causing microorganisms such as the human pathogen *Staphylococcus aureus* is of major importance.

Infection related virulence factors are either displayed at the surface of the staphylococcal cell or released into the medium. In order to understand and evaluate the pathogenic potential of these organisms it is of major importance to map their pathways for protein transport. Currently, the machinery for protein transport of *Escherichia coli* (gram negative) and *B. subtilis* (gram positive) are best described [4, 5]. Many of the known components that are involved in the different routes for protein export in these organisms are also conserved in *S. aureus*. Genomic and proteomic studies enable an in-depth study of the secretion machinery [6]. The understanding of which factors are responsible for causing infection and which proteins are why and how associated with infections carries high potential for new findings in terms of infection control and treatment.

Furthermore, contamination of medical devices such as catheters or endoscopes can also cause infections. Medical devices which are made of bio-compatible polymers such as polyethylene (PE) or polyethylenterephthalat (PET) are thermo labile materials. Besides numerous advantages for the patient, they are poorly resistant to high temperatures (autoclave sterilization). Alternative chemical treatments such as ethylene oxide sterilization bare side effects or risks which are neither desired nor acceptable [7, 8].

Therefore, the use of alternative decontamination procedures for heat sensitive materials such as low temperature plasma is in the focus of not only physicist but also biologist and medical staff.

As low temperature plasmas generated at atmospheric pressure consist of a variety of microbicidal active agents and chemical products e.g. atomic oxygen (O), ozone (O_3), hydroxyl

(OH), reactive oxygen (ROS) and nitrogen species (RNS), it becomes an appropriate tool for microbial decontamination. Recently, low temperature plasma was successfully applied for wound treatment. First studies revealed enormous potential in this area as improved wound healing could be shown. Clearly, the use of plasmas in medicine opens up new vistas of treatment—this is the vision. On the practical side many questions are still open such as: (i) which type of plasma is applicable for which purpose; (ii) what are the advantages of plasma compared to current medical treatments; (iii) whether plasmas are a more economical alternative to current applications and standards [9]?

Before plasma can be safely routinely used in hospitals, it is furthermore of major importance to evaluate the interaction of microorganisms (pro- and eukaryotic cells) with plasma. When these fundamental questions are well investigated and understood, a safe, successful and most important widely accepted implementation in the field of life science will be achieved.

This work is divided into two parts. First, investigations of secretion mechanisms in the human pathogen *S. aureus* and the posttranslational protein folding catalyst dsbA will be presented followed by results about the interaction between bacteria and low temperature plasma.

1. Secretion

The Gram-positive bacterium *Staphylococcus aureus* is a frequent component of the human microbial flora that can turn into a dangerous pathogen. As such, *S. aureus* is capable of infecting almost every tissue and organ system in the human body causing three basic syndromes: (i) superficial lesions such as skin abscesses and wound infections; (ii) deep-seated and systemic infections such as osteomyelitis, endocarditis, pneumonia, and bacteremia; and (iii) toxemic syndromes such as toxic shock syndrome (TSS) and staphylococcal scarlet fever [10-13]. The molecular basis of *S. aureus* pathogenicity is multifactorial, depending on the expression of a large class of accessory gene products that comprise cell wall-associated and extracellular proteins [6, 14].

The translocation of proteins from the cytoplasmatic compartment to the extracellular space is called secretion and plays an important role in bacterial physiology. About 25% to 30% of the bacterial proteins function in the cell envelope or outside of the cell. But the present cell envelope is an export barrier for the proteins which are synthesized at ribosomes localized in the cytosol. Besides its barrier characteristics, the cell envelope fulfills a variety of duties such as the protection of the underlying protoplast and maintenance of the cell shape. Furthermore, the cell wall is involved in the cell division, metal ion homeostasis and interactions between the cell and its environment [15-17].

1.1. Signal peptides

Various transport mechanisms have evolved to allow proteins to cross membranes without compromising the barrier function [4]. Proteins that are transported to an extracytoplasmic location generally contain an N-terminal signal sequence peptide which is needed to target the preprotein from the ribosome to a particular transport pathway and gets removed after translocation. Signal sequences have a tripartite structure with an N-terminal region encompassing one to three positively charged amino acids residues (N domain), a hydrophobic core region consisting of 10-15 residues (H domain) and a more polar C terminus, which constitutes the signal peptidase cleavage site (C domain).
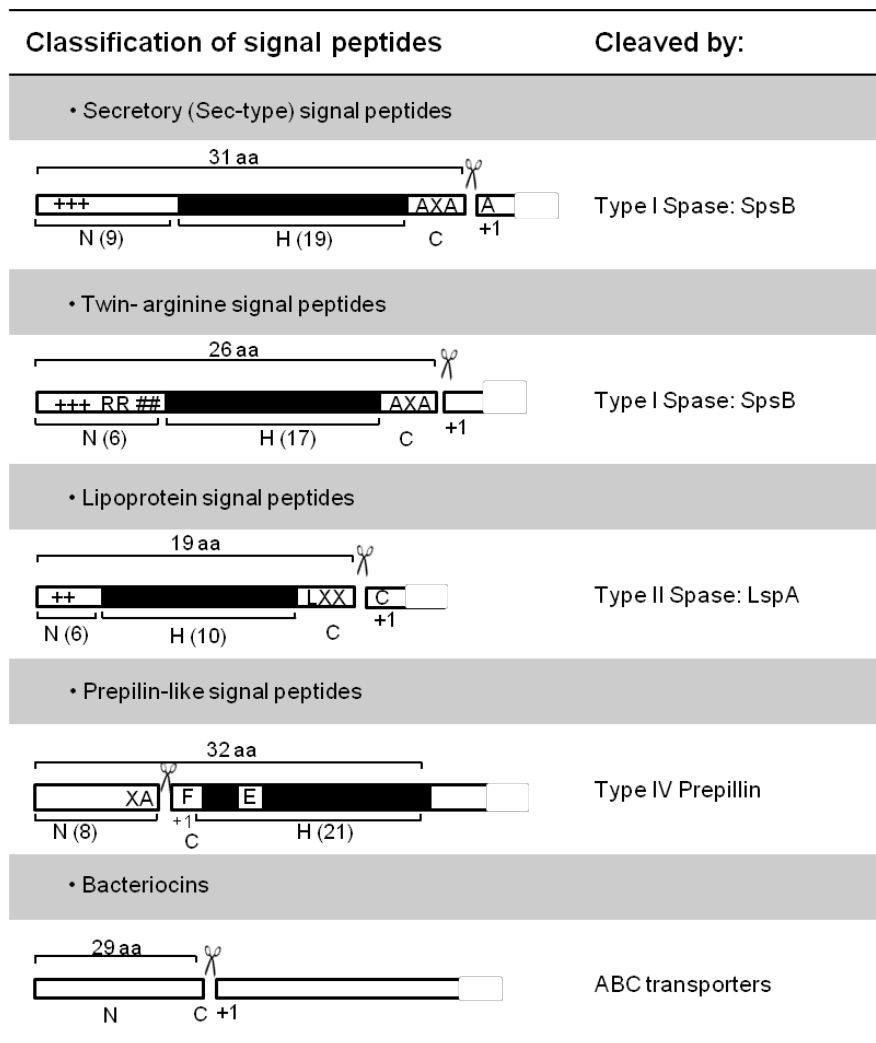
Fig.1. General features and classification of *S. aureus* signal peptides. The predicted signal peptides are divided into five distinct classes: secretory (Sec-type) signal peptides, twin-arginine (RR/KR) signal peptides, lipoprotein signal peptides, pseudopilin-like signal peptides, and bacteriocin leader peptides. Most of these signal peptides have a tripartite structure, with a positively charged N domain (N) containing lysine and/or arginine residues (indicated by plus signs), a hydrophobic H domain (H, indicated by a black box), and a C domain (C) that specifies the cleavage site for a specific SPase. Where appropriate, the most frequently occurring amino acid residues at particular positions in the signal peptide or mature protein are indicated as well as the SPase (on the basis of Sibbald et al. [6]).

1.2. Translocation

Next, the protein is threaded through the membrane in an either folded or unfolded state-depending on the used pathway. During this translocation step, or shortly afterwards, the signal peptide is removed by a so-called signal peptidase (SPase). Upon complete membrane translocation, the protein has to fold into its correct conformation and will then be retained in an extracytoplasmic compartment of the cell or secreted into the extracellular milieu [6]. In recent

years, genomic and proteomic tools have been employed to generate an inventory of the so-called secretome. By definition, the secretome includes both the various pathways for the protein transport across the cytoplasmic membrane to the membrane –cell wall interface, the cell wall or the extracellular environment and the secretory proteins themselves [17, 18]. Based on the cell envelope setup in Gram-positive bacteria such as *S. aureus*, four different final protein destinations for secreted proteins can be named which are (i) membrane anchored proteins, (ii) lipoproteins, (iii) cell wall associated proteins und (vi) extracellular proteins.

1.3. Virulence of *S. aureus*

The pathogenicity of *S. aureus* is caused by the expression of an arsenal of virulence factors (see Tab. 1) which are either displayed at the surface of the staphylococcal cell or secreted into the host milieu. Therefore it is of major importance to obtain a clear understanding of the protein transport pathways that are active in this organism [6].

	Virulence factor	Pathogenic action	function	Proteins or other compounds	Clinical consequences
1	Surface proteins	Colonization and atttachement of host tissues and blood clots	Adhesins, fibronectin- and fibrinogen-binding proteins	ClfA, ClfB, FnbA, FnbB, IsdA, SdrC, SdrD, SdrE,	endocarditis, prosthetic
2	Membrane damaging toxins, invasins	Lysis of eukaryotic cell membranes and promotion of bacterial spread in tissue	Hemolysins, hyaluronidase, leukocidin, leukotoxin, lipases, nucleases	Geh, Hla, Hld, HlgA-C, HysA, Lip, LukD, LukE, LukF, LukS, Nuc	tissue invasion and destruction
3	Surface factors	Evade opsonization and phagocytosis	Capsule, protein A	CapA-P, Efb, Spa	deep and metastatic infections
4	Biochemical compounds	Survival in phagocytes	Carotenoids, catalase production	KatA, staphyloxanthin	
5	Surface proteins	immunological disguises and modulation	Clumping factor, coagulase, protein A	ClfA, ClfB, Coa, Spa	
6	Exotoxins	Host tissue damage, provocation of symptoms of septic shock	Enterotoxins SEA to SEG, exfoliative toxin, TSST	Eta, Etb, SEA-G, TSST-1	gastroenteritis, food poisoning, toxic shock syndrome, scalded skin syndrome
7	Resistance proteins	Inherent and acquired resistance to antimicrobial agents	Methicillin and vancomycin resistance	BlaZ, MecA, VanA	

Tab. 1: Virulence factors of *S. aureus* (on the basis of Sibbald et al. and Raygada et al. [6, 19])

At least six distinct pathways for protein transport have been indentified in *S. aureus*. Besides the general secretion (Sec) pathway, *S. aureus* has a twin-arginine translocation "Tat" pathway, a pseudopilin export (Com) pathway, phage-like holins and certain ATP-binding cassette (ABC) transporters.

In general, the export of proteins can be divided into the following three stages:
(i) targeting the membrane translocation machinery by export-specific or general chaperones,
(ii) translocation across the membrane and
(iii) posttranslocational folding and modification.

If the translocated proteins of gram-positive bacteria lack specific retention signals for the membrane or cell wall, they are secreted into the growth medium [6].

1.4. Sec-pathway

The majority of secretory proteins are transported by the general secretion (Sec) pathway. Proir to translocation, the preproteins with a signal peptides SPase I or II, are recognized by the signal recognition particle (SRP) or by the secretion-dedicated chaperone SecB. Subsequently, they are targeted to the Sec translocase in the cytoplasmic membrane, a multimeric membrane protein complex composed of a highly conserved protein-conducting channel, SecYEG, and a peripherally bound ribosome or ATP-dependent motor protein SecA.

The Sec translocase mediates the translocation of unfolded proteins across the membrane and the insertion of membrane proteins into the cytoplasmic membrane [16, 18]. 130 to 145 proteins are predicted to be exported, depending on the investigated *S. aureus* strain. Typical proteins which are transported through the Sec pathway are degradative enzymes (e.g. carbohydrases, DNAses, lipases, phosphatases, proteases and RNAses), proteins involved in cell wall biosynthesis, substrate binding proteins and even pheromones involved in sensing the cell population density for onset of developmental processes such as natural competence and sporulation [6, 18].
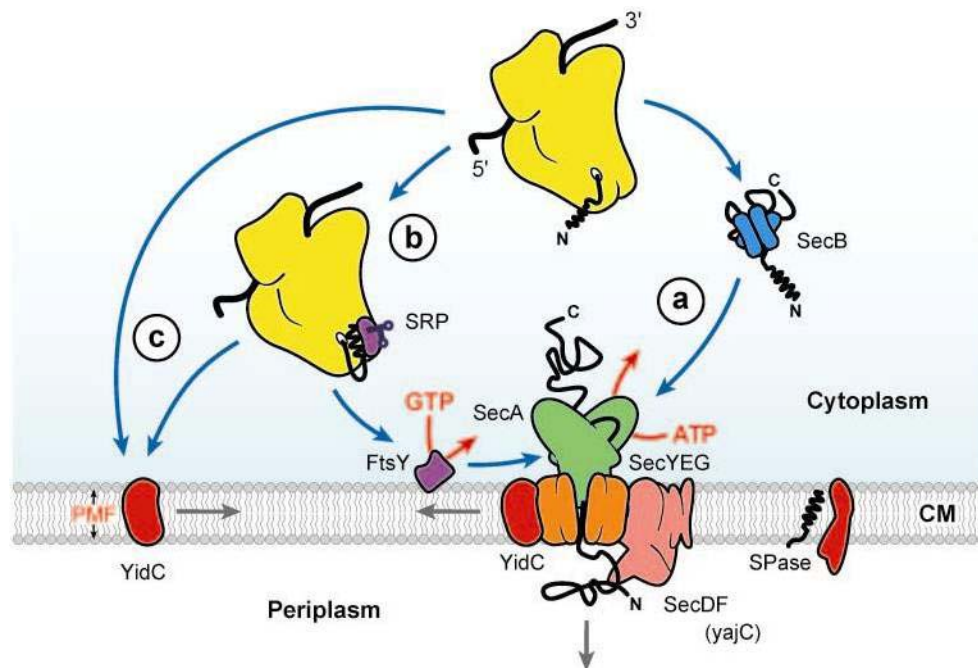
Fig. 2. Scheme of protein targeting to the Sec translocase. The bacterial Sec translocase is a protein complex in the cytoplasmic membrane (CM), which comprises a peripheral motor domain SecA (*green*), the protein-conducting channel, SecYEG (*orange*), and the accessory proteins SecDF(yajC) (*pink*) and YidC (*red*). Signal peptidase (SPase) is a membrane-bound peptidase that cleaves the signal sequence from preproteins at the periplasmic face of the membrane. (*a*) Secretory proteins (*yellow*) are posttranslationally targeted to the Sec translocase by virtue of their signal sequence, which is recognized directly by SecA, the motor domain of the Sec translocase, or by the aid of the molecular chaperone SecB (*blue*). (*b*) Membrane proteins and some preproteins are cotranslationally targeted to the Sec translocase as ribosome-bound nascent chains by the SRP and the SRP-receptor FtsY (*purple*). (*c*) Some membrane proteins insert into the cytoplasmic membrane via YidC [16].

1.5. Accessory secretion pathway

Interestingly, the genome of *S. aureus* contains a second set of chromosomal *secA* and *secY* genes named *secA2* and *secY2*, respectively. Several other pathogens, including *Streptococcus gordonii*, *Streptococcus pneumoniae*, *Bacillus anthracis* and *Bacillus cereus* have the same duplication in their genome [6, 20]. It is known that SecA2/Y2 is required for the transport of certain proteins related to virulence. In *S.gordonii*, the SecA2 system is responsible for exporting GspB, a large serine-rich glycoprotein to the cell surface [21]. Exported GspB promotes *S. gordonii* binding to platelets. Therefore, the SecA2 system is likely to contribute to pathogenesis, as platelet binding is believed to be important for *S. gordonii* attachment to damaged cardiac tissue and subsequent infective endocarditis [20].

Recently, Siboo and coworkers were able to show that the accessory Sec system of *S. aureus* is required for the export of SraP (Serine-rich adhesin for platelets) and it seems that this

system is dedicated to the transport of this substrate exclusively [22]. SraP shares similarity with a group of cell wall-associated glycoproteins. Among the best characterized members of such glycoproteins is the platelet binding protein GspB of *S. gordonii*. Compared to streptococci, however, SraP of *S. aureus* is predicted to differ in its signal peptide and glycosylation, which may affect its dependence on a specialized system for transport. In addition, two genes (*asp4* and *asp5*) essential for export of SraP in *S. gordonii* are missing in *S. aureus* (Fig.3).
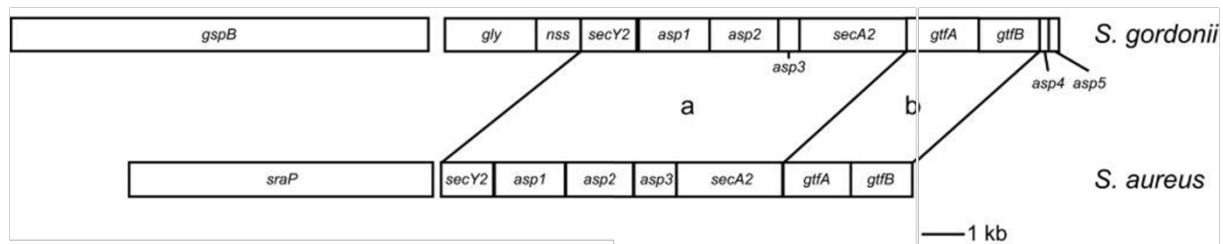
Fig.3. Schematic diagram of the accessory Sec loci of *S.aureus* and *S. gordonii* [22].

Despite these findings, it was still unclear what determines the different specificity of the SecA1/SecY1 and SecA2/SecY2 translocases. It is also not known whether the SecA2/SecY2 translocase shares SecE and/or SecG with the SecA1/SecY1 translocase, whether these translocases function completely independently from each other, or whether
mixed translocases can occur. Clearly, the *secE* and *secG* genes are not duplicated in *S. aureus*. The SecE and SecG functions in the SecA2/SecY2 translocase may, however, be performed by the *S. aureus* homologues of the Asp4 and Asp5 proteins of *S. gordonii*, for which SecE- and SecG-like functions have been proposed [23].

1.6. Synthetic effects of secG and secY2 mutations on exoproteome biogenesis in Staphylococcus aureus

Sibbald, M.J*., Winter, T*, van der Kooi-Pol, M. M., Buist, G., Tsompanidou, E., Bosma, T., Schäfer, T., Ohlsen, K., Hecker, M., Antelmann, H., Engelmann, S., van Dijl, J.M. (2010)
Journal of Bacteriology, *192*, 3788-3800
* both authors contributed equally to this work

1.6.1. Goal of study

So far, relatively few functional studies have addressed the protein export pathways of *S. aureus*. Notably, the Sec pathway is generally regarded as the main pathway for protein export,

but, to date, this has not been verified experimentally in *S. aureus*. Therefore, the present studies were aimed at defining the roles of two Sec channel components in the biogenesis of the *S. aureus* exoproteome. We focused attention on the nonessential channel component SecG as this allowed a facile co-assessment of the nonessential accessory Sec channel component SecY2 [24].

1.6.2. Results of study

Our results show that *secG* and *secY2* are not essential for growth and viability of *S. aureus*. We could prove that SecG is more important for Sec-dependent protein secretion in *S. aureus* than in *B. subtilis* or *E. coli.*, since studies for *E. coli* [25] and *B. subtilis* [26] have shown that deletion of *secG* had fairly moderate effects on protein secretion *in vivo*. The extracellular accumulation of proteins is affected to different extents by the absence of SecG: some proteins are present in reduced amounts, some are not affected, and some are present in elevated amounts. But all altered proteins have Sec-type signal peptides in common.

The effects of the absence of SecG are exacerbated by deletion of SecY2, suggesting that SecY2 directly or indirectly influences the functionality of the general Sec pathway. This is remarkable since the absence of SecY2 by itself had no detectable effects on the composition of the extracellular proteome of *S. aureus*.

Importantly, the transcription of genes for three proteins (Geh, Hlb, and Spa) that were affected in major ways by the absence of SecG was not changed and all observed effects of the *secG* mutation could be reversed by ectopic expression of *secG*. This suggests that the observed changes in the exoproteome composition of the *S. aureus secG* mutant strain relate to changes in the translocation efficiency of proteins through the Sec channel rather than to regulatory responses at the gene expression level.

Since we were unable to detect secretion defects for *secY2* single mutant strains, our studies confirm that only very few proteins are translocated across the membrane in a SecA2/SecY2-dependent manner, as has previously been suggested by Siboo et al. [22, 24].

Own contribution to manuscript

Cultivation, proteins preparation, SDS PAGE, analysis of 2D gels and Maldi data, RNA preparations, Northern blots and analysis of Northern blots as well as contributed writing of the manuscript.

2. Post-translocational folding

Most of the secretory proteins are translocated across the cytoplasmic membrane in an unfolded form. But once translocated across the membrane, proteins must be folded rapidly into their native conformation. This is not only requires for the activity of exported proteins but also for their stability, since the membrane-cell wall interface is a highly proteolytic environment that monitors and maintains the quality of secreted proteins. Furthermore, proteins may not block the translocation machinery in the membrane, form illegitimate interactions with the cell wall or, through intermolecular interactions, form insoluble aggregates [18]. To ensure correct processing, folding catalysts have evolved such as PrsA and thiol-disulphide oxidoreductases.

2.1. Thiol-disulphide oxidoreductases (TDORs)

A disulphide bond is a sulphur-sulphur chemical bond that results from an oxidative process that links two nonadjacent cysteines of a protein. In all three domains of life, disulphide bonds play major roles in the correct folding of many different proteins, maintaining their structural integrity and regulating their activity [27, 28]. Proteins containing disulphide bonds are found predominantly in the membranes and periplasm of Gram-negative bacteria, or the membrane/cell wall interface and extracellular milieu of Gram-positive bacteria [29].

Proteins that contain disulfide bonds can be divided into two classes: (i) those in which the cysteine-cysteine linkage is a stable part of their final folded structure and (ii) those in which pairs of cysteines alternate between the reduced and oxidized states. For the first class, the disulfide bond may contribute to the folding pathway of the protein and to the stability of its native state. For the second, the oxidative-reductive cycling of the disulfide bond may be central to a protein's activity as an enzyme [30].

For both classes of proteins, disulphide bonds are essential for their activity. The formation of disulphide bonds can occur spontaneously under oxidizing conditions. This process is very slow and non-specific [31]. For this reason enzymes have evolved that catalyze the formation (oxidation) or breakage (reduction) of disulphide bonds *in vivo*. These enzymes are called thiol-disulphide oxidoreductases (TDORs) [32].
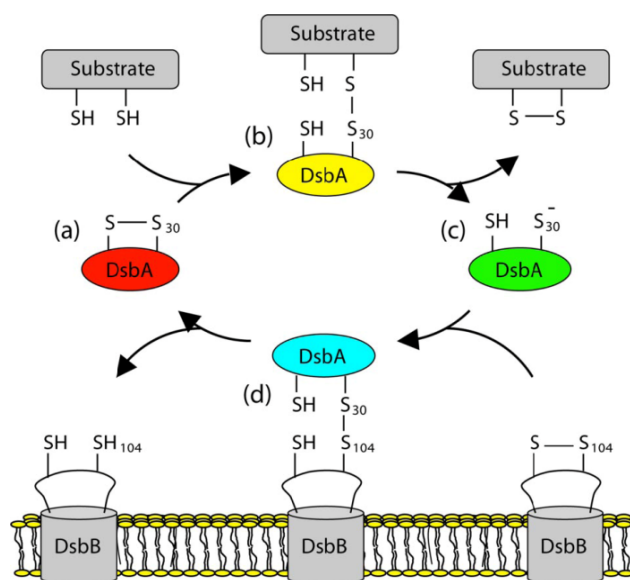
Fig: 4. Catalytic cycle of DsbA. In this reaction cycle, oxidized DsbA (a) reacts with a substrate protein to generate a mixed disulfide intermediate (b). This covalent reaction intermediate is rapidly resolved to release the oxidized substrate and reduced DsbA (c). Reduced DsbA is in turn reoxidized by the inner membrane protein DsbB (d). Image taken from Paxmann et al. [33].

Among the best known bacterial extracytoplasmic TDORs are the Dsb proteins of the Gram-negative bacterium *Escherichia coli* [30]. These proteins are characterized by a CxxC motif (two cysteine residues separated by two amino acids), which forms the core of the active site [34]. The catalytic mechanism involves a disulphide exchange process in which the disulphide bond is transferred from the enzyme to the substrate protein (or *vice versa*) via a short-lived intermediate as it is displayed in Fig. 4 [35].

2.2. Thiol-disulphide oxidoreductase modules in the low-GC Gram-positive Bacteria

Kouwen, T. R., van der Goot, A., Dorenbos, R., <u>Winter, T</u>., Antelmann, H., Plaisier, M. C., Quax, W. J., van Dijl, J. M., Dubois, J. Y. (2007)
Molecular Microbiology, 64(4):984-99

2.2.1. Goal of study

Compared with Gram-negative bacteria, such as *E. coli*, relatively little information is currently available about extracytoplasmic TDORs in Gram-positive bacteria. The current knowledge on TDORs from Gram-positive bacteria was obtains mainly in studies with *Bacillus subtilis* [32]. We focus on the mode of action and build up of TDORs of low-GC Gram-positive bacteria and compared the biological activity of TDORs from *B. subtilis* (BdbA-D) and *S. aureus* (DsbA).

2.2.2. Results of study

Blast research with BdbC and BbdD from *B. subtilis* against annotated *S. aureus* strains revealed the presence of a BdbD homologue (DsbA). But a BdbC homologue is missing in *S. aureus*.

The contruction of a *B. subtilis* XdsbA strain allowed the expression of *S. aureus* lipoprotein *dsbA* in *B. subtilis.* This strain enabled the successful investigation of three disulphide bond-containing reporter proteins for TDOR activity (PhoA, ComGC and sublancin 168) in terms of DsbA functionality. First, we were able to prove that DsbA produced in *B. subtilis* is active and able to promote specifically the folding of the secreted *E. coli* PhoA (Alkaline phosphatase) in a protease-resistant and active conformation. Furthermore, DsbA can replace all four Bdb proteins of *B. subtilis* for folding of *E. coli* PhoA.

Interestingly, DsbA does not need the presence of a BdbC-like protein for this activity in PhoA folding. This suggests that DsbA is reoxidized in a BdbC-independent manner.

Secondly, DsbA is able to complement, at least partly, for the absence of BdbC and BdbD in the correct folding of ComGC to a protease-resistant and biologically active conformation. The pseudopilin ComGC, which is an important element of the DNA uptake machinery of *B. subtilis*, was previously shown to require both BdbC and BdbD for folding and biological activity [36].

For the secretion of active sublancin 168 in *B. subtilis*, BdbB and BdbC are required. A *bdbBC-XdsbA* strain was constructed and it was shown that the *S. aureus* DsbA is able to complement, at least partially for both BdbB and BdbC in sublancin 168 production.

Own contribution to manuscript
Cultivation, proteins preparation, SDS PAGE as well as contributed writing of the manuscript.

3. **Low temperature plasma**

3.1. Introduction

Plasmas are by far the most common phase of matter (99%) in the universe, both by mass and by volume. In 1879 the British chemist and physicist William Crookes first described it as "radiant matter " [37]. The term "plasma" itself comes from Greek ("something molded") and was introduced in 1928 by Irving Langmuir [38].

In physics plasma is, as shown in Fig. 5, considered the fourth state of matter following by order of increasing energy, the solid state, the liquid state and the gaseous state.
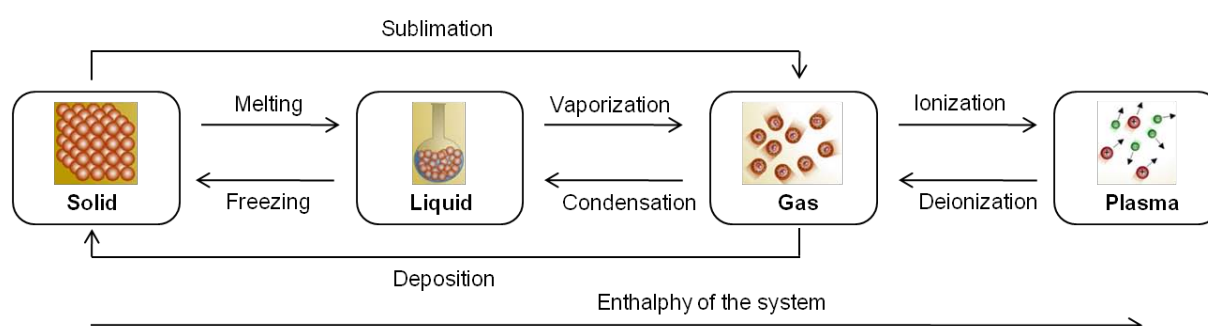
Fig. 5: Matter of states

Strictly speaking, this fourth state is a gas made up of particles and photons in permanent interaction. As displayed in Fig. 6, these particles include electrons, positive and negative ions, atoms, free radicals and excited or non-excited atoms and molecules [7].
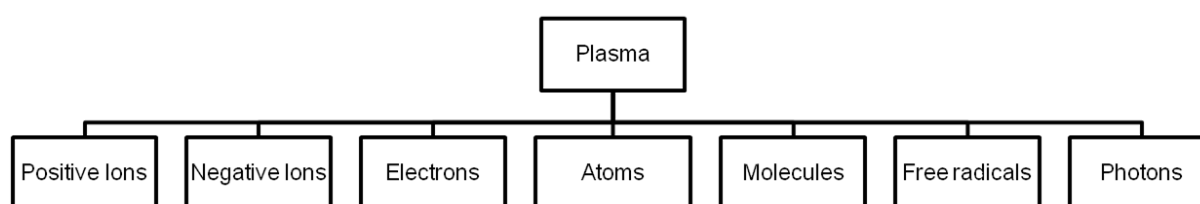
Fig. 6: Constituents of plasma

Plasma can exist over an extremely wide range of temperature and pressure. It can be produced at low-pressure or atmospheric pressure by coupling energy to a gaseous medium by several means such as mechanical, thermal, electrical, chemical, radiant, nuclear and also by a combination of these to dissociate the gaseous component atoms and molecules into a collection of ions, electrons and neutral species. It is thus an energetic chemical environment that combines particles and radiations of a diverse nature, an incredibly diverse source of chemistry that is normally not available in other states of matter [39].

3.2. Classification of plasma

Plasma can be distinguished into two main groups, namely high temperature and low temperature plasma. The classification of plasma is based on the relative energetic levels of electrons and heavy species of the plasma (see Fig. 7).

- *High temperature plasma* implies that light electrons and heavy ions are in a thermal equilibrium state. That means that both have the same temperature. Due to the extreme high gas temperature in those plasmas of up to 10^8 K, the degree of ionizations is almost 1 and hence almost the entire amount of neutral species is ionized. This type of plasma is found in the sun.

- *Low temperature plasma* is further subdivided into thermal (quasi-equilibrium plasma) and non-thermal plasmas (non-equilibrium plasma).

    - o *Thermal plasmas* are characterized by equilibrium or near equilibrium between electrons, ions and neutrals. Plasma torches, arc or microwave plasma are common thermal plasma applications. These sources produce high temperatures ($2x10^4$ K) and are mainly used in areas such as in plasma material processing and plasma treatment of waste materials. Due to the high temperature, thermal plasmas are not applicable for direct medical applications.

    - o In *non-thermal plasmas* (NTP), most of the coupled electrical energy is primarily channeled in the electron component, while the plasma ions and neutral components remain at or near room temperature. Because the ions and the neutrals remain relatively cold, this characteristic provides the possibility for using cold plasmas for low temperature plasma chemistry and for the treatment of heat sensitive materials including polymers and biological tissues. The strong thermodynamic non-equilibrium nature and the presence of reactive chemical species offer a tremendous potential for cold plasma to utilize these plasma sources in a wide range of applications [7, 39]. Examples for commonly used non-thermal plasma devices are plasma jets and Dielectric barrier discharges (DBD). The latter was used in our studies, due to its just mentioned advantages.
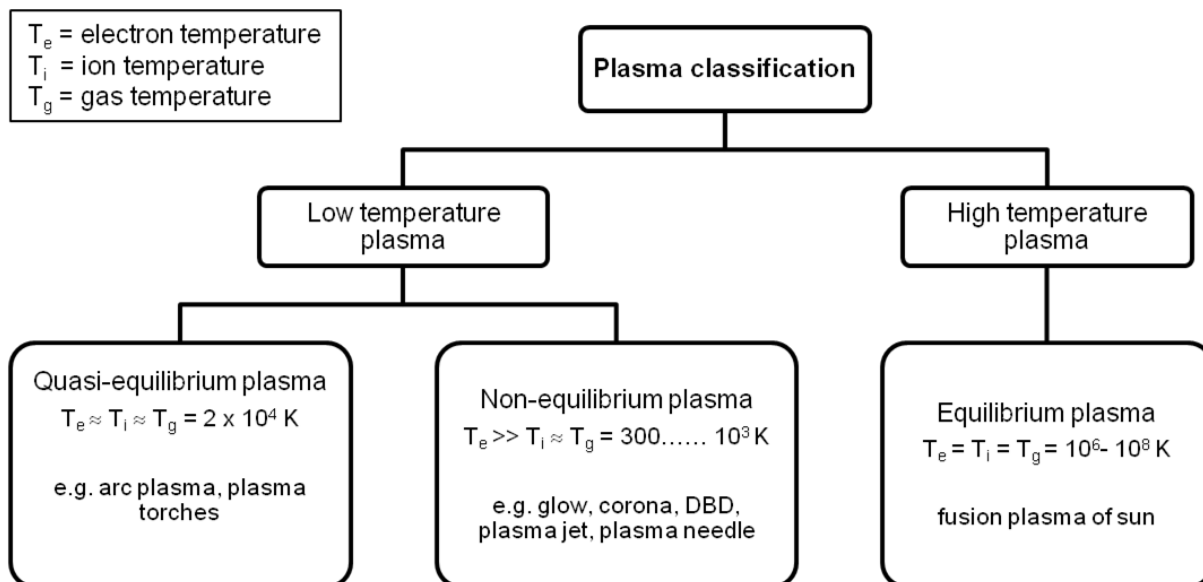
Plasma classification

T_e = electron temperature
T_i = ion temperature
T_g = gas temperature

Low temperature plasma

High temperature plasma

Quasi-equilibrium plasma
$T_e \approx T_i \approx T_g = 2 \times 10^4$ K

e.g. arc plasma, plasma torches

Non-equilibrium plasma
$T_e \gg T_i \approx T_g = 300 \ldots\ldots 10^3$ K

e.g. glow, corona, DBD, plasma jet, plasma needle

Equilibrium plasma
$T_e = T_i = T_g = 10^6 - 10^8$ K

fusion plasma of sun

Fig. 7: Plasma classification

3.3. Fields of applications of non-thermal plasma

In recent years, the application of non-thermal plasma has become more and more diverse. Industrial applications range from surface treatment, high-power CO_2 lasers, excimer ultraviolet lamps, pollution control, various thin film deposition processes, and most recently, also in large-area at plasma display panels [40]. Besides this rather technical use of plasma, a variety of non-thermal plasma applications evolved in the area of life science ranging from teeth bleaching [41, 42], skin treatments to wound healing [8, 43-45].

This quite novel field of non-thermal plasma applications with the main focus on the latter mentioned skin and wound treatment methods is called plasma medicine [9, 46-48].

Besides these direct patient treatments also other infection relevant plasma applications such as decontamination of heat sensitive medical devices (e.g. endoscopes, central venous catheters) have great potential in the medical field. With its non-equilibrium plasma conditions and moderate gas temperatures, non-thermal plasmas present a promising new alternative to inactivate pathogenic microorganisms and it might prove to be a new, faster, noncorrosive, more economical alternative to existing decontamination methods.

3.3.1. Microbial decontamination with non-thermal plasma

Microbial decontamination means the decomposition or removal of microorganisms. The major goal of any microbicidal treatment is the prevention of infections. In general, the inactivation of microorganisms and the removal of biological hazardous contaminants is of great interest

29

especially in the clinical sector [8]. The development of bio-compatible polymers and the constraints of industrial safety have driven the emergence of new technologies for bio-decontamination. As most of these polymers are poorly resistant to heating, oven or autoclave sterilization processes are generally inapplicable. Chemical treatments, using for instance ethylene oxide might be an alternative, but traces of the active compound often remain on the treated devices and constitute an unacceptable risk [7].

In general an optimal sterilization process has to be effective, fast in process, economical, nontoxic and nonhazardous for the staff, the operator and the patient, environmentally friendly, energy saving and should prevent material from damage [8].

Non-thermal plasma generated at atmospheric pressure consists of a variety of microbicidal active agents and is likely to become an appropriate tool for microbial decontamination. Since there is no need of expensive vacuum facilities, atmospheric pressure plasma sources are easily applicable to even complex devices and conventional processes. Hence, their development and characterization has been in the focus of research for more than two decades and until now their entire potential is not yet predictable.

3.3.2. Non-thermal plasma in contact with biological material/cells

Besides the just described plasma applications for decontamination purposes, the treatment of skin and wounds with plasma is becoming more and more of interest.

Clearly, the interaction of plasma with living systems is complex, owing partly to the complexity of plasma and mainly to the overwhelming complexity of biology [49].

Besides plain physical effects such as heat, high energy UV radiation, radiation in the visible and infrared spectral range, alternating electric fields, plasma has another huge arsenal of medically relevant therapeutic active agents [8]. Plasma generates various biologically active agents such as charged particles (electrons, ions), electronically excited atoms and molecules. Additionally, plasma treated cells or tissue surfaces are exposed to active short and long lived neutral atoms and molecules, including for instance atomic oxygen (O), ozone (O_3), nitric oxide (NO), hydroxyl (OH), and singlet oxygen ($O_2(a\Delta)$) [50].

This long list of possible reactive species produced by plasma suggests the complexity of plasma itself and to go one step further- its complex interaction mechanisms with living cells. The whole topic gets even more complex by the fact, that these different biological active agents are produced in dependence on the adjusted parameters like gas composition, flow rate, moisture, temperature and excitation properties.

3.4. Motivation for biological investigation on non-thermal plasma

The investigation of the actual plasma compositions itself is only one aspect that needs to be investigated. This can be achieved by plasma diagnostics tools such as temperature measurements, optical emission spectroscopy (OES) and Fourier transformed infrared spectroscopy (FTIR). But the individual or combined impact of each reactive species on cells is by far the more difficult task which lies ahead. The identification of plasma components responsible for the observed effect in prokaryotic and eukaryotic cells is an essential task and needs the expertise of multidisciplinary research teams. So far only a few selective studies about the interaction of plasma with living cells have been published [50, 51].

3.5. Characterization of the global impact of low temperature gas plasma on vegetative microorganisms

Winter, T., Winter, J., Polak, M., Kusch, K., Mader, U., Sietmann, R., Ehlbeck, J., van Hijum, S., Weltmann, K. D., Hecker, M., Kusch, H. (2011)
Proteomics 11(17): 3518-3530

3.5.1. Goal of study

Despite numerous successful applications of low temperature gas plasmas in medicine and decontamination, the fundamental nature of the interactions between plasma and microorganisms is, to a large extent, unknown. Furthermore, sufficient analytical methods to investigate the effects of the interaction of plasma with microorganism have not been described so far. Our goal was to treat- but not destroy microorganisms with low temperature plasma in order to understand their responses towards that stressor. The Gram-positive model organism *B. subtilis* was chosen, because of the extensive knowledge of its stress response mechanisms. Proteomic and transcriptomic analysis were performed in combination plasma diagnostics in order to connect the biological finding with the reactive plasma species.

3.5.2. Results of study

The construction of a novel growth camber system allowed a reproductive growth and plasma treatment of vegetative bacteria. With connected plasma diagnostic tools such as optical emission spectroscopy (OES), Fourier transformed infrared spectroscopy (FTIR) and temperature measurements, the plasma composition were determined. Temperature

measurements revealed a temperature increase in dependency of the applied plasma power of 48°C to 55.4°C in the discharge region. The temperature of the growth broth was not elevated. The biologically active agents produced by the plasma in this experimental setup are excited argon species, hydroxyl-radicals, UV-B radiation and high energy particles such as ions and electrons.

A growth retardation of the bacteria, depending on the discharge power was observed leading to a significant growth curve decline with increasing power. The argon gas influx led also to a short oxygen deprivation which was not detected on the transcriptional level. Plasma treatment led to morphological changes of the cells, which were made visible via electron microscopy. Dents on the cell surface appear not directly after the plasma treatment, but after 60 min, they are considered to be secondary effects resulting from the deregulation of other cell mechanisms.

Proteome analysis revealed numerous changes in the protein pattern as shown in Fig. 8. In total, 70 proteins exhibit changes in abundance (ratio <0.5 ;>2 ; p-value 0.01). 32 proteins displayed an increase and 38 a decreased protein amount on the 2-D gels.

Fig. 8: False-colored dual-channel image of 2-D gels of intracellular *B. subtilis* proteins (15min argon influx) (green) and *B. subtilis* (15min 2.5W argon plasma treatment) (red).

Additionally, the experiments were performed for different discharge voltages in order to evaluate the plasma power impact. We were able to show that the increased plasma power does not automatically result in more affected proteins. Proteins belonging to the functional categories of protein synthesis, modification and degradation were mainly affected, as well as proteins which belong functionally to the cell wall category. Several PerR regulon associated proteins were affected, too.

Transcriptome data shows that plasma treatment led to a rapid and global transcriptional response. 280 genes were found to be significantly regulated (ratio <0.5;>2;p-value 0.01) as a consequence of plasma treatment. The two most induced gene (*mrgA* and *katA*) are oxidative stress marker genes. Almost all significantly regulated genes belonging to the functional categories cell wall, motility and chemotaxis, coping with stress, prophages, sporulation and homeostasis were up regulated. In contrast, all genes, belonging to the functional categories metabolism of nucleotids and nucleic acids and carbon metabolism were down regulated. Several regulons were well covered by the 280 genes, e.g. LexA, PerR, Spx and Fur.

Taken together, we were able to investigate for the first time the molecular response of vegetative growing microorganism towards low temperature plasma treatment. Due to a novel growth chamber, reproducible growth and plasma treatment was possible. Effect on the growth behavior, the morphology and several cellular targets- such as cell wall, protein and DNA were found due to plasma treatment. The clear oxidative stress response, made visible with the proteomic and transcriptomic analysis could nicely be linked with the reactive species in the plasma which were detected by OES measurements.

3.6. Common versus noble- *Bacillus subtilis* differentially responds to air and argon gas plasma

Winter, T.., Bernhardt, J., Winter, J., Mäder, U., Schlüter, R., Weltmann, K. D., Hecker, M., Kusch, H. (2011)
Submitted to *PLoS ONE*

3.6.1. Goal of study

In order to gain further insight in this topic, a second kind of plasma treatment was applied and combined proteomic and transcriptomic analysis were used to investigate the specific stress response of *B. subtilis* cells to treatment with not only argon but also air plasma. The completely different properties of air plasma (e.g. reactive species, heat, radiation) compared to argon plasma seemed an adequate way to gain further understanding about the impact of plasma composition and its direct effect on the cells. The experimental design was identical to the previous study in order to assure reproducibility and comparability.

3.6.2. Results of study

The constructed growth camber system allowed a reproductive growth and plasma treatment of vegetative bacteria for both gas admixtures and ensured comparability between the experiments.

Once again, plasma diagnostics (OES, FTIR and temperature measurements) were applied.

Temperature measurements revealed significant differences between argon and air plasma. Whereas the temperature in the discharge region increased up to 55.4°C during argon plasma treatment, the temperatures increased up to 90.4°C during air plasma treatment. This severe temperature increase was also detected on the molecular level by the induction of heat shock genes. The temperature of the growth broth did not alter under both plasma treatment conditions.

Besides similar biological active agents under both plasma treatment conditions (UV-B radiation and high energy particles such as ions and electrons), the composition differs significantly in terms of hydroxyl radicals, heat and excited oxygen/nitrogen species.

In contrast to the clear growth retardation due to argon plasma treatment, only the highest applied discharge voltage during air plasma resulted in a detectable growth retardation.

In order to visualize the possible differential effects of argon and air plasma treatment on the cell envelope, samples for were taken for electron microscopy. In both cases, the morphological changes become first visible after 60 min and not directly after the plasma treatment. Argon plasma treated *B. subtilis* cells display noticeably dents on their surface. Air plasma treated cells look speckled 60 min after plasma treatment and 120 min later, these speckles turn into spider web-like filaments between cells.

With proteome analysis, 84 proteins were found to be altered due to air plasma treatment proteins (ratio <0.5 ;>2 ; p-value 0.01) in contrast to 70 proteins under argon plasma conditions. 614 altered genes were detected in transcriptomic analysis due to air plasma treatment (ratio <0.5;>2; p-value 0.01). *TrpC, trpF* (>200fold), *trpB*, *trpD*, *trpE* are part of the biosynthesis of tryptophan and are more than 100fold up regulated after air plasma treatment and so are *hxlA*, *hxlB* and the oxidative stress marker genes *hmp* and *katA*. The induction of the *trp* genes is a response to photo oxidative damage to amino acids. The effect was only observed under air plasma conditions.

Additionally acquired data allowed the evaluation of the impact of argon gas only on the microorganisms. By comparing the air control and argon gas control, a considerably number of affected genes was revealed. Argon gas only resulted in the significant alteration of 774 genes. When deleting argon gas only affected genes from the original argon plasma gene list, 219 "real" argon plasma affected gene remain. This finding reveals that the impact of argon gas is higher than previously envisioned. Argon gas only resulted in the clear induction of three

extracytoplasmic function (ECF) σ factors, (σ^W, σ^M and σ^X) which are related to cell envelope homeostasis and antibiotic resistance as well as in the induction of σ^B genes.

Our data showed clearly that the simple replacement of argon gas by atmospheric air resulted in a broad spectrum of similar but also plasma specific stress responses. Both plasma stresses provoked an oxidative-, as well as a SOS stress response which is displayed by the induction of the PerR-, Fur- and LexA regulons. Argon plasma induced many genes associated with functions of cell wall synthesis and degradation- especially the induction of the phosphate starvation response regulon PhoP which does not apply for air plasma, respectively. In contrast, air plasma specifically induced heat shock genes as well as the *trp* and *cymR* genes as a clear response to photo oxidative damage of amino acids.

<u>Own contribution to both manuscripts</u>

Experimental planning, cultivation, plasma treatment of cells, proteins preparation, SDS PAGE, analysis of 2D gels and Maldi data, RNA preparation for Array analysis and analysis of array data, as well as writing of the manuscript.

4. Literature

[1] WHO, *Life in the 21st century - A vision for all, The World Health Report* Geneva 1998.

[2] Brandi, L., Fabbretti, A., Gualerzi, C. O., How to cope with the quest for new antibiotics. *Febs Letters* 2011, *585*, 1673-1681.

[3] Norrby, S. R., Nord, C. E., Finch, R., In, E. S. C. M., Lack of development of new antimicrobial drugs: a potential serious threat to public health. *Lancet Infectious Diseases* 2005, *5*, 115-119.

[4] de Keyzer, J., van der Does, C., Driessen, A. J., The bacterial translocase: a dynamic protein channel complex. *Cell Mol Life Sci* 2003, *60*, 2034-2052.

[5] Tjalsma, H., Antelmann, H., Jongbloed, J. D., Braun, P. G*., et al.*, Proteomics of protein secretion by Bacillus subtilis: separating the "secrets" of the secretome. *Microbiol Mol Biol Rev* 2004, *68*, 207-233.

[6] Sibbald, M. J., Ziebandt, A. K., Engelmann, S., Hecker, M*., et al.*, Mapping the pathways to staphylococcal pathogenesis by comparative secretomics. *Microbiol Mol Biol Rev* 2006, *70*, 755-788.

[7] Moreau, M., Orange, N., Feuilloley, M. G., Non-thermal plasma technologies: new tools for bio-decontamination. *Biotechnol Adv* 2008, *26*, 610-617.

[8] Ehlbeck, J., Schnabel, U., Polak, M., Winter, J*., et al.*, Low temperature atmospheric pressure plasma sources for microbial decontamination. *Journal of Physics D-Applied Physics* 2011, *44*.

[9] Morfill, G. E., Kong, M. G., Zimmermann, J. L., Focus on Plasma Medicine. *New Journal of Physics* 2009, *11*.

[10] Arbuthnott, J. P., Coleman, D. C., de Azavedo, J. S., Staphylococcal toxins in human disease. *Soc Appl Bacteriol Symp Ser* 1990, *19*, 101S-107S.

[11] Lina, G., Gillet, Y., Vandenesch, F., Jones, M. E*., et al.*, Toxin involvement in staphylococcal scalded skin syndrome. *Clin Infect Dis* 1997, *25*, 1369-1373.

[12] Novick, R. P., Mobile genetic elements and bacterial toxinoses: the superantigen-encoding pathogenicity islands of Staphylococcus aureus. *Plasmid* 2003, *49*, 93-105.

[13] Novick, R. P., Schlievert, P., Ruzin, A., Pathogenicity and resistance islands of staphylococci. *Microbes Infect* 2001, *3*, 585-594.

[14] Jarraud, S., Mougel, C., Thioulouse, J., Lina, G*., et al.*, Relationships between Staphylococcus aureus genetic background, virulence factors, agr groups (alleles), and human disease. *Infect Immun* 2002, *70*, 631-641.

[15] Harwood, C. R., Cranenburgh, R., Bacillus protein secretion: an unfolding story. *Trends Microbiol* 2008, *16*, 73-79.

[16] Driessen, A. J., Nouwen, N., Protein translocation across the bacterial cytoplasmic membrane. *Annu Rev Biochem* 2008, *77*, 643-667.

[17] Tjalsma, H., Bolhuis, A., Jongbloed, J. D., Bron, S., van Dijl, J. M., Signal peptide-dependent protein transport in Bacillus subtilis: a genome-based survey of the secretome. *Microbiol Mol Biol Rev* 2000, *64*, 515-547.

[18] Sarvas, M., Harwood, C. R., Bron, S., van Dijl, J. M., Post-translocational folding of secretory proteins in Gram-positive bacteria. *Biochim Biophys Acta* 2004, *1694*, 311-327.

[19] Raygada, J. L., Levine, D.P. , Methicillin-Resistant *Staphylococcus aureus*: A Growing Risk in the Hospital and in the Community. *AMERICAN HEALTH & DRUG BENEFITS* 2009, *2*, 86- 95.

[20] Rigel, N. W., Braunstein, M., A new twist on an old pathway--accessory Sec [corrected] systems. *Mol Microbiol* 2008, *69*, 291-302.

[21] Bensing, B. A., Sullam, P. M., An accessory sec locus of Streptococcus gordonii is required for export of the surface protein GspB and for normal levels of binding to human platelets. *Mol Microbiol* 2002, *44*, 1081-1094.

[22] Siboo, I. R., Chaffin, D. O., Rubens, C. E., Sullam, P. M., Characterization of the accessory Sec system of Staphylococcus aureus. *J Bacteriol* 2008, *190*, 6188-6196.

[23] Takamatsu, D., Bensing, B. A., Sullam, P. M., Two additional components of the accessory sec system mediating export of the Streptococcus gordonii platelet-binding protein GspB. *J Bacteriol* 2005, *187*, 3878-3883.

[24] Sibbald, M. J., Winter, T., van der Kooi-Pol, M. M., Buist, G.*, et al.*, Synthetic effects of secG and secY2 mutations on exoproteome biogenesis in Staphylococcus aureus. *J Bacteriol* 2010, *192*, 3788-3800.

[25] Nishiyama, K., Mizushima, S., Tokuda, H., A novel membrane protein involved in protein translocation across the cytoplasmic membrane of Escherichia coli. *EMBO J* 1993, *12*, 3409-3415.

[26] van Wely, K. H., Swaving, J., Broekhuizen, C. P., Rose, M.*, et al.*, Functional identification of the product of the Bacillus subtilis yvaL gene as a SecG homologue. *J Bacteriol* 1999, *181*, 1786-1792.

[27] Collet, J. F., Bardwell, J. C., Oxidative protein folding in bacteria. *Mol Microbiol* 2002, *44*, 1-8.

[28] Ritz, D., Beckwith, J., Roles of thiol-redox pathways in bacteria. *Annu Rev Microbiol* 2001, *55*, 21-48.

[29] Aslund, F., Beckwith, J., Bridge over troubled waters: sensing stress by disulfide bond formation. *Cell* 1999, *96*, 751-753.

[30] Kadokura, H., Katzen, F., Beckwith, J., Protein disulfide bond formation in prokaryotes. *Annu Rev Biochem* 2003, *72*, 111-135.

[31] Anfinsen, C. B., Principles that govern the folding of protein chains. *Science* 1973, *181*, 223-230.

[32] Kouwen, T. R., van der Goot, A., Dorenbos, R., Winter, T.*, et al.*, Thiol-disulphide oxidoreductase modules in the low-GC Gram-positive bacteria. *Mol Microbiol* 2007, *64*, 984-999.

[33] Paxman, J. J., Borg, N. A., Horne, J., Thompson, P. E.*, et al.*, The structure of the bacterial oxidoreductase enzyme DsbA in complex with a peptide reveals a basis for substrate specificity in the catalytic cycle of DsbA enzymes. *J Biol Chem* 2009, *284*, 17835-17845.

[34] Newton, G. L., Arnold, K., Price, M. S., Sherrill, C.*, et al.*, Distribution of thiols in microorganisms: mycothiol is a major thiol in most actinomycetes. *J Bacteriol* 1996, *178*, 1990-1995.

[35] Kadokura, H., Tian, H., Zander, T., Bardwell, J. C., Beckwith, J., Snapshots of DsbA in action: detection of proteins in the process of oxidative folding. *Science* 2004, *303*, 534-537.

[36] Meima, R., Eschevins, C., Fillinger, S., Bolhuis, A.*, et al.*, The bdbDC operon of Bacillus subtilis encodes thiol-disulfide oxidoreductases required for competence development. *J Biol Chem* 2002, *277*, 6994-7001.

[37] Crookes, W., On Radiant Matter Spectroscopy: A New Method of Spectrum Analysis. *Proc Roy Soc* 1883, *35*, 262–271.

[38] Langmuir, I., Oscillations in Ionized Gases. *Proc Natl Acad Sci U S A* 1928, *14*, 627-637.

[39] Nehra, V., Kumar, A., Dwivedi, H. K., Atmospheric non-thermal plasma sources. *International journal of engineering* 2008, *2*, 53-68.

[40] Kogelschatz, U., Eliasson, B., Egli, W., From ozone generators to flat television screens: history and future potential of dielectric-barrier discharges. *Pure and Applied Chemistry* 1999, *71*, 1819-1828.

[41] Bussiahn, R., Brandenburg, R., Gerling, T., Kindel, E.*, et al.*, The hairline plasma: An intermittent negative dc-corona discharge at atmospheric pressure for plasma medical applications. *Applied Physics Letters* 2010, *96*, -.

[42] Sladek, R. E. J., Stoffels, E., Walraven, R., Tielbeek, P. J. A., Koolhoven, R. A., Plasma treatment of dental cavities: A feasibility study. *Ieee Transactions on Plasma Science* 2004, *32*, 1540-1543.

[43] Daeschlein, G., von Woedtke, T., Kindel, E., Brandenburg, R.*, et al.*, Antimicrobial Activity of an Atmospheric Pressure Plasma Jet Agian Relevant Wound Pathogens in vitro on a Simulated Wound Environment. *Plasma Processes and Polymers* 2010, *7*, 224-230.

[44] Fridman, G., Peddinghaus, M., Ayan, H., Fridman, A.*, et al.*, Blood coagulation and living tissue sterilization by floating-electrode dielectric barrier discharge in air. *Plasma Chemistry and Plasma Processing* 2006, *26*, 425-442.

[45] Shekhter, A. B., Serezhenkov, V. A., Rudenko, T. G., Pekshev, A. V., Vanin, A. F., Beneficial effect of gaseous nitric oxide on the healing of skin wounds. *Nitric Oxide-Biology and Chemistry* 2005, *12*, 210-219.

[46] Fridman, G., Friedman, G., Gutsol, A., Shekhter, A. B*., et al.*, Applied plasma medicine. *Plasma Processes and Polymers* 2008, *5*, 503-533.

[47] Weltmann, K. D., Kindel, E., von Woedtke, T., Hahnel, M*., et al.*, Atmospheric-pressure plasma sources: Prospective tools for plasma medicine. *Pure and Applied Chemistry* 2010, *82*, 1223-1237.

[48] Weltmann, K. D., von Woedtke, T., Brandenburg, R., Ehlbeck, J., Biomedical applications of atmospheric pressure plasma. *Chem. Listy* 2008, *102*, 1450-1451.

[49] Fridman, G., Dobrynin, D., Friedman, G., Fridman, A., Physical and biological mechanisms of direct plasma interaction with living tissue. *New Journal of Physics* 2009, *11*.

[50] Kalghatgi, S., Kelly, C. M., Cerchar, E., Torabi, B*., et al.*, Effects of non-thermal plasma on mammalian cells. *PLoS One* 2011, *6*, e16270.

[51] Landsberg, K., Scharf, C., Darm, K., Wende, K*., et al.*, The use of proteomics to investigate plasma- cell interaction. *Plasma Medicine* 2010, *1*, 55-63.

5. Orginal manuscripts

5.1. Synthetic effects of *secG* and *secY2* mutations on exoproteome biogenesis in *Staphylococcus aureus*

Sibbald, M.J*., Winter, T*, van der Kooi-Pol, M. M., Buist, G., Tsompanidou, E., Bosma, T., Schäfer, T., Ohlsen, K., Hecker, M., Antelmann, H., Engelmann, S., van Dijl, J.M. (2010)

* both authors contributed equally to this work

Own contribution to manuscript

Cultivation, proteins preparation, SDS PAGE, analysis of 2D gels and Maldi data, RNA preparations, Northern blots and analysis of Northern blots, as well as writing of the manuscript.

Synthetic Effects of *secG* and *secY2* Mutations on Exoproteome Biogenesis in *Staphylococcus aureus*[▽]

Mark J. J. B. Sibbald,[1]† Theresa Winter,[2]† Magdalena M. van der Kooi-Pol,[1] G. Buist,[1]
E. Tsompanidou,[1] Tjibbe Bosma,[3] Tina Schäfer,[4] Knut Ohlsen,[4] Michael Hecker,[2]
Haike Antelmann,[2] Susanne Engelmann,[2] and Jan Maarten van Dijl[1]*

*Department of Medical Microbiology, University Medical Center Groningen and University of Groningen, Hanzeplein 1,
P.O. Box 30001, 9700 RB Groningen, Netherlands[1]; Institut für Mikrobiologie, Ernst Moritz Arndt Universität Greifswald,
D-17487 Greifswald, Germany[2]; BioMaDe Technology, Nijenborgh 4, 9747 AG Groningen, Netherlands[3]; and
Universität Würzburg, Institut für Molekulare Infektionsbiologie, Josef Schneider Strasse 2,
D-97080 Würzburg, Germany[4]*

The Gram-positive pathogen *Staphylococcus aureus* secretes various proteins into its extracellular milieu. Bioinformatics analyses have indicated that most of these proteins are directed to the canonical Sec pathway, which consists of the translocation motor SecA and a membrane-embedded channel composed of the SecY, SecE, and SecG proteins. In addition, *S. aureus* contains an accessory Sec2 pathway involving the SecA2 and SecY2 proteins. Here, we have addressed the roles of the nonessential channel components SecG and SecY2 in the biogenesis of the extracellular proteome of *S. aureus*. The results show that SecG is of major importance for protein secretion by *S. aureus*. Specifically, the extracellular accumulation of nine abundant exoproteins and seven cell wall-bound proteins was significantly affected in an *secG* mutant. No secretion defects were detected for strains with a *secY2* single mutation. However, deletion of *secY2* exacerbated the secretion defects of *secG* mutants, affecting the extracellular accumulation of one additional exoprotein and one cell wall protein. Furthermore, an *secG secY2* double mutant displayed a synthetic growth defect. This might relate to a slightly elevated expression of *sraP*, encoding the only known substrate for the Sec2 pathway, in cells lacking SecG. Additionally, the results suggest that SecY2 can interact with the Sec1 channel, which would be consistent with the presence of a single set of *secE* and *secG* genes in *S. aureus*.

Staphylococcus aureus is a well-represented component of the human microbiota as nasal carriage of this Gram-positive bacterium has been shown for 30 to 40% of the population (32). This organism can, however, turn into a dangerous pathogen that is able to infect almost every tissue in the human body. *S. aureus* has become particularly notorious for its high potential to develop resistance against commonly used antibiotics (20, 49). Accordingly, the *S. aureus* genome encodes an arsenal of virulence factors that can be expressed when needed at different stages of growth. These include surface proteins and invasins that are necessary for colonization of host tissues, surface-exposed factors for evasion of the immune system, exotoxins for the subversion of protective host barriers, and resistance proteins for protection against antimicrobial agents (37, 57).

Most proteinaceous virulence factors of *S. aureus* are synthesized as precursors with an N-terminal signal peptide to direct their transport from the cytoplasm across the membrane to an extracytoplasmic location, such as the cell wall or the extracellular milieu (38, 45). As shown for various Gram-positive bacteria, the signal peptides of *S. aureus* are

generally longer and more hydrophobic than those of Gram-negative bacteria (38, 54). On the basis of signal peptide predictions using a variety of algorithms, it is believed that most exoproteins of *S. aureus* are exported to extracytoplasmic locations via the general secretory (Sec) pathway (38). This seems to involve precursor targeting to the Sec machinery via the signal recognition particle instead of the well-characterized proteobacterial chaperone SecB, which is absent from Gram-positive bacteria (16, 19, 53). The preproteins are then bound by the translocation motor protein SecA (38, 45). Through repeated cycles of ATP binding and hydrolysis, SecA pushes the protein in an unfolded state through the membrane-embedded SecYEG translocation channel (12, 30, 33, 52). Upon initiation of the translocation process, the proton motive force is thought to accelerate preprotein translocation through the Sec channel (26). Recently, the structure of the SecA/SecYEG complex from the Gram-negative bacterium *Thermotoga maritima* was solved at 4.5 Å resolution (58). In this structure, one SecA molecule is bound to one set of SecYEG channel proteins. The core of the Sec translocon consists of the SecA, SecY, and SecE proteins, which are essential for growth and viability of bacteria, such as *Escherichia coli* and *Bacillus subtilis* (6, 9, 22). In contrast, the channel component SecG is dispensable for growth, cell viability, and protein translocation (26, 48). Nevertheless, SecG does enhance the efficiency of preprotein translocation through the SecYE channel (26, 48). This is of particular relevance at low temperatures and in the

---

* Corresponding author. Mailing address: Department of Medical Microbiology, University Medical Center Groningen, Hanzeplein 1, P.O. Box 30001, 9700 RB Groningen, Netherlands. Phone: 31 50 3615187. Fax: 31 50 3619105. E-mail: J.M.van.Dijl@med.umcg.nl.
† M.J.J.B.S. and T.W. contributed equally to this work.
▽ Published ahead of print on 14 May 2010.

absence of a proton motive force (17). Several studies suggest that *E. coli* SecG undergoes topology inversion during preprotein translocation (25, 27, 43). Even so, van der Sluis et al. reported that SecG cross-linked to SecY is fully functional despite its fixed topology (46). During or shortly after membrane translocation of a preprotein through the Sec channel, the signal peptide is removed by signal peptidase. This is a prerequisite for the release of the translocated protein from the membrane (1, 47).

Several pathogens, including *Streptococcus gordonii*, *Streptococcus pneumoniae*, *Bacillus anthracis*, *Bacillus cereus*, and *S. aureus*, contain a second set of chromosomal *secA* and *secY* genes named *secA2* and *secY2*, respectively (39). Comparison of the amino acid sequences of the SecY1 and SecY2 proteins shows that their similarity is low (about 20% identity) and that the conserved regions are mainly restricted to the membrane-spanning domains. It has been shown for *S. gordonii* that transport of at least one protein is dependent on the presence of SecA2 and SecY2. This protein, GspB, is a large cell surface glycoprotein that is involved in platelet binding (4). The protein contains an unusually long N-terminal signal peptide of 90 amino acids, large serine-rich repeats, and a C-terminal LPXTG motif for covalent cell wall binding. The *gspB* gene is located in a gene cluster with the *secA2* and *secY2* genes. Two other genes in this cluster encode the glycosylation proteins GftA and GftB, which seem to be necessary for stabilization of pre-GspB. Furthermore, the *asp4* and *asp5* genes in the *secA2 secY2* gene cluster show similarity to *secE* and *secG*, and they are important for GspB export by *S. gordonii* (44). Despite this similarity, SecE and SecG cannot complement for the absence of Asp4 and Asp5, respectively. The *secA2-secY2* gene cluster is also present in *S. aureus*, but homologues of the *asp4* and *asp5* genes are lacking. This seems to suggest that SecA2 and SecY2 of *S. aureus* share the SecE and SecG proteins with SecA1 and SecY1. The *sraP* gene in the *secA2-secY2* gene cluster of *S. aureus* encodes a protein with features similar to those described for GspB. Siboo and colleagues (41) have shown that SraP is glycosylated and capable of binding to platelets. Importantly, the disruption of *sraP* resulted in a decreased ability to initiate infective endocarditis in a rabbit model. Consistent with the findings in *S. gordonii*, SraP export was shown to depend on SecA2/SecY2 (40). However, it has remained unclear whether other *S. aureus* proteins are also translocated across the membrane in an SecA2/SecY2-dependent manner.

The present studies were aimed at defining the roles of two Sec channel components, SecG and SecY2, in the biogenesis of the *S. aureus* exoproteome. The results show that *secG* and *secY2* are not essential for growth and viability of *S. aureus*. While the absence of SecY2 by itself had no detectable effect, the absence of SecG had a profound impact on the composition of the exoproteome of *S. aureus*. Various extracellular proteins were present in decreased amounts in the growth medium of *secG* mutant strains, which is consistent with impaired Sec channel function. However, a few proteins are present in increased amounts. Furthermore, the absence of *secG* caused a serious decrease in the amounts of the cell wall-bound Sbi protein. Most notable, a *secG secY2* double mutant strain displayed synthetic growth and secretion defects.

MATERIALS AND METHODS

Bacterial strains and plasmids. All strains used in this study are listed in Table 1. Unless stated otherwise, *E. coli* strains were grown in Luria-Bertani broth (LB). *S. aureus* strains were grown at 37°C in tryptic soy broth (TSB) or B medium (1% peptone, 0.5% yeast extract, 0.5% NaCl, 0.1% K_2HPO_4, 0.1% glucose), under vigorous shaking, or on tryptic soy agar (TSA) plates or B plates. If appropriate, medium for *E. coli* was supplemented with 100 μg/ml ampicillin or 100 μg/ml erythromycin, and medium for *S. aureus* was supplemented with 5 μg/ml erythromycin, 5 μg/ml tetracycline, or 20 μg/ml kanamycin. To monitor β-galactosidase activity in cells of *E. coli* and *S. aureus*, 5-bromo-4-chloro-3-indolyl-β-D-galactopyranoside (X-Gal) was added to the plates at a final concentration of 80 μg/ml.

Construction of *S. aureus* mutant strains. Mutants of *S. aureus* were constructed using the temperature-sensitive plasmid pMAD (2) and previously described procedures (23). Primers (Table 2) were designed using the genome sequence of *S. aureus* NCTC8325 (http://www.ncbi.nlm.nih.gov/nuccore/NC_007795). All mutant strains were checked by isolation of genomic DNA using a GenElute Bacterial Genomic DNA Kit (Sigma) and PCR with specific primers.

To delete the *secG* or *secY2* gene, primer pairs with the designations F1/R1 and F2/R2 were used for PCR amplification of the respective upstream and downstream regions (each, ~500 bp) and their fusion with a 21-bp linker. The fused flanking regions were cloned in pMAD, and the resulting plasmids were used to delete the chromosomal *secG* or *secY2* genes of *S. aureus* RN4220. To delete the *secG* or *secY2* genes from the *S. aureus* SH1000 genome, the respective pMAD constructs were transferred from the RN4220 strain to the SH1000 strain by transduction with phage φ85 (29).

To create the *spa sbi* double mutant of *S. aureus* Newman, the *sbi* gene was deleted from a *spa* mutant strain kindly provided by T. Foster (31). For this purpose, the kanamycin resistance marker encoded by pDG783 was introduced between the *sbi* flanking regions via PCR with the primer pairs *sbi*-F1/*sbi*-R1, *sbi*-F2/*sbi*-R2, and *kan*-F1/*kan*-R1. The obtained ~2,000-bp fragment was ligated into pMAD, and the resulting plasmid was used to transform competent *S. aureus* Newman *spa* cells. Blue colonies were selected on TSA plates with erythromycin and kanamycin, and the *spa sbi* double mutant was subsequently identified following the previously described protocol (23).

For complementation studies, the *secG* or *secY2* gene was cloned into plasmid pCN51 (11). Expression of genes cloned in this plasmid is directed by a cadmium-inducible promoter. Primer pairs with the F3/R3 designation (Table 2) were used to amplify the *secG* or *secY2* gene. These primers contain an EcoRI restriction site at the 5′ end and an SalI restriction site at the 3′ end of the amplified gene. PCR products were purified using a PCR Purification Kit (Roche) and ligated into a TOPO vector (Invitrogen). The resulting constructs were then cut with EcoRI and SalI, and the *secG* or *secY2* gene (284 and 1,233 bp, respectively) was isolated from an agarose gel and ligated into pCN51 cut with EcoRI and SalI. This resulted in the *secG*- and *secY2*-pCN51 plasmids. Competent *S. aureus* RN4220 Δ*secG*, Δ*secY2*, or Δ*secG* Δ*secY2* cells were transformed with these plasmids by electroporation, and colonies were selected on TSA plates containing erythromycin. The plasmids were then transferred to *S. aureus* SH1000 by transduction as described above.

Analytical and preparative 2-D PAGE. Extracellular proteins from 100 ml of culture supernatant were precipitated, washed, dried, and resolved as described previously (56). The protein concentration was determined using Roti-Nanoquant (Carl Roth GmbH & Co., Karlsruhe, Germany). Preparative two-dimensional (2-D) PAGE was performed by using the immobilized pH gradient technique (5, 13). The protein samples (350 μg) were separated on immobilized pH gradient strips (Amersham Pharmacia Biotech, Piscataway, NJ) with a linear pH gradient from 3 to 10. The resulting protein gels were stained with colloidal Coomassie blue G-250G (10) and scanned with a light scanner. Each experiment was performed at least three times.

For identification of proteins by matrix-assisted laser desorption ionization–time of flight mass spectrometry (MALDI-TOF MS), Coomassie-stained protein spots were excised from gels using a spot cutter (Proteome Work) with a picker head of 2 mm and transferred into 96-well microtiter plates. Digestion with trypsin and subsequent spotting of peptide solutions onto the MALDI targets were performed automatically in an Ettan Spot Handling Workstation (GE-Healthcare, Little Chalfont, United Kingdom) using a modified standard protocol. MALDI-TOF MS analyses of spotted peptide solutions were carried out on a Proteome-Analyzer 4700/4800 (Applied Biosystems, Foster City, CA) as described previously (13). MALDI with tandem TOF (TOF-TOF) analysis was performed for the three highest peaks of the TOF spectrum as described previously (13, 51). Database searches were performed using the GPS explorer software, version 3.6 (build 329), with organism-specific databases.

TABLE 1. Plasmids and bacterial strains used

Plasmid or strain	Description or genotype	Reference or source
Plasmids		
TOPO	pCR-Blunt II-TOPO vector; Km^r	Invitrogen Life Technologies
pCN51	*E. coli*/*S. aureus* shuttle vector that contains a cadmium-inducible promoter	11
pMAD	*E. coli*/*S. aureus* shuttle vector that is temp-sensitive in *S. aureus* and contains the *bgaB* gene; Ery^r Amp^r	2
pUC18	Amp^r, ColE1, φ80d*lacZ*; *lac* promoter	28
pDG783	1.5-kb kanamycin resistance cassette in pSB118; Amp^r	15
secG-pCN51	pCN51 with *S. aureus secG* gene; Amp^r Ery^r	This work
secY2-pCN51	pCN51 with *S. aureus secY2* gene; Amp^r Ery^r	This work
Strains		
E. coli		
DH5α	λ$^-$ φ80d*lacZ*ΔM15 Δ(*lacZYA-argF*)U169 *recA1 endA hsdR17*(r$_K^-$ m$_K^-$) *supE44 thi-1 gyrA relA1*	18
TOP10	Cloning host for TOPO vector; F$^-$ *mcrA* Δ(*mrr-hsdRMS-mcrBC*) φ80*lacZ*ΔM15 Δ*lacX74 recA1 araD139* Δ(*ara-leu*)7697 *galU galK rpsL* (Str^r) *endA1 nupG*	Invitrogen Life Technologies
S. aureus RN4220		
Parental strain	Restriction-deficient derivative of NCTC 8325; cured of all known prophages	24
Δ*secG* strain	*secG* mutant	This work
Δ*secY2* strain	*secY2* mutant	This work
Δ*secG* Δ*secY2* strain	*secG secY2* mutant	This work
S. aureus SH1000		
Parental strain	Derivative of NCTC 8325-4; *rsbU$^+$ agr$^+$*	21
Δ*secG* strain	*rsbU$^+$ agr$^+$* Δ*secG*	This work
Δ*secY2* strain	*rsbU$^+$ agr$^+$* Δ*secY2*	This work
Δ*secG* Δ*secY2* strain	*rsbU$^+$ agr$^+$* Δ*secG* Δ*secY2*	This work
S. aureus Newman		
Δ*spa* strain	*spa* mutant	31
Δ*spa* Δ*sbi* strain	*spa sbi* mutant	This work

By using the MASCOT search engine, version 2.1.0.4. (Matrix Science, London, United Kingdom), the combined MS and tandem MS (MS/MS) peak lists for each protein spot were searched against a database containing protein sequences derived from the genome sequences of *S. aureus* NCTC8325. Search parameters were as described previously (51). For comparison of protein spot volumes, the Delta 2D software package was used (Decodon GmbH Germany). The induction ratio of mutant to parental strain was calculated for each spot (normalized intensity of a spot on the mutant image/normalized intensity of the corresponding spot on the parental image). The significance of spot volume differences of 2-fold or higher was assessed by the a Student's *t* test (α of <0.05; Delta 2D statistics table).

Transcriptional analysis. Total RNA from *S. aureus* RN4220 was isolated using the acid-phenol method (14). Digoxigenin (DIG)-labeled RNA probes were prepared by *in vitro* transcription with T7 RNA polymerase using a DIG-RNA labeling mixture (Roche, Indianapolis, IN) and appropriate PCR fragments as templates. The PCR fragments were generated by using the respective oligonucleotides (Table 2) and chromosomal DNA of *S. aureus* RN4220 isolated with the chromosomal DNA isolation kit (Promega, Madison, WI) according to the manufacturer's recommendations. Reverse primers contain the T7 RNA polymerase recognition sequence at the 5′ end. Northern blot and slot blot analyses were performed as described previously (50, 57). Before hybridization, each RNA blot was stained with methylene blue in order to check the RNA amount blotted onto the membrane. Only blots showing equal amounts of 16S and 23S rRNAs for each sample loaded onto the respective gels were used for hybridization experiments. The hybridization signals of the Northern blots were detected with a Lumi-Imager (Roche, Indianapolis, IN) and analyzed with the software package LumiAnalyst (Roche, Indianapolis, IN). Slot blot signal detection was performed with the Intas ChemoCam system and analyzed with LabImage1D software (Intas Science Imaging Instruments GmbH, Göttingen, Germany). In slot blot experiments, the induction ratios were calculated by dividing the volumes obtained for the different RNA samples by the volume of the signals of the exponentially grown RN4220 parental strain. An internal RNA standard was spotted onto each membrane to correct for intermembrane variations.

Cell fractionation, SDS-PAGE, and Western blotting. Overnight cultures were diluted to an optical density at 540 nm (OD$_{540}$) of 0.05 and grown in 25 ml of TSB under vigorous shaking. For complementation of mutant strains with pCN51-based plasmids, CdSO$_4$ was added after 3 h of growth to a final concentration of 0.25 μM. Samples were taken after 6 h of growth and separated into growth medium and whole-cell and noncovalently cell wall-bound protein fractions. Cells were separated from the growth medium by centrifugation of 1 ml of the culture. The proteins in the growth medium were precipitated with 250 μl of 50% trichloroacetic acid (TCA), washed with acetone, and dissolved in 100 μl of loading buffer (Invitrogen). Cells were resuspended in 300 μl of loading buffer (Invitrogen) and disrupted with glass beads using a Precellys 24 bead-beating homogenizer (Bertin Technologies). From the same culture 20 ml was used for the extraction of noncovalently bound cell wall proteins using KSCN. Cells were collected by centrifugation, washed with PBS, and incubated for 10 min with 1 M KSCN on ice. After centrifugation the noncovalently cell wall-bound proteins were precipitated from the supernatant fraction with TCA, washed with acetone, and dissolved in 100 μl of loading buffer (Invitrogen). Upon addition of reducing agent (Invitrogen), the samples were incubated at 95°C. Proteins were separated by SDS-PAGE using precast NuPage gels (Invitrogen) and subsequently blotted onto a nitrocellulose membrane (Protran; Schleicher and Schuell). The presence of a cytoplasmic marker protein (TrxA), a lipoprotein (DsbA), and several cell wall-associated proteins (Sle1, Aly, ClfA, and IsaA) or extracellular proteins (Sle1, Aly, IsaA, and SspB) was monitored by immunodetection with specific polyclonal antibodies raised in mice or rabbits. Bound primary antibodies were visualized using fluorescent IgG secondary antibodies (IRDye 800 CW goat anti-mouse/anti-rabbit; LiCor Biosciences). Mem-

TABLE 2. Primers used in this study

Primer	Sequence (5′→3′)[a]
secG-F1	TTAAAACAGGACGCTTTATTG
secG-R1	**TTACGTCAGTCAGTCACCATGGCA**AAATTGTCCTCCGTTCCTTAT
secG-F2	**TGCCATGGTGACTGACTGACGTAA**GGTCCGGCGATGTAAATGTCG
secG-R2	GCGTGCATATTCTAAAAAGCC
secY2-F1	TGTCTGGTTCACAAAGCATTT
secY2-R1	**TTACGTCAGTCAGTCACCATGGCA**GTTGCACCTCTTTTATATCAA
secY2-F2	**TGCCATGGTGACTGACTGACGTAA**GGAGGTAATTATGAAATACTT
secY2-R2	GCCTCTCCCTGATCATCAAAA
sbi-F1	TGTGTTCCTTTATTTTCTGCG
sbi-R1	**GAACTCCAATTCACCCATGGCCCCCCCCCC**AACTAGCAACTTCGAG
sbi-F2	**CCGCAACTGTCCATACCATGGCCCCC**GGAAATAATCAATCAAAAATATCTTCTC
sbi-R2	CTATTAAACCAACTGCTAAAGTTGC
kan-F1	GGGGG<u>CCATGG</u>GTGAATTGGAGTTCGTCTTG
kan-R1	GGGGG<u>CCATGG</u>TATGGACAGTTGCGGATGTA
secG-F3	GGGGG<u>GTCGAC</u>GGGATATACTACTTGTCGTATATA
secG-R3	GGGGG<u>GAATTC</u>CCTTACATACCAAGATAACTTATGCA
secY2-F3	GGGGG<u>GTCGAC</u>GTCTTTTTAATGTTTTTGATA
secY2-R3	GGGGG<u>GAATTC</u>CCTTACCAATACTGGTTTAAAAATGG
*spa*_for	ACCTGCTGCAAATGCTGCGC
*spa*_rev[b]	*CTAATACGACTCACTATAGGGAGA* GGTTAGCACTTTGGCTTGGG
*geh*_for	CACATCAAATGCAGTCAGG
*geh*_rev[b]	*CTAATACGACTCACTATAGGGAGA* AATCGACATGATCCCATCC
*hlb*_for	ATCAAACACCTGTACTCGG
*hlb*_rev[b]	*CTAATACGACTCACTATAGGGAGA* CGTAGTAATATGGGAACGC
*sraP*_for	CCATCTAATGTAGCTGGTGG
*sraP*_rev[b]	*CTAATACGACTCACTATAGGGAGA*CACTGATTGTCCAGCATTCG

[a] The overlap in primers is shown in boldface; restriction sites are underlined.
[b] Oligonucleotides containing the recognition sequence for T7 polymerase at the 5′ end (shown in italics).

branes were scanned for fluorescence at 800 nm using an Odyssey Infrared Imaging System (LiCor Biosciences).

Mouse infection studies. All animal studies were approved by the Animal Care and Experimentation Committee of the district government of Lower Franconia, Germany, and conformed to University of Würzburg guidelines. Female BALB/c mice (16 to 18 g; Charles River, Sulzfeld, Germany) were housed in polypropylene cages and received food and water *ad libitum*. *S. aureus* isolates were cultured for 18 h in B medium, washed three times with sterile phosphate-buffered saline (PBS), and suspended in sterile PBS to 1.0×10^8 CFU/100 μl. As a control, selected dilutions were plated on B agar. Mice were inoculated with 100 μl of *S. aureus* via the tail vein. Control mice were treated with sterile PBS. For each strain, eight mice were used. Three days after challenge, kidneys and livers were aseptically harvested and homogenized in 3 ml of PBS using Dispomix (Bio-Budget Technologies Gmbh, Krefeld, Germany). Serial dilutions of the organ homogenates were cultured on mannitol salt-phenol red agar plates for at least 48 h at 37°C. The numbers of CFU were calculated as the number of CFU/organ. The statistical significance of bacterial load was determined using Mann-Whitney tests.

RESULTS

The exoproteomes of *secG* and *secY2* mutant *S. aureus* strains. To investigate the roles of SecG and SecY2 in the biogenesis of the *S. aureus* exoproteome, the respective genes were completely deleted from the chromosome of *S. aureus* strain RN4220. This resulted in the single mutant ΔsecG and ΔsecY2 strains and the double mutant ΔsecG ΔsecY2. Next, cells of these mutants were grown in TSB medium until they reached the stationary phase (Fig. 1; not shown for the ΔsecY2 strain). All three mutants displayed exponential growth rates similar to the rate of the parental strain. However, the *secG secY2* double mutant entered the stationary phase at a lower optical density (OD_{540} of 8) than the parental strain and the ΔsecG mutant (OD_{540} of 15). Since the amounts of most exo-
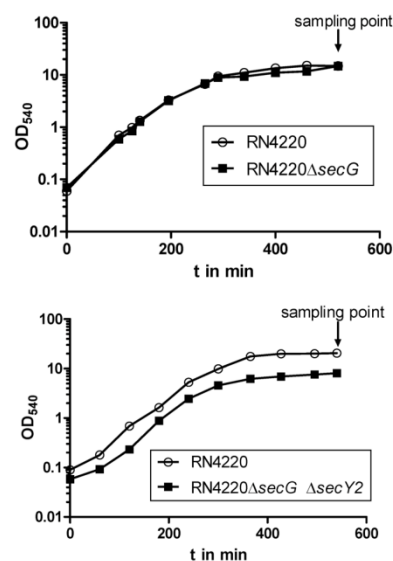

FIG. 1. Growth of *S. aureus secG* and *secG secY2* mutants. The *S. aureus* RN4220 ΔsecG (top) and ΔsecG ΔsecY2 (bottom) strains and the parental strain RN4220 were grown in 100 ml of TSB medium under vigorous shaking at 37°C. Sampling points for the preparation of extracellular proteins for 2-D PAGE analyses shown in Fig. 2 are indicated in the growth curves by arrows. *t*, time.
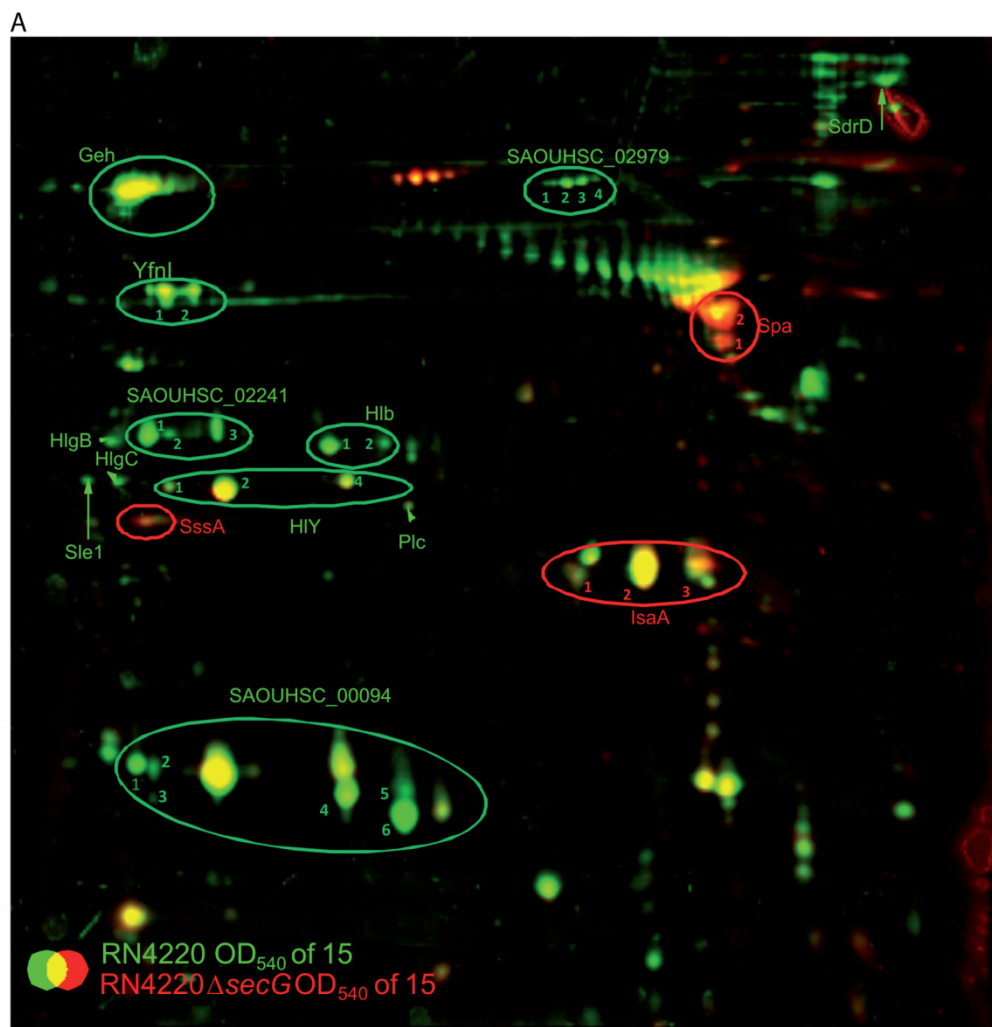
FIG. 2. The extracellular proteomes of *S. aureus secG* and *secG secY2* mutants. (A) False-colored dual-channel image of 2-D gels of extracellular proteins of *S. aureus* RN4220 (green) and *S. aureus* RN4220 Δ*secG* (red). Proteins (350 μg) isolated from the supernatant of *S. aureus* RN4220 and *S. aureus* RN4220 Δ*secG* grown in TSB medium to an OD_{540} of 15 were separated on 2-D gels by using immobilized pH gradient strips with a linear pH range of 3 to 10. Proteins were stained with colloidal Coomassie brilliant blue. Protein spots present in equal amounts in both strains appear in yellow, protein spots present in larger amounts in the *secG* mutant appear in red, and protein spots present in larger amounts in the parental strain appear in green. Only proteins with a Sec-type signal peptide of which the extracellular amounts were reproducibly affected by the *secG* mutation have been marked. (B) False-colored dual-channel image of 2-D gels of extracellular proteins of *S. aureus* RN4220 (green) and *S. aureus* RN4220 Δ*secG* Δ*secY2* (red). For experimental details see the legend for panel A. Protein spots present in equal amounts in both strains appear in yellow, protein spots present in larger amounts in the *secG secY2* mutant appear in red, and protein spots present in larger amounts in the parental strain appear in green. (C) False-colored dual-channel image of 2-D gels of extracellular proteins of *S. aureus* RN4220 (green) and *S. aureus* RN4220 Δ*secG* *secG*-pCN51 (red). For experimental details see the legend for panel A. All protein spots are yellow, indicating that both strains secreted the respective proteins in equal amounts.

proteins of *S. aureus* increase mainly in the stationary growth phase at high cell densities (37, 56), extracellular proteins for 2-D PAGE analyses were collected from the supernatant of cell cultures that had reached stationary phase (Fig. 1 and 2). Comparison of the exoproteomes of the *secG* mutant and its parental strain revealed that 11 proteins with Sec-type signal peptides and type I signal peptidase cleavage sites (i.e., SAOUHSC_00094, SdrD, Sle1, Geh, Hlb, HlY, HlgB, HlgC,

Plc, SAOUHSC_02241, and SAOUHSC_02979) were present in significantly decreased amounts when SecG was absent from the cells. This was also true for the secreted moiety of the polytopic membrane protein YfnI, which is processed by signal peptidase I as was previously shown for the YfnI homologue of *B. subtilis* (1). In contrast, the amounts of three other exoproteins (i.e., IsaA, Spa, and SsaA) were considerably increased due to the *secG* deletion (Fig. 2A; Table 3). These effects of the
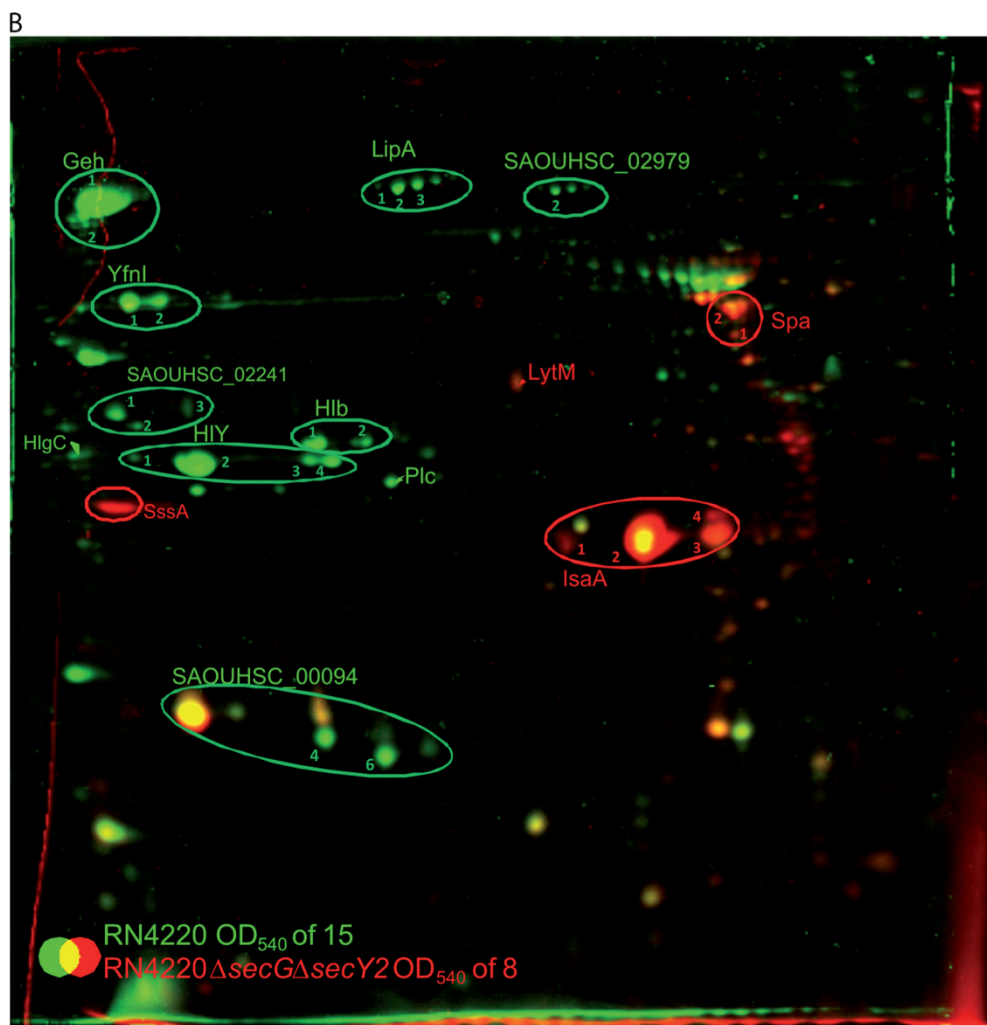
FIG. 2—*Continued.*

secG mutation were fully compensated when *secG* was ectopically expressed from plasmid *secG*-pCN51 (Fig. 2C). Northern blot analyses revealed similar transcript levels for *geh*, *hlb*, and *spa* in the *secG* mutant and the parental strain RN4220. This shows that the changes in the amounts of the respective exoproteins in the *secG* mutant were not caused by decreased transcription of the corresponding genes (Fig. 3).

Deletion of the *secY2* gene encoding a channel component of the accessory Sec system in *S. aureus* did not affect the extracellular protein pattern (data not shown). However, the deletion of both *secG* and *secY2* caused additional changes in the extracellular proteome compared to the *secG* single mutant (Fig. 2B). Specifically, one additional exoprotein was identified in decreased amounts (i.e., LipA), and one additional exoprotein (i.e., LytM) was identified in increased amounts (Table 3). Furthermore, proteins such as IsaA, Spa, and SsaA were secreted in larger amounts not only by the *secG* mutant but also by the *secG secY2* double mutant. This effect was significantly exacerbated for IsaA and SsaA in the *secG secY2* double mutant. It is interesting that IsaA, LytM, Spa, and SsaA represent cell surface-associated proteins (34, 37, 42). In contrast, most proteins that were secreted in reduced amounts in the *secG* or *secG secY2* mutant are secretory proteins without retention signals, except for SAOUHSC_00094 (Table 3). Importantly, the secretion and growth defects of the *secG secY2* mutant strain could also be fully reversed by ectopic expression of *secG* from plasmid *secG*-pCN51, and the synthetic effects of the *secG* and *secY2* mutations could be reversed by plasmid *secY2*-pCN51 (data not shown).

Elevated expression of *sraP* in *secG* mutant cells during the transition phase. To test whether the synthetic effects of the *secG secY2* double mutation might relate to jamming of the SecYE translocation channel by SraP, the only known substrate for the Sec2 pathway, we tried to construct an *secG secY2 sraP*
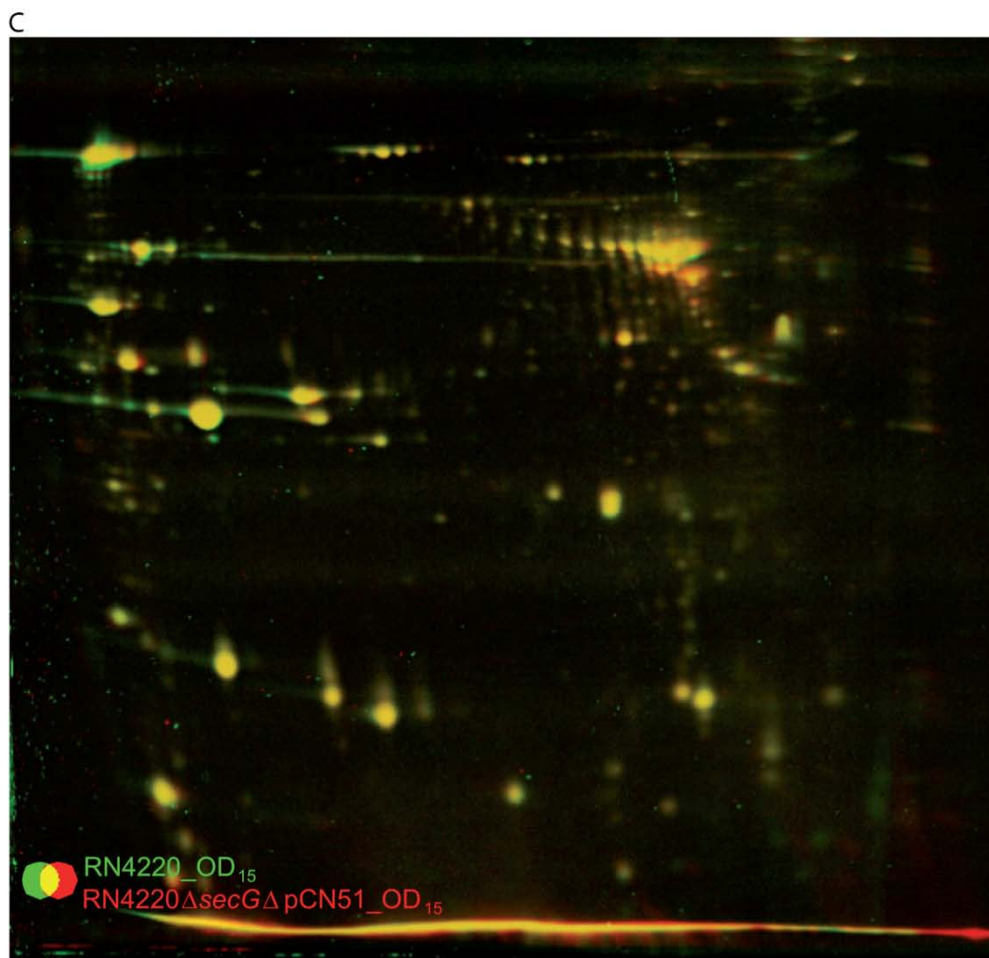
C

FIG. 2—*Continued.*

triple mutant. Unfortunately, despite several attempts, we did not manage to obtain this triple mutant for reasons that have so far remained obscure. To obtain further insights into the expression of *sraP* under the conditions tested, we performed Northern blotting and slot blot experiments with RNA extracted from the *secG* single mutant, the *secG secY2* double mutant, and the parental strain RN4220. These experiments revealed that *sraP* expression is highest in the transient phase between the exponential and stationary growth phases (Fig. 4). Furthermore, the deletion of *secG* reproducibly triggered a 2-fold elevation in the *sraP* transcript level during the transient phase. This moderate but reproducible effect was observed both in the *secG* single mutant and in the *secG secY2* double mutant, which argues to some extent against the possible jamming of SecYE by SraP, at least when SecY2 is still present in the cells.

Impaired export of cell wall-bound Sbi in *secG* mutant cells. Western blotting experiments were performed to investigate whether particular protein export defects of the *secG* and

secY2 mutants had remained unnoticed in the proteomic analyses. These analyses included secreted proteins in the growth medium (Sle1, Aly, IsaA, and SspB), noncovalently attached cell wall proteins (Sle1, Aly, and IsaA), a covalently attached cell wall protein (ClfA), a lipoprotein (DsbA), and a cytoplasmic marker protein (TrxA) in *S. aureus* strains RN4220 and *S. aureus* SH1000. For most tested proteins no differences were detectable between the *secG* and/or *secY2* mutant strains and their parental strain. However, these analyses showed that a band of ~50 kDa, which was cross-reactive with all tested sera, had disappeared from the fraction of noncovalently bound cell wall proteins of the *secG* mutant. It is known that proteins, such as protein A (36) and Sbi (55), have IgG-binding properties. To investigate whether the missing band would relate to protein A or Sbi, protein fractions from an *spa* mutant and an *spa sbi* double mutant were included in the Western blotting analyses. As shown in Fig. 5A, the band of ~50 kDa that was missing from the noncovalently bound cell wall proteins in the *secG* mutant was also missing from these proteins in the *spa sbi*

TABLE 3. Extracellular and cell wall proteins with altered secretion patterns in *S. aureus* Δ*secG* and Δ*secG* Δ*secY2* strains

Protein (spot no.)[a]	Function	M_r/pI coordinates[b]	*S. aureus* NCTC8325 ORF	NCBI accession no.	Predicted location[c]	Induction ratio of the indicated mutant to the parental strain[d]	
						Δ*secG*	Δ*secG* Δ*secY2*
IsaA (1)	Immunodominant antigen A	24.2/6.6	SAOUHSC_02887	88196515	Cell wall	2.0	4.2
IsaA (2)	Immunodominant antigen A	24.2/6.6	SAOUHSC_02887	88196515	Cell wall	2.4	8.6
IsaA (3)	Immunodominant antigen A	24.2/6.6	SAOUHSC_02887	88196515	Cell wall	2.9	4.8
IsaA (4)	Immunodominant antigen A	24.2/6.6	SAOUHSC_02887	88196515	Cell wall		12.4
LytM	Peptidoglycan hydrolase, putative	34.3/6.7	SAOUHSC_00248	88194055	Cell wall		4.3
SAOUHSC_00094 (1)	Hypothetical protein	21.8/9.4	SAOUHSC_00094	88193909	Cell wall	0.2	
SAOUHSC_00094 (2)	Hypothetical protein	21.8/9.4	SAOUHSC_00094	88193909	Cell wall	0.3	
SAOUHSC_00094 (3)	Hypothetical protein	21.8/9.4	SAOUHSC_00094	88193909	Cell wall	0.4	
SAOUHSC_00094 (4)	Hypothetical protein	21.8/9.4	SAOUHSC_00094	88193909	Cell wall	0.3	0.3
SAOUHSC_00094 (5)	Hypothetical protein	21.8/9.4	SAOUHSC_00094	88193909	Cell wall	0.5	
SAOUHSC_00094 (6)	Hypothetical protein	21.8/9.4	SAOUHSC_00094	88193909	Cell wall	0.2	0.3
SdrD (1)	SdrD protein, putative	14.6/3.9	SAOUHSC_00545	88194324	Cell wall	0.3	
Sle1/Aaa	Autolysin precursor, putative	35.8/9.9	SAOUHSC_00427	88194219	Cell wall	0.4	
Spa (1)	Protein A	55.6/5.4	SAOUHSC_00069	88193885	Cell wall	3.7	3.3
Spa (2)	Protein A	55.6/5.4	SAOUHSC_00069	88193885	Cell wall	5.0	2.9
SsaA	Secretory antigen precursor, putative	29.3/9.1	SAOUHSC_02571	88196215	Cell wall	5.0	9.9
Geh	Lipase precursor	76.4/9.6	SAOUHSC_00300	88194101	Extracellular	0.4	0.2
Hlb (1)	Truncated β-hemolysin	31.3/8.2	SAOUHSC_02240	88195913	Extracellular	0.1	0.2
Hlb (2)	Truncated β-hemolysin	31.3/8.2	SAOUHSC_02240	88195913	Extracellular	0.4	0.4
HlY (1)	α-Hemolysin precursor	35.9/9.1	SAOUHSC_01121	88194865	Extracellular	0.3	0.5
HlY (2)	α-Hemolysin precursor	35.9/9.1	SAOUHSC_01121	88194865	Extracellular	0.4	0.2
HlY (3)	α-Hemolysin precursor	35.9/9.1	SAOUHSC_01121	88194865	Extracellular		0.2
HlY (4)	α-Hemolysin precursor	35.9/9.1	SAOUHSC_01121	88194865	Extracellular	0.4	0.2
HlgB	Leukocidin F subunit precursor	36.7/9.8	SAOUHSC_02710	88196350	Extracellular	0.3	
HlgC	Leukocidin S subunit precursor, putative	35.7/9.7	SAOUHSC_02709	88196349	Extracellular	0.3	0.4
LipA (1)	Lipase	76.7/7.7	SAOUHSC_03006	88196625	Extracellular		0.5
LipA (2)	Lipase	76.7/7.7	SAOUHSC_03006	88196625	Extracellular		0.3
LipA (3)	Lipase	76.7/7.7	SAOUHSC_03006	88196625	Extracellular		0.4
Plc	1-Phosphatidylinositol phosphodiesterase precursor, putative	37.1/8.6	SAOUHSC_00051	88193871	Extracellular	0.3	0.3
SAOUHSC_02241 (1)	Hypothetical protein	38.7/9.1	SAOUHSC_02241	88195914	Extracellular	0.1	0.2
SAOUHSC_02241 (2)	Hypothetical protein	38.7/9.1	SAOUHSC_02241	88195914	Extracellular	0.3	0.4
SAOUHSC_02241 (3)	Hypothetical protein	38.7/9.1	SAOUHSC_02241	88195914	Extracellular	0.2	0.4
SAOUHSC_02979 (1)	Hypothetical protein	69.3/6.3	SAOUHSC_02979	88196599	Extracellular	0.4	
SAOUHSC_02979 (2)	Hypothetical protein	69.3/6.3	SAOUHSC_02979	88196599	Extracellular	0.3	0.3
SAOUHSC_02979 (3)	Hypothetical protein	69.3/6.3	SAOUHSC_02979	88196599	Extracellular	0.3	
SAOUHSC_02979 (4)	Hypothetical protein	69.3/6.3	SAOUHSC_02979	88196599	Extracellular	0.5	
YfnI (1)	Polytopic membrane protein, signal peptidase I substrate	74.4/9.5	SAOUHSC_00728	88194493	Extracellular	0.4	0.2
YfnI (2)	Polytopic membrane protein, signal peptidase I substrate	74.4/9.5	SAOUHSC_00728	88194493	Extracellular	0.4	0.2

[a] Several proteins are detectable as multiple spots. The spot numbers as marked in Fig. 2 are indicated in parentheses.

[b] Mature form.

[c] Protein localization was predicted as described in Sibbald et al. (38); SceD, SsaA, and IsaA were shown to be bound ionically to the cell wall by Stapleton et al. (42); Sle1 (Aaa) has three LysM domains that can bind to peptidoglycan (7).

[d] The induction ratio of mutant to parental strain was calculated for each spot (normalized intensity of a spot on the mutant image/normalized intensity of the corresponding spot on the parental image). The significance of spot volume differences of 2-fold or higher was assessed by the Student's t test ($\alpha < 0.05$; Delta 2D statistics table).

double mutant but not from those in the *spa* single mutant (only the results for *S. aureus* SH1000 are shown, but essentially the same results were obtained for *S. aureus* RN4220). Taken together, these findings show that Sbi is noncovalently bound to the cell wall of *S. aureus* strains RN4220 and SH1000 and that SecG is required for export of Sbi from the cytoplasm to the cell wall. As was the case for the secreted *S. aureus* proteins detected by proteomics, Sbi export to the cell wall was not affected by the absence of SecY2 (Fig. 5B). Finally, it is noteworthy that Sbi is detectable only among the noncovalently bound cell wall proteins of *S. aureus* strains RN4220 and SH1000, whereas it is detectable both in a cell wall-bound and a secreted state in *S. aureus* Newman.

Deletion of *secG* and *secY2* does not affect virulence in a mouse model. To test whether the deletion of *secG* and/or

secY2 would affect the virulence of *S. aureus* SH1000, a mouse infection model was used. The results revealed no significant differences in virulence of the Δ*secG*, Δ*secY2*, or Δ*secG* Δ*secY2* strains compared to the parental strain SH1000 (Fig. 6). This shows that SecG and SecY2 have no important roles in the virulence of strain SH1000 in the context of the mouse infection model used.

DISCUSSION

The extracellular and surface-associated proteins of bacterial pathogens, such as *S. aureus*, represent an important reservoir of virulence factors (38, 39, 57). Accordingly, protein export mechanisms will contribute to the virulence of these organisms. While protein export has been well characterized in
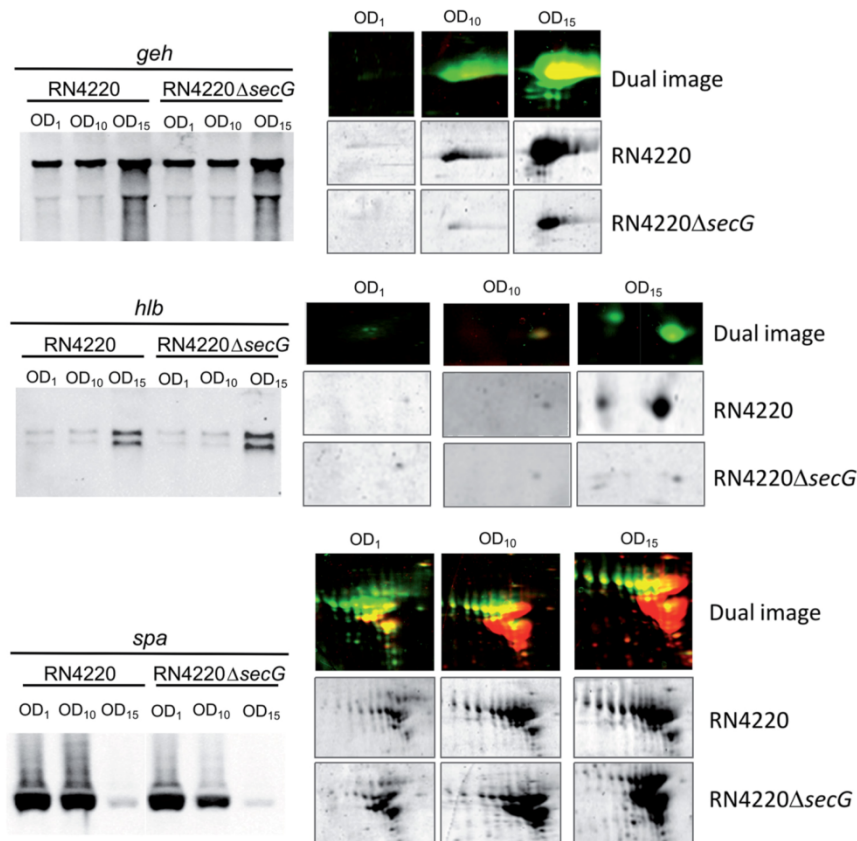
FIG. 3. Expression of SecG-dependent exoproteins. RNA and exoproteins were collected from *S. aureus* RN4220 and *S. aureus* RN4220 Δ*secG* grown in TSB medium at 37°C. Samples were collected at three different points during growth (OD$_{540}$s of 1, 10, and 15). In the Northern blotting experiments, membranes were hybridized with digoxigenin-labeled RNA probes specific for *geh*, *hlb*, or *spa*. Protein spots from 2-D PAGE analyses of the respective proteins collected at OD$_{540}$s of 1, 10, and 15 are shown for the *secG* mutant and its parental strain both separately and as dual-channel images.

model organisms, such as *E. coli* and *B. subtilis*, relatively few functional studies have addressed the protein export pathways of *S. aureus*. Notably, the Sec pathway is generally regarded as the main pathway for protein export, but, to date, this has not been verified experimentally in *S. aureus*. Therefore, the present studies were aimed at assessing the role of the Sec pathway in establishing the extracellular proteome of *S. aureus*. We focused attention on the nonessential channel component SecG as this allowed a facile coassessment of the nonessential accessory Sec channel component SecY2. Our results show that the extracellular accumulation of proteins is affected to different extents by the absence of SecG: some proteins are present in reduced amounts, some are not affected, and some are present in elevated amounts. Furthermore, the effects of the absence of SecG are exacerbated by deletion of SecY2, suggesting that SecY2 directly or indirectly influences the functionality of the general Sec pathway. This is all the more remarkable since the absence of SecY2 by itself had no detectable effects on the composition of the extracellular proteome of *S. aureus*.

The observation that the secretion of a wide range of pro-

teins was affected by the absence of SecG is consistent with the fact that all of these proteins contain Sec-type signal peptides. On the other hand, this finding is remarkable since studies of other organisms, such as *E. coli* (26) and *B. subtilis* (48), have shown that deletion of *secG* had fairly moderate effects on protein secretion *in vivo*. In *B. subtilis*, a phenotype of the *secG* mutation was observed only under conditions of high overproduction of secretory proteins (48). Clearly, our present data show that SecG is more important for Sec-dependent protein secretion in *S. aureus* than in *B. subtilis* or *E. coli*. Importantly, the transcription of genes for three proteins (Geh, Hlb, and Spa) that were affected in major ways by the absence of SecG was not changed, and all observed effects of the *secG* mutation could be reversed by ectopic expression of *secG*. This suggests that the observed changes in the exoproteome composition of the *S. aureus secG* mutant strain relate to changes in the translocation efficiency of proteins through the Sec channel rather than to regulatory responses at the gene expression level. This could be due to altered recognition of the respective signal peptides or mature proteins by the SecG-less Sec channel or combinations thereof. However, some indirect effects, for ex-
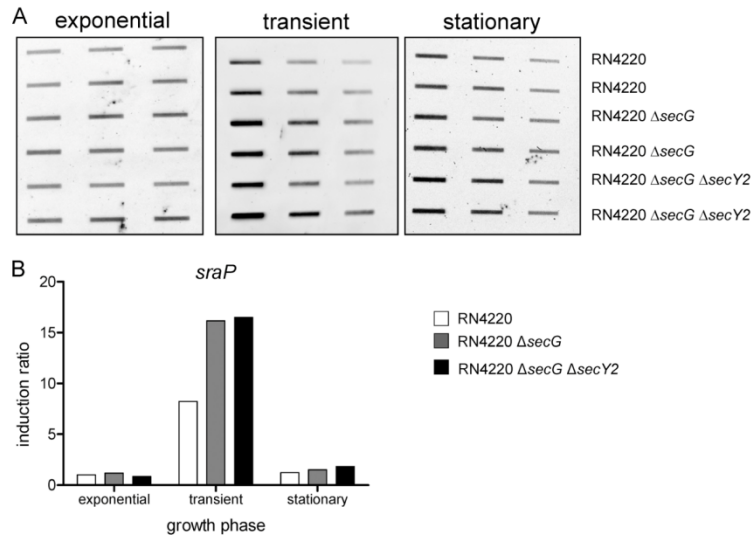
FIG. 4. Transcriptional analysis of *sraP*. RNA was prepared from *S. aureus* RN4220, *S. aureus* RN4220 Δ*secG*, and *S. aureus* RN4220 Δ*secG* Δ*secY2* cells grown in TSB medium (37°C) at three different stages of growth: exponential phase (OD$_{540}$ of 1), transient phase (RN4220 and Δ*secG* at an OD$_{540}$ of 10; Δ*secG* Δ*secY2* at an OD$_{540}$ of 6), and stationary phase (RN4220 and Δ*secG* at an OD$_{540}$ of 15; Δ*secG* Δ*secY2* at an OD$_{540}$ of 8). (A) Serial dilutions of total RNA of the wild-type and the mutant strains were blotted and cross-linked onto positively charged nylon membranes. The membrane-bound RNA was hybridized with a digoxigenin-labeled RNA probe complementary to *sraP*. (B) Quantification of changes in the *sraP* mRNA levels during growth of *S. aureus* RN4220 and its Δ*secG* or Δ*secG* Δ*secY2* mutant derivatives. Induction ratios relate to *sraP* mRNA levels in exponentially growing cells of the RN4220 parental strain as described in Materials and Methods.

ample, at the level of translation of exported proteins, post-translocational folding, proteolysis, or cell wall binding of proteins like IsaA, LytM, Spa, and SsaA, can currently not be excluded, especially since no proteins were found to accumulate inside the *secG* mutant cells (data not shown). It remains to be shown why the extracellular accumulation of particular proteins is affected by the absence of SecG while that of other proteins remains unaffected.

Unexpectedly, our studies revealed that export of the IgG-binding protein Sbi to the cell wall was almost completely blocked in *secG* mutant strains. The reason that this export defect was not detected by 2-D PAGE relates to the fact that Sbi is predominantly cell wall bound in the tested *S. aureus* strains under the experimental conditions used. It has been proposed previously that Sbi would remain cell wall attached through a proline-rich wall-binding domain and electrostatic
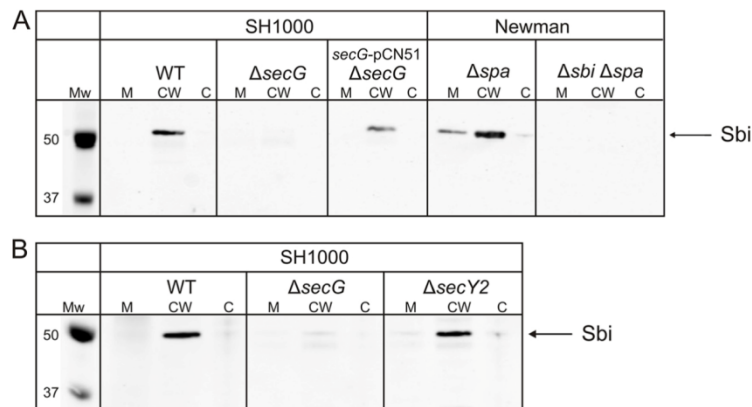

FIG. 5. Sbi localization to the cell wall of *S. aureus* depends on SecG. (A) *S. aureus* SH1000 (wild type [WT]), *S. aureus* SH1000 Δ*secG*, and *S. aureus* SH1000 Δ*secG* secG-pCN51 were grown in TSB medium at 37°C to early stationary phase. Samples of extracellular proteins isolated from the growth medium (M), noncovalently cell wall-bound proteins (CW), and total cells (C) were used for Western blotting and immunodetection with serum of mice immunized with IsaA. As a control for Sbi production, the *S. aureus* Newman Δ*spa* and *S. aureus* Newman Δ*spa* Δ*sbi* strains were included in the analyses. (B) Proteins of *S. aureus* SH1000 (WT), *S. aureus* SH1000 Δ*secG*, and *S. aureus* SH1000 Δ*secY2* were used for Western blotting and immunodetection as described for panel A. The position of Sbi is marked with an arrow.
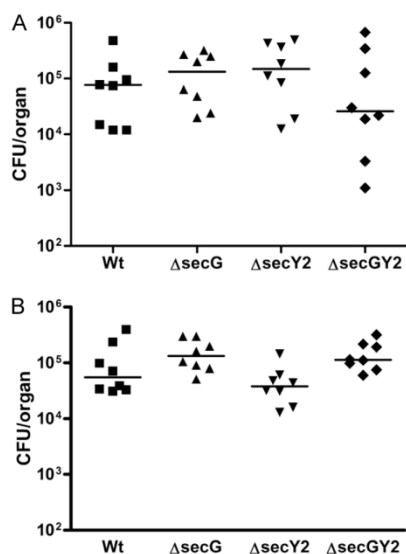
FIG. 6. Mouse infection studies with *S. aureus secG* and *secG secY2* mutants. Eight mice were challenged with 1×10^8 CFU of *S. aureus* SH1000 Δ*secG*, *S. aureus* SH1000 Δ*secY2*, *S. aureus* SH1000 Δ*secG* Δ*secY2*, or the parental SH1000 (Wt) Strain. After 3 days, the bacterial loads of the kidneys (A) and livers (B) were determined as described in Materials and Methods.

interactions (55). Nevertheless, Burman and colleagues showed that Sbi is extracellular, and they suggested that cell surface-bound Sbi might be disadvantageous for the bacterium due to its role in modulating the complement system (8). On the other hand, cell surface localization of Sbi would be appropriate for interference with the adaptive immune system through IgG binding (3). Irrespective of these previously reported findings, our Western blotting analyses show that Sbi is noncovalently bound to the cell wall, not only in *S. aureus* SH1000 and *S. aureus* RN4220 but also in *S. aureus* Newman. However, consistent with the findings of Burman et al., Sbi was also detected in the growth medium of *S. aureus* Newman, which indicates that the location of Sbi in the cell wall or extracellular milieu may differ for different *S. aureus* strains. In case of the Newman strain, the release of Sbi into the growth medium could be due to the fact that this strain produces Sbi and several other cell wall-bound proteins at increased levels compared to the RN4220 and SH1000 strains (35). Conceivably, this increased production of wall-bound proteins might lead to a saturation of available cell wall binding sites for Sbi.

Remarkably, the absence of SecG was shown to impact the relative amounts of various extracellular proteins while effects of the absence of SecG were detected for only one cell wall-associated protein, namely, Sbi. We do not believe that these differences in the numbers of identified proteins relate to the method that was used to monitor effects of the absence of SecG. Specifically, the analysis of proteins secreted by *secG* mutant strains via regular one-dimensional (1-D) SDS-PAGE already revealed major differences in the composition of the exoproteome (data not shown). It was for this reason that we initiated our 2-D PAGE analyses to identify the affected pro-

teins. On the other hand, a 1-D SDS-PAGE analysis of cell wall-associated proteins did not reveal any major differences, and this was in fact the reason why we investigated potentially wall-associated proteins by Western blotting. Furthermore, we have no evidence from the different studies that we performed that the time point at which the sampling was done during the stationary phase had any major influence on the outcomes of our analyses.

Many of the proteins for which the absence of SecG affects extracellular amounts are considered to be important virulence factors of *S. aureus*. These proteins are involved in host colonization (e.g., the serine-aspartic acid repeat proteins SdrC and SdrD), invasion of host tissues (e.g., hemolysins and leukocidins), cell wall turnover (LytM), and evasion of the immune system (Spa and Sbi). The altered amounts of these proteins suggest that *S. aureus* strains depleted of SecG might perhaps be less virulent. However, in the mouse infection model used, no changes in virulence of the *S. aureus* SH1000 *secG*, *secY2*, or *secG secY2* mutant strains could be detected. This implies that the presence or absence of SecG or SecY2 is not critical for the virulence of *S. aureus* SH1000, at least under the conditions tested in the mouse infection model used. Clearly, this does not rule out the possibility that such mutants are attenuated in virulence in other infection models that have not yet been tested.

Since we were unable to detect secretion defects for *secY2* single mutant strains, our studies confirm that only very few proteins are translocated across the membrane in an SecA2/SecY2-dependent manner, as has previously been suggested by Siboo et al. (40). Furthermore, we did not detect differences in the export of glycosylated proteins by the *secY2* mutants (data not shown), which is in line with the suggestion that glycosylated proteins are not strictly dependent on the accessory Sec pathway for export (40). It was therefore quite surprising that the *secY2* mutation exacerbated the secretion defect of the *S. aureus secG* mutant. In fact, the secretion of two additional proteins was found to be affected in the *secG secY2* double mutant. Moreover, a synthetic growth defect was observed for this double mutant. At this stage, it is possible that both the growth defect and the secretion defects are consequences of an impaired Sec channel function. In addition, the exacerbated secretion defects may relate to SecYE jamming by SraP, which is the only known SecA2/SecY2 substrate. As shown by Northern blotting analyses, the deletion of *secG* somehow triggers a 2-fold elevation in *sraP* transcript level during the transition between exponential and postexponential growth in not only the *secG* single mutant but also the *secG secY2* double mutant. This argues to some extent against the jamming of SecYE by SraP, at least when SecY2 is still present in the cells. In the absence of SecG and SecY2, indeed, jamming of SecYE by the overexpressed SraP may occur in the transient phase. On the other hand, *sraP* expression seems relatively low in the stationary phase during which we harvested the extracellular proteins for proteomics analyses, which would suggest that any jamming effects of SraP are relatively slight in this growth phase. Unfortunately, we have so far not been able to assess the possibility of SecYE jamming by SraP directly because we were unable to obtain an *secG secY2 sraP* triple mutant. Notably, it is also possible that the exacerbated secretion defects are, to some extent, a secondary consequence of the growth

defect of the double mutant. Irrespective of their primary cause, these synthetic effects of the *secG* and *secY2* mutations suggest that the regular Sec channel can somehow interact with the Sec2 channel. Whether this means that mixed Sec channels with both SecY and SecY2 exist remains to be determined. However, this possibility would be consistent with the observation that *S. aureus* lacks a second set of *secE* and *secG* genes. It would thus be important to focus future research activities in this area on possible interactions between the regular Sec channel components and SecY2.

REFERENCES

1. **Antelmann, H., H. Tjalsma, B. Voigt, S. Ohlmeier, S. Bron, J. M. van Dijl, and M. Hecker.** 2001. A proteomic view on genome-based signal peptide predictions. Genome Res. **11:**1484–1502.
2. **Arnaud, M., A. Chastanet, and M. Debarbouille.** 2004. New vector for efficient allelic replacement in naturally nontransformable, low-GC-content, gram-positive bacteria. Appl. Environ. Microbiol. **70:**6887–6891.
3. **Atkins, K. L., J. D. Burman, E. S. Chamberlain, J. E. Cooper, B. Poutrel, S. Bagby, A. T. Jenkins, E. J. Feil, and J. M. van den Elsen.** 2008. *S. aureus* IgG-binding proteins SpA and Sbi: host specificity and mechanisms of immune complex formation. Mol. Immunol. **45:**1600–1611.
4. **Bensing, B. A., and P. M. Sullam.** 2002. An accessory *sec* locus of *Streptococcus gordonii* is required for export of the surface protein GspB and for normal levels of binding to human platelets. Mol. Microbiol. **44:**1081–1094.
5. **Bernhardt, J., K. Büttner, C. Scharf, and M. Hecker.** 1999. Dual channel imaging of two-dimensional electropherograms in *Bacillus subtilis*. Electrophoresis **20:**2225–2240.
6. **Brundage, L., J. P. Hendrick, E. Schiebel, A. J. Driessen, and W. Wickner.** 1990. The purified *E. coli* integral membrane protein SecY/E is sufficient for reconstitution of SecA-dependent precursor protein translocation. Cell **62:**649–657.
7. **Buist, G., A. Steen, J. Kok, and O. P. Kuipers.** 2008. LysM, a widely distributed protein motif for binding to (peptido)glycans. Mol. Microbiol. **68:**838–847.
8. **Burman, J. D., E. Leung, K. L. Atkins, M. N. O'Seaghdha, L. Lango, P. Bernado, S. Bagby, D. I. Svergun, T. J. Foster, D. E. Isenman, and J. M. van den Elsen.** 2008. Interaction of human complement with Sbi, a staphylococcal immunoglobulin-binding protein: indications of a novel mechanism of complement evasion by *Staphylococcus aureus*. J. Biol. Chem. **283:**17579–17593.
9. **Cabelli, R. J., L. Chen, P. C. Tai, and D. B. Oliver.** 1988. SecA protein is required for secretory protein translocation into *E. coli* membrane vesicles. Cell **55:**683–692.
10. **Candiano, G., M. Bruschi, L. Musante, L. Santucci, G. M. Ghiggeri, B. Carnemolla, P. Orecchia, L. Zardi, and P. G. Righetti.** 2004. Blue silver: a very sensitive colloidal Coomassie G-250 staining for proteome analysis. Electrophoresis **25:**1327–1333.
11. **Charpentier, E., A. I. Anton, P. Barry, B. Alfonso, Y. Fang, and R. P. Novick.** 2004. Novel cassette-based shuttle vector system for gram-positive bacteria. Appl. Environ. Microbiol. **70:**6076–6085.
12. **Driessen, A. J., and N. Nouwen.** 2008. Protein translocation across the bacterial cytoplasmic membrane. Annu. Rev. Biochem. **77:**643–667.
13. **Eymann, C., A. Dreisbach, D. Albrecht, J. Bernhardt, D. Becher, S. Gentner, T. Tam le, K. Büttner, G. Buurman, C. Scharf, S. Venz, U. Völker, and M. Hecker.** 2004. A comprehensive proteome map of growing *Bacillus subtilis* cells. Proteomics **4:**2849–2876.
14. **Gertz, S., S. Engelmann, R. Schmid, K. Ohlsen, J. Hacker, and M. Hecker.** 1999. Regulation of σ^B-dependent transcription of *sigB* and *asp23* in two different *Staphylococcus aureus* strains. Mol. Gen. Genet. **261:**558–566.
15. **Guérout-Fleury, A. M., K. Shazand, N. Frandsen, and P. Stragier.** 1995. Antibiotic-resistance cassettes for *Bacillus subtilis*. Gene **167:**335–336.
16. **Gutierrez, J. A., P. J. Crowley, D. G. Cvitkovitch, L. J. Brady, I. R. Hamilton, J. D. Hillman, and A. S. Bleiweis.** 1999. *Streptococcus mutans ffh*, a gene encoding a homologue of the 54 kDa subunit of the signal recognition particle, is involved in resistance to acid stress. Microbiology **145:**357–366.
17. **Hanada, M., K. Nishiyama, and H. Tokuda.** 1996. SecG plays a critical role in protein translocation in the absence of the proton motive force as well as at low temperature. FEBS Lett. **381:**25–28.
18. **Hanahan, D.** 1983. Studies on transformation of *Escherichia coli* with plasmids. J. Mol. Biol. **166:**557–580.
19. **Hasona, A., P. J. Crowley, C. M. Levesque, R. W. Mair, D. G. Cvitkovitch, A. S. Bleiweis, and L. J. Brady.** 2005. Streptococcal viability and diminished stress tolerance in mutants lacking the signal recognition particle pathway or YidC2. Proc. Natl. Acad. Sci. U. S. A. **102:**17466–17471.
20. **Hiramatsu, K., H. Hanaki, T. Ino, K. Yabuta, T. Oguri, and F. C. Tenover.** 1997. Methicillin-resistant *Staphylococcus aureus* clinical strain with reduced vancomycin susceptibility. J. Antimicrob. Chemother. **40:**135–136.
21. **Horsburgh, M. J., J. L. Aish, I. J. White, L. Shaw, J. K. Lithgow, and S. J. Foster.** 2002. σ^B modulates virulence determinant expression and stress resistance: characterization of a functional *rsbU* strain derived from *Staphylococcus aureus* 8325-4. J. Bacteriol. **184:**5457–5467.
22. **Kobayashi, K., S. D. Ehrlich, A. Albertini, G. Amati, K. K. Andersen, M. Arnaud, K. Asai, S. Ashikaga, S. Aymerich, P. Bessieres, F. Boland, S. C. Brignell, S. Bron, K. Bunai, J. Chapuis, L. C. Christiansen, A. Danchin, M. Debarbouille, E. Dervyn, E. Deuerling, K. Devine, S. K. Devine, O. Dreesen, J. Errington, S. Fillinger, S. J. Foster, Y. Fujita, A. Galizzi, R. Gardan, C. Eschevins, T. Fukushima, K. Haga, C. R. Harwood, M. Hecker, D. Hosoya, M. F. Hullo, H. Kakeshita, D. Karamata, Y. Kasahara, F. Kawamura, K. Koga, P. Koski, R. Kuwana, D. Imamura, M. Ishimaru, S. Ishikawa, I. Ishio, C. D. Le, A. Masson, C. Mauel, R. Meima, R. P. Mellado, A. Moir, S. Moriya, E. Nagakawa, H. Nanamiya, S. Nakai, P. Nygaard, M. Ogura, T. Ohanan, M. O'Reilly, M. O'Rourke, Z. Pragai, H. M. Pooley, G. Rapoport, J. P. Rawlins, L. A. Rivas, C. Rivolta, A. Sadaie, Y. Sadaie, M. Sarvas, T. Sato, H. H. Saxild, E. Scanlan, W. Schumann, J. F. Seegers, J. Sekiguchi, A. Sekowska, S. J. Seror, M. Simon, P. Stragier, R. Studer, H. Takamatsu, T. Tanaka, M. Takeuchi, H. B. Thomaides, V. Vagner, J. M. van Dijl, K. Watabe, A. Wipat, H. Yamamoto, M. Yamamoto, Y. Yamamoto, K. Yamane, K. Yata, K. Yoshida, H. Yoshikawa, U. Zuber, and N. Ogasawara.** 2003. Essential *Bacillus subtilis* genes. Proc. Natl. Acad. Sci. U. S. A. **100:**4678–4683.
23. **Kouwen, T. R., E. N. Trip, E. L. Denham, M. J. Sibbald, J. Y. Dubois, and J. M. van Dijl.** 2009. The large mechanosensitive channel MscL determines bacterial susceptibility to the bacteriocin sublancin 168. Antimicrob. Agents Chemother. **53:**4702–4711.
24. **Kreiswirth, B. N., S. Löfdahl, M. J. Betley, M. O'Reilly, P. M. Schlievert, M. S. Bergdoll, and R. P. Novick.** 1983. The toxic shock syndrome exotoxin structural gene is not detectably transmitted by a prophage. Nature **305:**709–712.
25. **Nagamori, S., K. Nishiyama, and H. Tokuda.** 2000. Two SecG molecules present in a single protein translocation machinery are functional even after crosslinking. J. Biochem. **128:**129–137.
26. **Nishiyama, K., S. Mizushima, and H. Tokuda.** 1993. A novel membrane protein involved in protein translocation across the cytoplasmic membrane of *Escherichia coli*. EMBO J. **12:**3409–3415.
27. **Nishiyama, K., T. Suzuki, and H. Tokuda.** 1996. Inversion of the membrane topology of SecG coupled with SecA-dependent preprotein translocation. Cell **85:**71–81.
28. **Norrander, J., T. Kempe, and J. Messing.** 1983. Construction of improved M13 vectors using oligodeoxynucleotide-directed mutagenesis. Gene **26:**101–106.
29. **Novick, R. P.** 1991. Genetic systems in staphylococci. Methods Enzymol. **204:**587–636.
30. **Papanikou, E., S. Karamanou, and A. Economou.** 2007. Bacterial protein secretion through the translocase nanomachine. Nat. Rev. Microbiol. **5:**839–851.
31. **Patel, A. H., P. Nowlan, E. D. Weavers, and T. Foster.** 1987. Virulence of protein A-deficient and α-toxin-deficient mutants of *Staphylococcus aureus* isolated by allele replacement. Infect. Immun. **55:**3103–3110.
32. **Peacock, S. J., I. de Silva, and F. D. Lowy.** 2001. What determines nasal carriage of *Staphylococcus aureus*? Trends Microbiol. **9:**605–610.
33. **Pohlschröder, M., W. A. Prinz, E. Hartmann, and J. Beckwith.** 1997. Protein translocation in the three domains of life: variations on a theme. Cell **91:**563–566.
34. **Ramadurai, L., K. J. Lockwood, M. J. Nadakavukaren, and R. K. Jayaswal.** 1999. Characterization of a chromosomally encoded glycylglycine endopeptidase of *Staphylococcus aureus*. Microbiology **145:**801–808.
35. **Rogasch, K., V. Rühmling, J. Pané-Farré, D. Höper, C. Weinberg, S. Fuchs, M. Schmudde, B. M. Bröker, C. Wolz, M. Hecker, and S. Engelmann.** 2006. Influence of the two-component system SaeRS on global gene expression in two different *Staphylococcus aureus* strains. J. Bacteriol. **188:**7742–7758.
36. **Sasso, E. H., G. J. Silverman, and M. Mannik.** 1991. Human IgA and IgG F(ab′)2 that bind to staphylococcal protein A belong to the VHIII subgroup. J. Immunol. **147:**1877–1883.

37. **Schneewind, O., P. Model, and V. A. Fischetti.** 1992. Sorting of protein A to the staphylococcal cell wall. Cell **70:**267–281.

38. **Sibbald, M. J., A. K. Ziebandt, S. Engelmann, M. Hecker, A. de Jong, H. J. Harmsen, G. C. Raangs, I. Stokroos, J. P. Arends, J. Y. Dubois, and J. M. van Dijl.** 2006. Mapping the pathways to staphylococcal pathogenesis by comparative secretomics. Microbiol. Mol. Biol. Rev. **70:**755–788.

39. **Sibbald, M. J. J. B., and J. M. van Dijl.** 2009. Secretome mapping in Gram-positive pathogens, p. 193–224. *In* K. Wooldridge (ed.), Bacterial secreted proteins: secretory mechanisms and role in pathogenesis. Horizon Scientific Press, Norwich, United Kingdom.

40. **Siboo, I. R., D. O. Chaffin, C. E. Rubens, and P. M. Sullam.** 2008. Characterization of the accessory Sec system of *Staphylococcus aureus*. J. Bacteriol. **190:**6188–6196.

41. **Siboo, I. R., H. F. Chambers, and P. M. Sullam.** 2005. Role of SraP, a serine-rich surface protein of *Staphylococcus aureus*, in binding to human platelets. Infect. Immun. **73:**2273–2280.

42. **Stapleton, M. R., M. J. Horsburgh, E. J. Hayhurst, L. Wright, I. M. Jonsson, A. Tarkowski, J. F. Kokai-Kun, J. J. Mond, and S. J. Foster.** 2007. Characterization of IsaA and SceD, two putative lytic transglycosylases of *Staphylococcus aureus*. J. Bacteriol. **189:**7316–7325.

43. **Sugai, R., K. Takemae, H. Tokuda, and K. Nishiyama.** 2007. Topology inversion of SecG is essential for cytosolic SecA-dependent stimulation of protein translocation. J. Biol. Chem. **282:**29540–29548.

44. **Takamatsu, D., B. A. Bensing, and P. M. Sullam.** 2005. Two additional components of the accessory *sec* system mediating export of the *Streptococcus gordonii* platelet-binding protein GspB. J. Bacteriol. **187:**3878–3883.

45. **Tjalsma, H., A. Bolhuis, J. D. Jongbloed, S. Bron, and J. M. van Dijl.** 2000. Signal peptide-dependent protein transport in *Bacillus subtilis*: a genome-based survey of the secretome. Microbiol. Mol. Biol. Rev. **64:**515–547.

46. **van der Sluis, E. O., E. van der Vries, G. Berrelkamp, N. Nouwen, and A. J. Driessen.** 2006. Topologically fixed SecG is fully functional. J. Bacteriol. **188:**1188–1190.

47. **van Roosmalen, M. L., N. Geukens, J. D. Jongbloed, H. Tjalsma, J. Y. Dubois, S. Bron, J. M. van Dijl, and J. Anne.** 2004. Type I signal peptidases of Gram-positive bacteria. Biochim. Biophys. Acta **1694:**279–297.

48. **van Wely, K. H., J. Swaving, C. P. Broekhuizen, M. Rose, W. J. Quax, and A. J. Driessen.** 1999. Functional identification of the product of the *Bacillus subtilis yvaL* gene as a SecG homologue. J. Bacteriol. **181:**1786–1792.

49. **Weigel, L. M., D. B. Clewell, S. R. Gill, N. C. Clark, L. K. McDougal, S. E. Flannagan, J. F. Kolonay, J. Shetty, G. E. Killgore, and F. C. Tenover.** 2003. Genetic analysis of a high-level vancomycin-resistant isolate of *Staphylococcus aureus*. Science **302:**1569–1571.

50. **Wetzstein, M., U. Völker, J. Dedio, S. Löbau, U. Zuber, M. Schiesswohl, C. Herget, M. Hecker, and W. Schumann.** 1992. Cloning, sequencing, and molecular analysis of the *dnaK* locus from *Bacillus subtilis*. J. Bacteriol. **174:**3300–3310.

51. **Wolff, S., H. Antelmann, D. Albrecht, D. Becher, J. Bernhardt, S. Bron, K. Büttner, J. M. van Dijl, C. Eymann, A. Otto, l. T. Tam, and M. Hecker.** 2007. Towards the entire proteome of the model bacterium *Bacillus subtilis* by gel-based and gel-free approaches. J. Chromatogr. B Analyt. Technol. Biomed. Life Sci. **849:**129–140.

52. **Yuan, J., J. C. Zweers, J. M. van Dijl, and R. E. Dalbey.** 2010. Protein transport across and into cell membranes in bacteria and archaea. Cell Mol. Life Sci. **67:**179–199.

53. **Zanen, G., H. Antelmann, R. Meima, J. D. Jongbloed, M. Kolkman, M. Hecker, J. M. van Dijl, and W. J. Quax.** 2006. Proteomic dissection of potential signal recognition particle dependence in protein secretion by *Bacillus subtilis*. Proteomics **6:**3636–3648.

54. **Zanen, G., E. N. Houben, R. Meima, H. Tjalsma, J. D. Jongbloed, H. Westers, B. Oudega, J. Luirink, J. M. van Dijl, and W. J. Quax.** 2005. Signal peptide hydrophobicity is critical for early stages in protein export by *Bacillus subtilis*. FEBS J. **272:**4617–4630.

55. **Zhang, L., K. Jacobsson, J. Vasi, M. Lindberg, and L. Frykberg.** 1998. A second IgG-binding protein in *Staphylococcus aureus*. Microbiology **144:**985–991.

56. **Ziebandt, A. K., D. Becher, K. Ohlsen, J. Hacker, M. Hecker, and S. Engelmann.** 2004. The influence of *agr* and σ^B in growth phase dependent regulation of virulence factors in *Staphylococcus aureus*. Proteomics **4:**3034–3047.

57. **Ziebandt, A. K., H. Kusch, M. Degner, S. Jaglitz, M. J. Sibbald, J. P. Arends, M. A. Chlebowicz, D. Albrecht, R. Pantucek, J. Doskar, W. Ziebuhr, B. M. Bröker, M. Hecker, J. M. van Dijl, and S. Engelmann.** 2010. Proteomics uncovers extreme heterogeneity in the *Staphylococcus aureus* exoproteome due to genomic plasticity and variant gene regulation. Proteomics **10:**1634–1644.

58. **Zimmer, J., Y. Nam, and T. A. Rapoport.** 2008. Structure of a complex of the ATPase SecA and the protein-translocation channel. Nature **455:**936–943.

5.2. Thiol-disulphide oxidoreductase modules in the low-GC Gram-positive bacteria

Kouwen, T. R., van der Goot, A., Dorenbos, R., Winter, T., Antelmann, H.,

Plaisier, M. C., Quax, W. J., van Dijl, J. M., Dubois, J. Y. (2007)

Molecular Microbiology, 64(4):984-99

Own contribution to manuscript

Cultivation, proteins preparation, SDS PAGE, as well as contributed to the writing of the manuscript.

Thiol-disulphide oxidoreductase modules in the low-GC Gram-positive bacteria

Thijs R. H. M. Kouwen,[1] Annemieke van der Goot,[1]
Ronald Dorenbos,[2†] Theresa Winter,[3]
Haike Antelmann,[3] Marie-Claire Plaisier,[1]
Wim J. Quax,[2] January Maarten van Dijl[1]* and
Jean-Yves F. Dubois[1]

[1]*Department of Medical Microbiology, University Medical
Center Groningen and University of Groningen,
Hanzeplein 1, PO Box 30001, 9700 RB Groningen, the
Netherlands.*
[2]*Department of Pharmaceutical Biology, University of
Groningen, A. Deusinglaan 1, 9713 AV Groningen, the
Netherlands.*
[3]*Institut für Mikrobiologie und Molekularbiologie,
Ernst-Moritz-Arndt-Universität Greifswald, D-17487
Greifswald, Germany.*

Summary

**Disulphide bond formation catalysed by thiol-
disulphide oxidoreductases (TDORs) is a universally
conserved mechanism for stabilizing extracytoplas-
mic proteins. In *Escherichia coli*, disulphide bond
formation requires a concerted action of distinct
TDORs in thiol oxidation and subsequent quinone
reduction. TDOR function in other bacteria has
remained largely unexplored. Here we focus on
TDORs of low-GC Gram-positive bacteria, in particu-
lar DsbA of *Staphylococcus aureus* and BdbA-D of
Bacillus subtilis. Phylogenetic analyses reveal that
the homologues DsbA and BdbD cluster in distinct
groups typical for *Staphylococcus* and *Bacillus*
species respectively. To compare the function of
these TDORs, DsbA was produced in various *bdb*
mutants of *B. subtilis*. Next, we assessed the ability
of DsbA to sustain different TDOR-dependent pro-
cesses, including heterologous secretion of *E. coli*
PhoA, competence development and bacteriocin
(sublancin 168) production. The results show that
DsbA can function in all three processes. While
BdbD needs a quinone oxidoreductase for activity,
DsbA activity appears to depend on redox-active
medium components. Unexpectedly, both quinone
oxidoreductases of *B. subtilis* are sufficient to
sustain production of sublancin. Moreover, DsbA
can functionally replace these quinone oxidoreduc-
tases in sublancin production. Taken together, our
unprecedented findings imply that TDOR systems of
low-GC Gram-positive bacteria have a modular
composition.**

Introduction

A disulphide bond is a sulphur-sulphur chemical bond that
results from an oxidative process that links two non-
adjacent cysteines of a protein. In all three domains of life,
disulphide bonds play major roles in the correct folding of
many different proteins, maintaining their structural integ-
rity and regulating their activity (Ritz and Beckwith, 2001;
Collet and Bardwell, 2002). Proteins containing disulphide
bonds are found predominantly in extracytoplasmic cell
compartments, such as the eukaryotic endoplasmic
reticulum, the membranes and periplasm of Gram-
negative bacteria, or the membrane/cell wall interface and
extracellular milieu of Gram-positive bacteria (Aslund and
Beckwith, 1999). These proteins are only biologically
active and/or stable when their cysteines are joined in
disulphide bonds.

The formation of disulphide bonds can occur spontane-
ously under oxidizing conditions, but this process is very
slow and non-specific (Anfinsen, 1973). For this reason
enzymes have evolved that catalyse the formation
(oxidation) or breakage (reduction) of disulphide bonds
in vivo. These enzymes are called thiol-disulphide oxi-
doreductases (TDORs). Cytoplasmic TDORs are gener-
ally reductases, while their extracytoplasmic equivalents
are oxidases or isomerases that catalyse a reorganization
of disulphide bonds (Tan and Bardwell, 2004; Dorenbos
et al., 2005). Among the best known bacterial extracyto-
plasmic TDORs are the Dsb proteins of the Gram-
negative bacterium *Escherichia coli* (Kadokura *et al.*,
2003; Nakamoto and Bardwell, 2004). These proteins are
characterized by a CxxC motif (two cysteine residues
separated by two amino acids), which forms the core of
the active site (Newton *et al.*, 1996). The catalytic mecha-
nism involves a disulphide exchange process in which the
disulphide bond is transferred from the enzyme to the
substrate protein (or *vice versa*) via a short-lived interme-
diate (Kadokura *et al.*, 2004).

Table 1. Different biological functions of the Bdb proteins of *B. subtilis*.

Process	BdbA	BdbB	BdbC	BdbD
E. coli PhoA secretion	None	Minor	Major	Major
Competence development	None	None	Major	Major
Sublancin production	None	Major	Minor	None

Compared with Gram-negative bacteria, such as *E. coli*, relatively little information is currently available about extracytoplasmic TDORs in Gram-positive bacteria, which lack a classical periplasmic space and have a thick cell wall instead of an outer membrane. The current knowledge on TDORs from Gram-positive bacteria comes mainly from studies with *Bacillus subtilis*, which is a paradigm of Gram-positive bacterial research (Bolhuis *et al.*, 1999; Dorenbos *et al.*, 2002; Erlendsson and Hederstedt, 2002; Meima *et al.*, 2002; Erlendsson *et al.*, 2003; 2004). In *B. subtilis*, four extracytoplasmic TDORs with presumed thiol oxidase activity have been described, which are known as BdbA, BdbB, BdbC and BdbD. Biological functions have been identified for BdbB, BdbC and BdbD, but not for BdbA (Table 1). Notably, the *bdbA* and *bdbB* genes are located within the SPβ prophage region, and are therefore only present in the sequenced *B. subtilis* strain 168. BdbB is of major importance for folding of the secreted SPβ-encoded antibiotic sublancin 168, which contains two disulphide bonds (Dorenbos *et al.*, 2002; Stein, 2005). The integral membrane protein BdbB shares a high degree of sequence similarity with BdbC (Bolhuis *et al.*, 1999). Nevertheless, their substrate specificities overlap only in part (Table 1). For example, BdbC contributes in a minor way to the folding of sublancin 168 (Dorenbos *et al.*, 2002). On the contrary, BdbC is of major importance for the biogenesis of the pseudopilin ComGC, while BdbB is dispensable for this process (Meima *et al.*, 2002). ComGC is an important element of the DNA-uptake machinery of *B. subtilis* and, consistent with its TDOR requirement for folding into a protease-resistant conformation, it contains an essential intramolecular disulphide bond (Chung *et al.*, 1998). In addition to BdbC, the biogenesis of ComGC requires activity of the membrane protein BdbD (Meima *et al.*, 2002). Therefore, both BdbC and BdbD have major roles in the development of natural competence in *B. subtilis*. Interestingly, BdbC and BdbD are also required for folding of a secreted heterologous protein by *B. subtilis*, namely the alkaline phosphatase PhoA of *E. coli* (Bolhuis *et al.*, 1999; Meima *et al.*, 2002; Darmon *et al.*, 2006) (Table 1). Most likely, this TDOR requirement relates to the fact that *E. coli* PhoA contains two disulphide bonds that are indispensable both for the enzymatic activity and stability of this protein (Sone *et al.*, 1997).

As judged by their importance for the folding of exported proteins with disulphide bonds, it appears that

BdbC and BdbD are members of an oxidation pathway in *B. subtilis* (Sarvas *et al.*, 2004). It has been proposed that BdbD functions as an electron acceptor for secreted cysteine-containing proteins, thereby facilitating the formation of the disulphide bond. Subsequently, the reduced BdbD would be re-oxidized by the action of BdbC, thereby recycling BdbD for another round of catalysis. BdbC would then donate its electrons to quinones in the electron transport chain. BdbD and BdbC are thus believed to cooperate as a redox pair. This view is supported by the fact that BdbC shares a high degree of similarity with the TDOR-quinone oxidoreductase DsbB of *E. coli*, whereas BdbD shares some very limited similarity with DsbA of *Haemophilus, Neisseria* and *Pseudomonas* species (Bolhuis *et al.*, 1999; Meima *et al.*, 2002). Both DsbA and DsbB of *E. coli* act pair-wise as oxidases in periplasmic disulphide bond formation (Rietsch and Beckwith, 1998; Regeimbal and Bardwell, 2002; Inaba *et al.*, 2006).

A well-known subclass of Gram-positive bacteria is formed by the so-called low-GC Gram-positive bacteria or Firmicutes, which include important pathogens such as *Staphylococcus aureus, Bacillus anthracis* and *Listeria monocytogenes*. Notably, also biotechnologically relevant bacteria, such as *B. subtilis*, belong to the low-GC Gram-positive bacteria. In relation to the TDORs of low-GC Gram-positives, it was previously reported that BdbD of *B. subtilis* shares a high degree of sequence similarity (55% identical residues and conservative replacements) with DsbA of *S. aureus* (Meima *et al.*, 2002). Interestingly however, a homologue of BdbC was not found in this organism (Dumoulin *et al.*, 2005). In fact, BdbC homologues appear to be absent from all sequenced *Staphylococcus* and *Listeria* species (Table 2). Conversely, certain *Bacillus, Geobacillus* and *Oceanobacillus* species do contain a BdbC homologue, but lack a BdbD homologue. These observations suggest that BdbC- and BdbD-like TDORs of different groups of low-GC Gram-positive bacteria are modules that can act either in concert, or independently from each other. This novel concept of modular TDOR function was investigated in the present studies. To this end, we employed single and multiple *bdb* mutant *B. subtilis* strains for a complementation analysis with DsbA of *S. aureus*. Specifically, we asked whether DsbA of *S. aureus* can replace different Bdb proteins for folding of secreted *E. coli* PhoA, competence development and ComGC biogenesis, and production of sublancin 168. The results show that DsbA of *S. aureus* can perform these functions of the BdbB, BdbC and BdbD proteins in a growth medium-dependent way, without the apparent need of a Bdb partner protein. Moreover, no BdbD-like protein was required for sublancin 168 production in *B. subtilis*. These findings demonstrate that BdbC- and BdbD-like TDORs can act both in concert and independently. This implies that TDOR systems for disul-

Table 2. BdbC and BdbD homologues in low-GC Gram-positive bacteria.

Organism	BdbC-homologue[a]	BdbD-homologue[a]	Accession numbers
Bacillus subtilis ssp. subtilis str. 168	BdbC/BdbB	BdbD[b]	NP_391227
			BG13587
			NP_391228
Bacillus licheniformis ATCC 14580	BdbC	BdbD	YP_080629
			YP_080630
Bacillus thuringiensis serovar konkukian str. 97–27	DsbB	BdbD	YP_035017
			YP_034804
Bacillus thuringiensis serovar israelensis ATCC 35646	DsbB	DsbA	ZP_00743025
			ZP_00741255
Bacillus anthracis str. 'Ames Ancestor'	DsbB	DsbA	NP_843282
			YP_017166
Bacillus anthracis str. A2012	DsbB	DsbA	ZP_00393849
			ZP_00390922
Bacillus anthracis str. Sterne	DsbB	DsbA	YP_026998
			YP_026791
Bacillus weihenstephanensis KBAB4	DsbB	DsbA	ZP_01185626
			ZP_01184592
Bacillus cereus ssp. cytotoxis NVH 391–98	DsbB	DsbA	ZP_01179254
			ZP_01181835
Bacillus cereus ATCC 14579	DsbB	DsbA	NP_830569
			NP_830362
Bacillus cereus ATCC 10987	DsbB	DsbA	NP_977147
			NP_976925
Bacillus cereus G9241	DsbB	DsbA	ZP_00235738
			ZP_00237820
Bacillus cereus E33L	BdbC	BdbD	YP_082265
			YP_082059
Bacillus halodurans C-125	DsbB	–	NP_242807
Geobacillus kaustophilus HTA426	DsbB	–	YP_146421
Bacillus sp. NRRL B-14911	DsbB	–	ZP_01170582
Bacillus clausii KSM-K16	DsbB	–	YP_177437
Oceanobacillus iheyensis HTE831	DsbB	–	NP_692084
Exiguobacterium sibiricum 255–15	DsbB	–	ZP_00540257
Staphylococcus aureus NCTC 8325	–	DsbA	YP_501156
Staphylococcus aureus RF122	–	DsbA	YP_417746
Staphylococcus saprophyticus ATCC 15305	–	DsbA	YP_300579
Staphylococcus aureus ssp. aureus MRSA252	–	YvgV	YP_041849
Staphylococcus haemolyticus JCSC1435	–	DsbG	YP_252559
Staphylococcus epidermidis ATCC 12228	–	DsbA	NP_765542
Staphylococcus epidermidis RP62A	–	DsbA	YP_189555
Listeria innocua Clip11262	–	DsbA	NP_470388
Listeria monocytogenes str. 1/2a F6854	–	DsbG	ZP_00233748
Listeria monocytogenes str. 4b F2365	–	DsbG	YP_013680
Lactobacillus sakei ssp. sakei 23K	–	DsbG	YP_395142
Enterococcus faecalis V583	–	DsbA	NP_814517

Homologues of *B. subtilis* BdbC or BdbD were identified by BLAST searches using all publicly available sequences of the low-GC Gram-positive bacteria. All identified protein sequences contain the typical CxxC motif for thiol-disulphide oxidoreductases.
a. Note that most of these names have not been attributed to the corresponding proteins on the basis of their phylogeny, but on the basis of very limited sequence similarity to known *E. coli* Dsb proteins.
b. BdbA of *B. subtilis* is not listed here, because its sequence similarity with the listed BdbD-like proteins is too limited for detection by BLAST searches. Homologues of BdbA can be found in *B. brevis* and *B. cereus*. The name BdbA is used in *B. subtilis* for historic reasons, but its potential TDOR activity has not been demonstrated experimentally.

phide bond formation in low-GC Gram-positive bacteria have a modular composition.

Results

Evolutionary conservation of TDORs in Low-GC Gram-positive bacteria

BLAST searches with BdbC or BdbD from *B. subtilis* 168 against the annotated genomes of low-GC Gram-positive bacteria revealed that all the sequenced *Staphylococcus* and *Listeria* species, as well as *Lactobacillus sakei* and *Enterococcus faecalis*, contain only a BdbD homologue, but lack a BdbC homologue (Table 2). In contrast, most sequenced *Bacillus* species contain both a homologue of BdbC and BdbD. In *B. subtilis* and *Bacillus licheniformis* the corresponding genes are organized in a *bdbDC* operon-like structure; in all other bacilli these genes are located at distinct genomic positions. Six sequenced
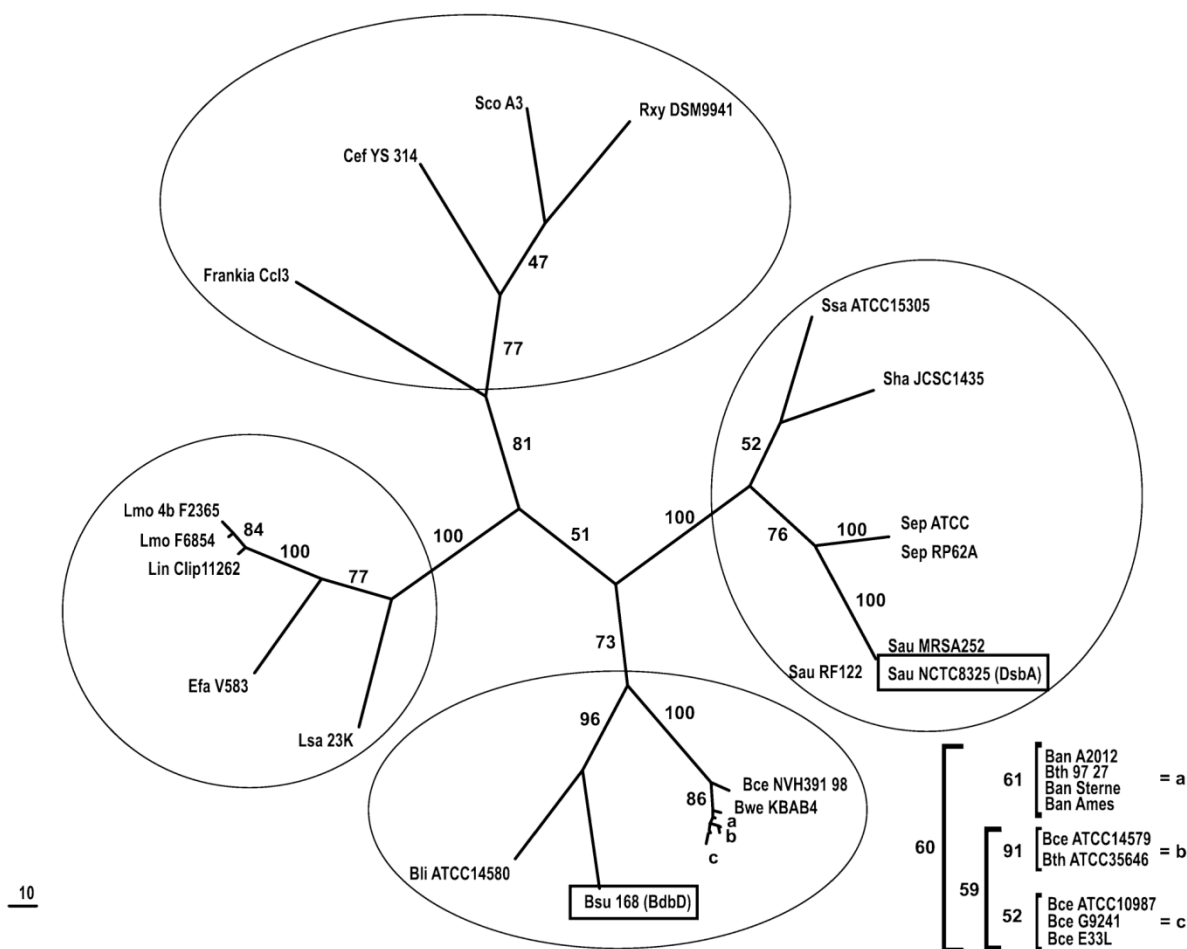
Fig. 1. Most parsimonious 50% majority rule tree of BdbD homologues from low-GC Gram-positive bacteria. Schematic representation of the evolutionary conservation of BdbD homologues in low-GC Gram-positive bacteria. Names of species used in this figure are abbreviations of the full names given in Table 2 (Ban, *B. anthracis*, Bce, *Bacillus cereus*, Bli, *B. licheniformis*, Bsu, *B. subtilis*, Bth, *B. thuringiensis*, Bwe, *B. weihenstephanensis*, Efa, *E. faecalis*, Lmo, *L. monocytogenes*, Lin, *L. inocua*, Lsa, *L. sakei*, Sau, *S. aureus*, Sep, *S. epidermidis*, Sha, *S. haemolyticus*, Ssa, *S. saprophyticus*). The calculated maximum parsimony values are shown at the nodes. Sequence accession numbers of the BdbD homologues used are depicted in Table 2. The tree is unrooted, although four BdbD homologues of high-GC Gram-positive bacteria were included to represent an outgroup. These outgroup species are *Frankia* sp. Ccl3; *Rubrobacter xylanophilus* (Rxy) DSM 9941; *Streptomyces coelicolor* (Sco) A3(2); and *Corynebacterium efficiens* (Cef) YS-314. The clusters of BdbD homologues from the *Bacillus*, *Staphylococcus* and *Listeria* species and the outgroup are encircled. BdbD of *B. subtilis* 168 and DsbA of *S. aureus* NCTC8325 are boxed. The tree branch for highly related BdbD homologues of *B. anthracis*, *B. cereus* and *B. thuringiensis* species is enlarged (marked a, b, c).

low-GC Gram-positive bacteria contain only a homologue of BdbC, but lack a homologue of BdbD. Remarkably, all other sequenced low-GC Gram-positive bacteria lack homologues of the known *B. subtilis* Bdb proteins (or *E. coli* Dsb proteins).

To obtain insight into the evolutionary relationships between the BdbD homologues of low-GC Gram-positive bacteria, we performed a most parsimonious tree analysis on the corresponding sequences. The maximum parsimony analysis resulted in three most parsimonious trees (973 steps long, CI excluding uninformative

characters = 0.7657, RI = 0.8265, RC = 0.6328). After testing these with bootstrap, one most parsimonious 50% majority rule tree was obtained as shown in Fig. 1. This tree clearly reveals distinct evolutionary groups that relate to different clusters of *Bacillus*, *Staphylococcus* and *Listeria* species. Notably, the 'listerial cluster' also includes *E. faecalis* and *L. sakei*. The clustering of BdbD homologues into three groups of low-GC Gram-positive bacteria is underscored by the results of topology predictions with the prediction programs SignalP, LipoP and TMHMM (data not shown). All the BdbD homologues of bacilli are

***amyE::XTC*dsbA**
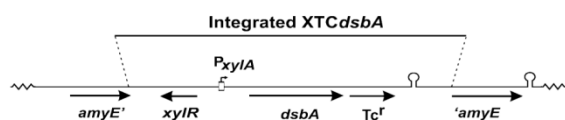
Fig. 2. Construction of the XdsbA strain. Schematic representation of the chromosomal region of strains containing the XTC*dsbA* cassette, integrated in the *amyE* gene via a double crossover recombination event. This cassette encodes the mature *dsbA* gene from *S. aureus* fused to the ribosomal binding site and signal sequence of *mntA* from *B. subtilis*. The hybrid *dsbA* gene is transcribed from a xylose-inducible promoter (P_{xylA}). *xylR*, gene specifying the XylR repressor protein; *amyE'*, 3′ truncated *amyE* gene; '*amyE*, 5′-truncated *amyE* gene; Tc^R, tetracycline resistance marker.

predicted membrane proteins, whereas the staphylococcal homologues are predicted lipoproteins. These predictions are fully consistent with the observations that BdbD of *B. subtilis* is a membrane protein (Tjalsma and van Dijl, 2005) and that DsbA of *S. aureus* is a lipoprotein (Dumoulin *et al.*, 2005). Remarkably, the BdbD homologues in the listerial cluster are predicted cytoplasmic proteins, suggesting that these proteins have evolved to biological functions that are completely different from those of the extracytoplasmic BdbD homologues of bacilli and staphylococci. For this reason, we excluded the BdbD homologues of the listerial cluster from further studies. Most importantly, the phylogenetic analyses imply that the closely related BdbD homologues of *Bacillus* species act in concert with cognate BdbC homologues, while the staphylococcal BdbD homologues seem to act independently of BdbC partner proteins.

Expression of S. aureus dsbA *in* B. subtilis

To test the hypothesis that staphylococcal DsbA can act independently of a BdbC homologue, we followed a heterologous approach for *dsbA* expression in *B. subtilis* BdbC-proficient or deficient host strains. For this purpose, we used the currently best characterized staphylococcal DsbA protein, DsbA from *S. aureus* NCTC 8325, hereafter referred to as DsbA.

To express DsbA in *B. subtilis*, the pXTC system was used, which allows xylose inducible expression from a chromosomally integrated cassette (Fig. 2). Unfortunately, the authentic *S. aureus* DsbA protein was not detectably produced in *B. subtilis*, despite efficient transcription from the *xylA* promoter (data not shown). Therefore, we fused the sequence encoding the mature DsbA lipoprotein to the ribosomal binding site and signal sequence of the *B. subtilis mntA* gene, which codes for an abundantly expressed lipoprotein of this organism (Antelmann *et al.*, 2001). Upon integration of the XTC*dsbA* cassette containing this hybrid *dsbA* gene into the *B. subtilis*

168 chromosome, xylose-inducible expression of cell-associated DsbA was obtained. Importantly, efficient xylose-inducible DsbA expression could be detected in all *B. subtilis bdb* mutant strains containing the XTC*dsbA* cassette (Fig. 3A; in what follows, strains containing this cassette are referred to as XdsbA). As expected, the cellular levels of DsbA depended on the amount of xylose added to the growth medium (Fig. 3B, upper left panel). Notably, overexposure of these membranes revealed that low amounts of DsbA were already produced by the uninduced XdsbA strain (Fig. 3B, upper right panel). This can be attributed to the fact that the *xylA* promoter is slightly leaky in the absence of added xylose (Tjalsma *et al.*, 1998). The largest levels of cellular DsbA were observed when the XdsbA cells were induced with 0.6% xylose or more (not shown). To estimate the amounts of expressed DsbA protein, ~3 μg of purified DsbA-His6 protein was loaded on the gels. This resulted in a signal that was comparable to the DsbA signal obtained for samples of cells grown in the presence of 0.2% xylose (Fig. 3B, upper left panel), indicating that these cells produced ~75 mg DsbA per litre.

To determine under which conditions the DsbA production levels are comparable with the BdbD levels in *B. subtilis*, semiquantitative Western blotting experiments were performed. For this purpose, we made use of the fact that our anti-BdbD serum cross-reacts with the his-tag in DsbA-His6. Accordingly, the pure DsbA-His6 could be used as a standard to compare the relative amounts of DsbA and BdbD. As shown in Fig. 3B (upper left panel), the amount of DsbA produced by XdsbA cells grown in Luria–Bertani (LB) medium with 0.2% xylose, is comparable to the amount of BdbD in these cells. Similarly, we investigated the production of DsbA by cells grown in S7 minimal medium with cysteine (Fig. 3C), or without cysteine (Fig. 3D). The results showed that higher amounts of xylose were needed to induce DsbA production by cells grown in the S7 minimal media. Specifically, comparable levels of DsbA and BdbD were produced when XdsbA cells were grown in the presence of 2% xylose. This effect can be attributed to the high amount of glucose present in S7 media, which is known to repress the xylose promoter.

DsbA production in B. subtilis *promotes folding of secreted* E. coli *PhoA*

Escherichia coli PhoA is a sensitive reporter for extracytoplasmic TDOR activity in *B. subtilis*, because this protein with two disulphide bonds requires these enzymes for folding into a protease-resistant conformation (Bolhuis *et al.*, 1999; Meima *et al.*, 2002). Especially in the absence of BdbC and/or BdbD, the unfolded PhoA is readily degraded in the highly proteolytic environments of
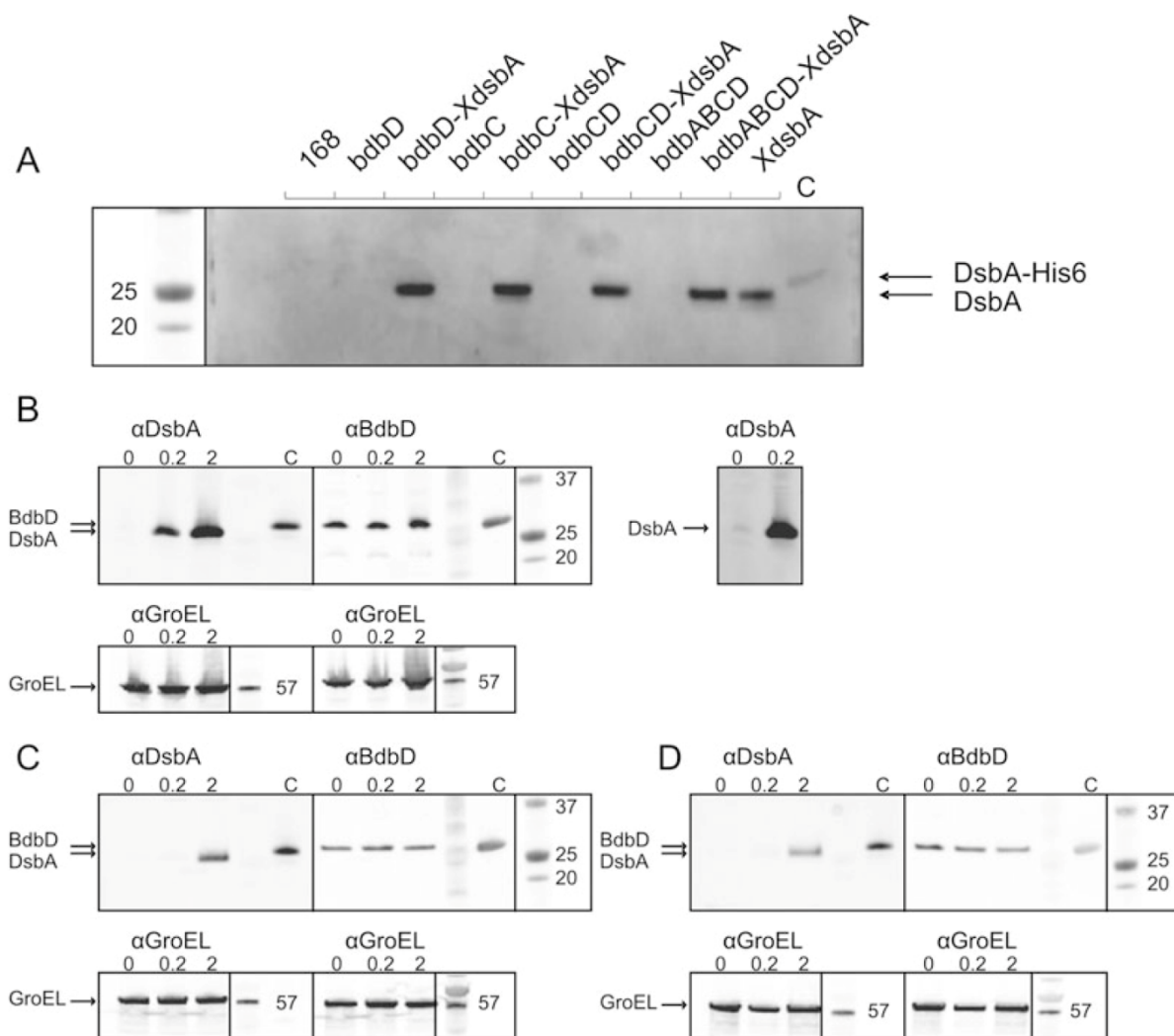
Fig. 3. Expression of *S. aureus dsbA* in *B. subtilis*.
A. The presence of DsbA in cells of the *B. subtilis* strains 168, bdbD, bdbD-XdsbA, bdbC, bdbC-XdsbA, bdbCD, bdbCD-XdsbA, bdbABCD, bdbABCD-XdsbA and XdsbA was investigated by SDS-PAGE and Western blotting with specific antibodies against DsbA. The different strains were grown overnight in the presence of 2% xylose in LB medium.
B. *B. subtilis* strain XdsbA was used to investigate the cellular levels of DsbA and BdbD by SDS-PAGE and Western blotting with specific antibodies against DsbA and BdbD. Cells were grown in LB medium without xylose (0), or with 0.2% (0.2) or 2% (2) xylose for induced DsbA production. Protein samples were loaded in duplicate on a gel, separated by elecrophoresis and electro-transferred to a membrane. For immunodetection, the membrane was cut in two halves, one of which was decorated with DsbA-specific antibodies and the other with BdbD-specific antibodies (upper left panel). Subsequently, the presence of GroEL on both membranes was monitored with specific antibodies against GroEL as a control for sample loading (lower panel). For visualization of low amounts of DsbA in uninduced cells of *B. subtilis* XdsbA, the upper right panel shows an overexposed image of the 0 and 0.2% xylose lanes of the membrane decorated with DsbA-specific antibodies.
C. Same as (B), except that *B. subtilis* XdsbA was grown in S7 minimal medium containing cysteine.
D. Same as (B), except that *B. subtilis* XdsbA was grown in S7 minimal medium without cysteine.
As a control, ~3 μg purified his-tagged DsbA was loaded onto each gel 'C'. Due to the presence of the His6-tag, the purified pre-DsbA has a lower mobility (~24 kDa) on SDS-PAGE than the corresponding mature DsbA form (~23 kDa) present in cells of *B. subtilis* (note that BdbD runs at ~25 kDa). Molecular weight markers are indicated. Each lane of the gels was loaded with an amount of protein that corresponds to 40 μl of cultured cells with an OD_{600} of 3.0.

the *B. subtilis* cell wall and growth medium (Sarvas *et al.*, 2004). This basically provides an *in vivo* protease protection assay for probing the folding efficiency of secreted PhoA. Accordingly, we investigated the possible effect of

DsbA on the extracellular accumulation of active PhoA. To this purpose, the *B. subtilis* XdsbA strain containing the integrated XTC*dsbA* cassette and the parental strain 168 were transformed with plasmid pPSPhoA5, which
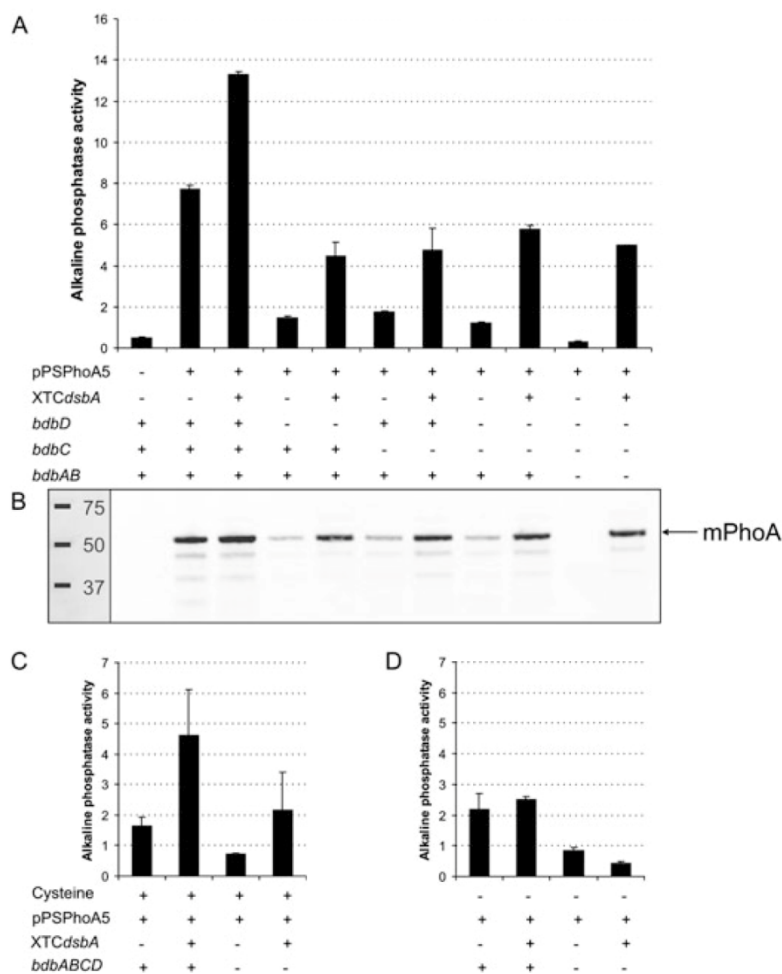
Fig. 4. Production of *E. coli* PhoA by *B. subtilis bdb* mutants also producing DsbA. A. The *B. subtilis* XdsbA, bdbD, bdbD-XdsbA, bdbC, bdbC-XdsbA, bdbCD, bdbCD-XdsbA, bdbABCD, bdbABCD-XdsbA strains, and the parental strain 168, were transformed with pPSPhoA5 for *E. coli* PhoA production. All strains were grown overnight in LB medium containing 0.2% xylose. Next, growth medium samples were withdrawn for alkaline phosphatase activity assays (A) as well as SDS-PAGE and Western blotting with PhoA specific antibodies (B). The presence or absence of pPSPhoA5, the XTC*dsbA* cassette, *bdbD*, *bdbC* or *bdbAB* is indicated for both panels. PhoA activity is given in U/ml/OD$_{600}$. The Arrow in panel B indicates the position of mature PhoA (mPhoA). Bands with a higher mobility on SDS-PAGE are breakdown products of PhoA. Molecular weight markers are indicated. C. The *B. subtilis* XdsbA, bdbABCD, bdbABCD-XdsbA strains, and the parental strain 168, were transformed with pPSPhoA5 for *E. coli* PhoA production. All strains were grown overnight in S7 medium with 2% xylose and cysteine. Next, growth medium samples were withdrawn for alkaline phosphatase activity assays. The presence or absence of cysteine, pPSPhoA5, the XTC*dsbA* cassette, or *bdbABCD* is indicated. PhoA activity is given in U/ml/OD$_{600}$. D. Same as for panel C, except that the medium was cysteine-free.

encodes secreted *E. coli* PhoA. Co-production of DsbA with PhoA resulted in significantly increased levels of PhoA activity in the LB growth medium of *B. subtilis* XdsbA, as compared with the parental strain (Fig. 4A). Maximum PhoA activity was observed when the XdsbA cells were induced with 0.2% xylose (data not shown). In fact, the very low amounts of DsbA, as produced by the uninduced XdsbA strain, were already sufficient to result in an increased extracellular accumulation of active PhoA. As demonstrated by proteomics analyses on LB growth medium fractions of *B. subtilis* XdsbA grown in the presence or absence of xylose and the parental strain 168, neither the presence of xylose in the growth medium, nor the production of DsbA caused any detectable changes in the composition of the extracellular proteome (data not shown). Taken together, these findings suggest that the DsbA produced in *B. subtilis* is active and able to promote specifically the folding of PhoA into a protease-resistant and active conformation.

DsbA can replace all the B. subtilis *Bbd proteins for secretion of active* E. coli *PhoA*

To functionally compare the DsbA system of *S. aureus* with the BdbABCD system of *B. subtilis*, we produced DsbA from the XTC*dsbA* cassette in various *bdb* mutant *B. subtilis* strains grown in LB medium with 0.2% xylose, and used PhoA (encoded by pPSPhoA5) as a reporter for extracytoplasmic TDOR activity. As shown above, addition of 0.2% xylose to LB medium resulted in the production of DsbA by *B. subtilis* XdsbA strains in amounts that were comparable with the amounts of BdbD. Therefore, we used this concentration of xylose in all experiments in which PhoA-producing cells were grown in LB. As shown in Fig. 4A, PhoA activity was restored to significant levels by the production of DsbA in strains lacking BdbC and/or BdbD. Even a strain lacking all four Bdb proteins produced active PhoA at similar levels as the strains lacking BdbC or BdbD upon DsbA production. However, the

Table 3. Transformability of various *bdb* mutant and DsbA-complementation strains.

strain	Relevant genotype	Transformability			
		Viable count (x 10⁶)	Cmᴿ colonies	Frequency	% of 168
168	Parental strain	38.0	180.3	4.7E-04	100.0
XdsbA	*amyE*::XTC*dsbA*	52.3	386.0	7.4E-04	155.4
bdbD	*bdbD*::pMutin2*mcs*	51.0	9.7	1.9E-05	4.0
bdbD-XdsbA	*bdbD*::pMutin2*mcs*; *amyE*::XTC*dsbA*	58.0	47.7	8.2E-05	17.3
bdbC	*bdbC*::*Km*ᴿ	50.3	135.7	2.7E-04	56.8
bdbC-XdsbA	*bdbC*::*Km*ᴿ; *amyE*::XTC*dsbA*	64.0	201.7	3.2E-04	66.4
bdbCD	*bdbCD*::*Sp*ᴿ	54.3	6.0	1.1E-05	2.3
bdbCD-XdsbA	*bdbCD*::*Sp*ᴿ; *amyE*::XTC*dsbA*	65.0	113.3	1.7E-04	36.7

Cells were grown in the presence of 2% xylose. Transformability was expressed as the percentage of chloramphenicol resistant transformants of the total viable count.

levels of extracellular PhoA activity of the complemented strains remained lower than that of the parental strain 168. Importantly, the levels of PhoA activity in the different growth medium samples correlated well with the levels of PhoA protein detected in the respective samples, as shown by Western blotting (Fig. 4B). These observations show that DsbA can replace all four Bdb proteins of *B. subtilis* for folding of *E. coli* PhoA into an active and protease resistant conformation. Moreover, DsbA does not need the presence of a BdbC-like protein for this activity in PhoA folding. This implies that DsbA was reoxidized in a BdbC-independent manner.

In order to investigate whether cystine, the readily air-oxidized form of cysteine present in cysteine-rich media, could play a role in the reoxidation of DsbA, PhoA activity measurements were performed with *B. subtilis* strains harbouring plasmid pPSPhoA5 grown on S7 minimal medium with or without cysteine. Both S7 media were supplemented with 2% xylose, because addition of this amount of xylose to S7 medium resulted in the production of DsbA by *B. subtilis* XdsbA strains in amounts that were comparable with the amounts of BdbD. As shown in Fig. 4C, expression of DsbA in *B. subtilis* grown on S7 medium containing cysteine resulted in higher PhoA activities compared with the parental strain 168, as was observed for cells grown in LB. In addition, DsbA was also able to replace at least partly all the Bdb proteins in PhoA folding. However, when cells were grown in S7 medium lacking cysteine (Fig. 4D), a contribution of DsbA to PhoA folding was no longer detectable because DsbA expression did not result in elevated PhoA activities in the growth medium. Together, these observations suggest that DsbA is most likely reoxidized by redox-active growth medium components, such as cystine, instead of a quinone oxidoreductase as is the case for BdbD.

DsbA complements bdbC/bdbD mutants for competence

The pseudopilin ComGC, which is an important element of the DNA uptake machinery of *B. subtilis*, was previously shown to require both BdbC and BdbD for folding and biological activity (Meima *et al.*, 2002). In contrast to *E. coli* PhoA secretion, the development of competence for DNA binding and uptake is a natural property of *B. subtilis* that can be used to study the extent to which DsbA can compensate for the absence of BdbC and/or BdbD. Therefore, we assessed competence development in the various *bdbC* and/or *bdbD* mutant strains, with or without expression of DsbA. Table 3 summarizes the results. Under the conditions tested, the deletion of both *bdbC* and *bdbD* impaired competence development almost completely, and the disruption of only *bdbD* had a major negative impact on this process. Mutation of *bdbC* also had a negative effect on competence development, but not as severely as previously reported (Meima *et al.*, 2002). Most likely, this is due to the specific competence regime used in this study. Interestingly, the expression of DsbA in these strains resulted in a significant increase in their transformability. This was most clearly evident in the strain lacking BdbC and BdbD.

Because the assayed competence development data are only an indirect indication of TDOR activity, we assayed the levels of ComGC in the various strains by Western blotting. Because not all cells in a culture become competent, only low amounts of ComGC are detectable unless ComGC production is stimulated artificially. This can be achieved by overproduction of the ComS peptide, through introduction of the multicopy plasmid pComS that carries the *comS* gene (Fig. 5; Hahn *et al.*, 1996). As shown in Fig. 5, ComGC was barely detectable in cells lacking the *bdbC* and *bdbD* genes. The level of ComGC was increased upon introduction of plasmid pHB-bdbCD, confirming that BdbC and BdbD are required for folding of ComGC into a stable conformation. Notably, the fact that the ComGC level remained lower than in the parental controls can be explained by the fact that the level of BdbD produced from plasmid pHB-bdbCD is much lower than the BdbD level in the parental strain (Fig. 5, lower panel), which explains for the partial restoration of the ComGC level in
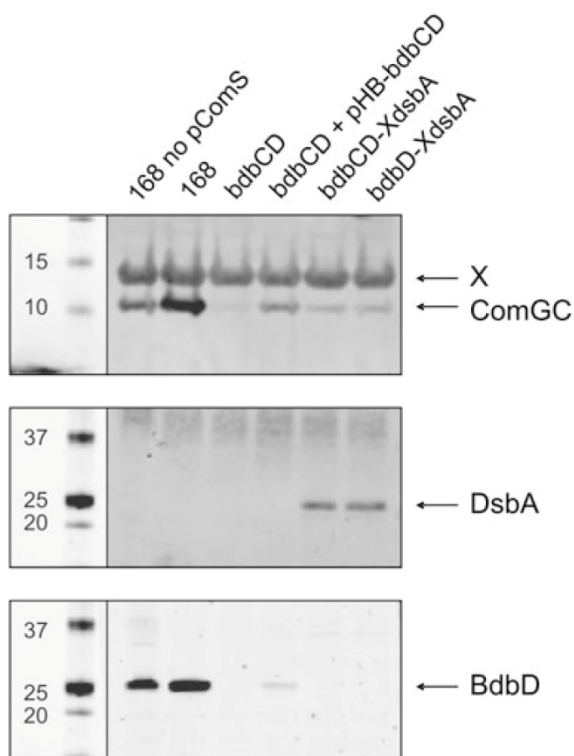
Fig. 5. Production of ComGC in *bdb* mutants also producing DsbA. The presence of ComGC in cell wall fractions of cells of *B. subtilis* 168, bdbCD, bdbCD + pHB-bdbCD, bdbCD-XdsbA and bdbD-XdsbA was detected by Western blotting with antibodies raised against ComGC. Cells were grown to maximum competence in PM medium with 2% xylose. Subsequently, the cells were protoplasted and the protoplast supernatant was used for blotting as previously described (Meima *et al.*, 2002). The cell wall fraction equivalent to 4.5 ml culture with an OD_{600} of ~3.0 was loaded in each lane of the gel. As a control, the presence of DsbA and BdbD was analysed in cell lysates. In this case, each lane of the gels was loaded with an amount of protein that corresponds to 40 μl of cultured cells with an OD_{600} of ~3.0. To increase the level of ComGC production, all assayed strains contained plasmid pComS, except a 168 control strain (marked 'no pComS'). The position of ComGC, DsbA and BdbD is indicated by arrows in the respective panels. X marks an unidentified cross-reacting band, which can be regarded as an internal standard. Molecular weight markers are indicated.

this strain. The production of ComGC was also restored when DsbA was expressed in *bdbD* or *bdbCD* mutant cells, albeit to levels that were lower than those observed in *bdbCD* mutant cells containing pHB-bdbCD (Fig. 5). This finding is consistent with the observation that DsbA production does not fully restore competence development in *bdbCD* mutant cells (Table 3). Nevertheless, the results show that DsbA is able to complement, at least partly, for the absence of BdbC and BdbD in the correct folding of ComGC to a protease-resistant and biologically active conformation.

DsbA can sustain sublancin 168 production

The secretion of active sublancin 168 by *B. subtilis* requires the presence of BdbB, and to a lesser extent BdbC (Dorenbos *et al.*, 2002). This makes sublancin 168 suitable as a reporter protein for TDOR activity. Furthermore, our previous studies have shown that BdbA is dispensable for the production of active sublancin 168. So far, it was not known, however, whether BdbD is involved in this process. To know precisely which Bdb proteins of *B. subtilis* are required for sublancin 168 production (before assessing possible effects of DsbA), we studied the role of BdbD in this process. For this purpose, production of sublancin 168 by a *bdbAD* double mutant was monitored, using *B. subtilis* ΔSPβ as a sublancin 168-sensitive indicator strain. The results in Fig. 6A show that there is no difference in sublancin 168-dependent growth inhibition of the ΔSPβ indicator strain by the *bdbAD* double mutant as compared with the parental strain. This shows that neither BdbA nor BdbD are required for sublancin 168 production and that, apparently, BdbB and BdbC are the only Bdb proteins required for this process.

Finally, we investigated whether DsbA could complement for the absence of both BdbB and BdbC in sublancin
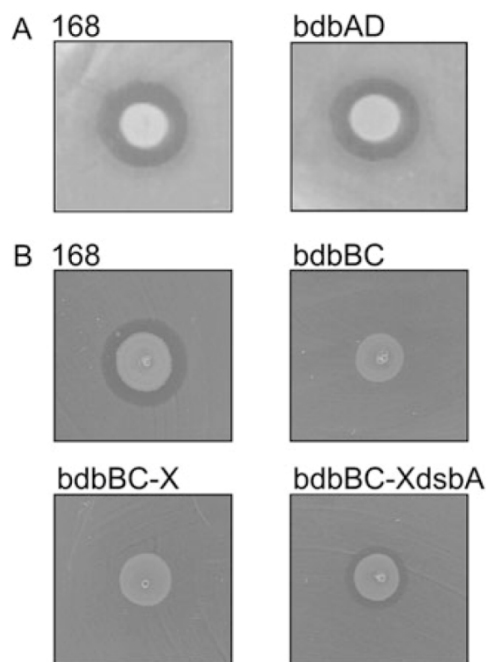
Fig. 6. Sublancin 168 Production by bdb mutants also producing DsbA. Sublancin 168 production by various strains was assayed with a sublancin-sensitive *B. subtilis* ΔSPβ indicator strain. Sublancin 168 activity is visualized by zones of growth inhibition around spotted cells producing this lantibiotic.
A. Sublancin 168 production by *B. subtilis* 168 and bdbAD.
B. Sublancin 168 production by *B. subtilis* 168, bdbBC, BdbBC-X and bdbBC-XdsbA.

168 production. For this purpose, we assayed the production of sublancin 168 by a *bdbBC*-X*dsbA* strain. It should be noted that xylose binds to sublancin 168, thereby inactivating this lantibiotic (Dorenbos *et al.*, 2002). Therefore, we assayed sublancin 168 production in the absence of xylose. As shown in Fig. 6B, deletion of both *bdbB* and *bdbC* resulted in a complete inhibition of sublancin 168 production. Introduction of the XTC*dsbA* cassette in this *bdbBC* mutant was sufficient to restore the sublancin 168 production to an intermediate level, while this was not the case when the 'empty' XTC cassette was introduced. However, the presence of increasing amounts of xylose did not result in increased growth inhibition of the ΔSPβ indicator by the bdbBC XdsbA strain. Together, these findings show that DsbA is able to complement at least partially for both BdbB and BdbC in sublancin 168 production.

Discussion

In the present studies, we compared the biological activity of TDORs from *B. subtilis* and *S. aureus*. Guided by the results of phylogenetic analyses, we addressed the question whether the TDOR systems of low-GC Gram-positive bacteria, such as *B. subtilis* and *S. aureus*, have a modular composition. The results show that this is indeed the case. Specifically, three novel findings are reported here. First, we show that the lipoprotein DsbA of *S. aureus* can perform its TDOR function by itself in a heterologous background, namely *B. subtilis* lacking all TDORs that have been implicated in extracytoplasmic oxidation of disulphide bond-containing proteins (i.e. *B. subtilis* BdbA-D). The second novelty is that DsbA does not need the presence of a TDOR-quinone oxidoreductase, like DsbB of *E. coli*, for its biological activity. Instead, it seems that DsbA can be reoxidized by redox-active compounds in the extracellular milieu. This is completely different from the situation in *B. subtilis*, where the DsbA homologue BdbD does require such a TDOR-quinone oxidoreductase, namely BdbC. A third novel observation is that the two known TDOR-quinone oxidoreductases of *B. subtilis*, BdbB and BdbC, can act independently of other Bdb proteins in the formation of sublancin 168.

Because at least three disulphide bond-containing reporter proteins, including two native proteins and one heterologous protein, are known to require TDOR activity in *B. subtilis*, we decided to study DsbA function in *B. subtilis* rather than *S. aureus*, where DsbA substrates have not yet been identified (Dumoulin *et al.*, 2005). Use of *B. subtilis* to study DsbA function *in vivo* has two major advantages. First, the cell envelope architecture of *B. subtilis* and *S. aureus* is very similar, both organisms being related low-GC Gram-positive bacteria. Second, none of the *B. subtilis* Bdb proteins implicated in extracy-

toplasmic protein oxidation is essential for cell growth and viability (Erlendsson and Hederstedt, 2002; Kobayashi *et al.*, 2003), which allowed the analysis of DsbA function in the absence of individual or multiple Bdb proteins. As previously shown by Dumoulin *et al.* (2005), DsbA is a very strong oxidase, at least *in vitro*. Our *in vivo* complementation experiments now show that DsbA can replace the known Bdb proteins of *B. subtilis* in three distinct processes that involve disulphide bond-containing proteins: folding of secreted *E. coli* PhoA (two disulphide bonds) into an active and protease-resistant conformation (Bolhuis *et al.*, 1999), folding of *B. subtilis* ComGC (one disulphide bond) into an active and protease-resistant conformation (Meima *et al.*, 2002), and secretion of *B. subtilis* sublancin 168 (two disulphide bonds) with bactericidal activity (Dorenbos *et al.*, 2002). On the contrary, our proteomics analyses show that DsbA does not impact on the remaining extracytoplasmic proteins that can be visualized by two-dimensional gel electophoresis. Together, these findings strongly support the view that DsbA can replace the Bdb proteins in the specific oxidation of certain extracytoplasmic proteins that are sorted to the membrane and cell wall (i.e. ComGC) or growth medium (i.e. PhoA and sublancin 168). Notably, the Bdb's of *B. subtilis* have evolved to different functions in ComGC (depends on BdbCD) and sublancin 168 biogenesis (depends on BdbBC) and this difference in substrate specificity is also reflected in the heterologous secretion of *E. coli* PhoA (depends on BdbBCD). It is therefore remarkable that DsbA can sustain all three processes, albeit with a reduced efficiency compared with the authentic Bdb proteins. This reduced efficiency may relate to the fact that DsbA has evolved in *S. aureus* to modulate the folding of *S. aureus*-specific proteins, to the expression level of DsbA in *B. subtilis*, or to a limited reoxidation of DsbA under the conditions tested.

An important conclusion from the present studies is that DsbA does not need other known TDORs for its re-oxidation. In particular, the results obtained with *E. coli* PhoA show unambiguously that DsbA can perform its function independently of the *B. subtilis* BdbABCD proteins in catalytic amounts, as the DsbA production level resembles that of BdbD. This is remarkable because BdbD, which is the *B. subtilis* homologue of DsbA, does not efficiently promote PhoA folding in the absence of the TDOR-quinone oxidoreductase BdbC (Bolhuis *et al.*, 1999; Meima *et al.*, 2002). Thus, it is reasonable to assume that BdbC is required for re-oxidation of BdbD even though this has not yet been shown biochemically (Sarvas *et al.*, 2004). This previous observation on BdbCD function, together with the present DsbA complementation studies in *B. subtilis*, raised the question how DsbA becomes re-oxidized after oxidizing a substrate protein. Possible answers to this intriguing question could

be that DsbA mainly functions as an isomerase and/or chaperone, or that DsbA transfers its electrons directly to as yet unidentified proteins or quinones in the electron transport chain, or that DsbA is directly reoxidized by molecular oxygen. The latter possibilities could perhaps be tested in future studies by growing DsbA-producing cells under anaerobic growth conditions. Another possibility was that certain other components in the extracellular milieu of *S. aureus*, such as cystine in the blood of colonized hosts, could be involved in the reoxidation of DsbA (Dumoulin *et al.*, 2005). This idea was tested by growing cells in minimal medium plus or minus cysteine, which is readily oxidized to cystine under aerobic conditions. Indeed, our experiments showed that the addition of cysteine was needed to detect the PhoA folding activity of DsbA when cells were grown in S7 minimal medium. This implies that DsbA is able to reduce certain medium compounds in order to become reoxidized for another catalytic cycle, at least when produced in *B. subtilis*. It is presently not known to what extent redox-active components of the different staphylococcal growth environments contribute to DsbA re-oxidation in *S. aureus.*

A completely unexpected observation was that the two TDOR-quinone oxidoreductases of *B. subtilis*, BdbB and BdbC, are sufficient to sustain the production of active sublancin 168. Although it has not yet been shown that these two proteins are directly involved in the oxidation of sublancin 168, their direct involvement seems a very likely possibility (Dorenbos *et al.*, 2002). Notably, DsbA does not show any structural similarity to BdbB and BdbC (this study; T.R.H.M. Kouwen *et al.*, unpubl. obs.). Therefore, it was a highly surprising finding that DsbA can replace these TDOR-quinone oxidoreductases in the production of active sublancin 168. This result seems to suggest that DsbA might also have a TDOR-quinone oxidoreductases function. However, we consider this possibility unlikely, because of the complete lack of sequence similarity between DsbA and known quinone oxidoreductases and, in particular, the absence of an additional pair of cysteines that would be required for the transfer of electrons from DsbA to quinones as was previously shown for the TDOR-quinone oxidoreductases DsbB of *E. coli* (Jander *et al.*, 1994). Such an additional cysteine pair is present in BdbB and BdbC (Bolhuis *et al.*, 1999). In any case, the function of BdbB and BdbC independent of a BdbD-like TDOR in a biological process is consistent with the observation that some low-GC Gram-positive bacteria, such as *Bacillus halodurans*, *Geobacillus kaustophilus*, *Bacillus clausii* and *Oceanonbacillus iheyenis*, have a BdbC homologue, but lack a BdbD homologue. It is thus conceivable that the presence of a TDOR-quinone oxidoreductase is sufficient to facilitate the oxidation of certain extracytoplasmic proteins in these species.

In summary, our present studies on the Bdb proteins of *B. subtilis* and DsbA of *S. aureus* justify the conclusion that analogous TDOR systems for the oxidation of extra-cytoplasmic proteins have evolved in the low-GC Gram-positive genera *Bacillus* and *Staphylococcus*. This view is supported by phylogenetic analyses combined with topological predictions, indicating that the *Bacillus* TDORs have evolved into integral membrane proteins, while the *Staphylococcus* TDORs have evolved into lipoproteins. Importantly, the present observations indicate that the BdbC-, BdbD- and DsbA-like TDORs can be regarded as functional modules that can act in different combinations. This modular composition of TDOR systems is probably also conserved in bacterial genera other than the low-GC Gram-positive bacteria because the presence of BdbC-, BdbD- and DsbA-like TDORs is widespread among all bacteria. Even though BdbD- and DsbA-like TDORs are homologous, they display functional differences. While DsbA can replace BdbC- and BdbD-like TDORs for all processes studied, the BdbC-like TDORs can either function individually, or in conjunction with BdbD-like TDORs. Whether BdbD-like TDOR modules can function independently of a BdbC-like TDOR is currently not known. To obtain a more comprehensive view on TDOR function in low-GC Gram-positive bacteria, our ongoing studies are aimed at identifying the natural TDOR substrates in *B. subtilis* and *S. aureus*, and at determining how the actions of *Bacillus* Bdb proteins are either concerted or separated in the different processes sustained by these TDORs.

Experimental procedures

Sequence similarity searches, alignment and tree reconstruction

Sequence similarity searches were performed with the standard protein-protein BLAST algorithm (BLASTP) (http://www.ncbi.nlm.nih.gov/sutils/genom_table.cgi) against all the annotated microbial genomes of the Firmicutes (i.e. low-GC Gram-positive bacteria) at NCBI, using GenBank as the database. Homologous sequences were obtained and used for alignment with ClustalX software (version 1.8), using the Blossum 30 matrix as pair-wise and multiple alignment parameters. Default gap opening and extension parameters were applied. Minor changes in the alignment were introduced manually. Multiple insertions and deletions were removed. Tree reconstruction was performed according to the maximum parsimony method as implemented in the program PAUP (version 4.0b10) and visualized with the program Treeview (version 1.616). Of the 159 total characters used for the heuristic search, six characters were constant and three variable characters were parsimony-uninformative, leaving 150 parsimony-informative characters. Ten random additions of sequences were applied with the branch swapping/tree-bisection-reconnection algorithm. Bootstrap values were calculated with 1000 replications. Four

Table 4. Plasmids and strains used in this study.

	Relevant properties	Reference
Plasmids		
pTOPO	pCR®-Blunt II-TOPO® vector; Km^R	Invitrogen Life technologies
pUC18	Ap^R, ColE1, Φ80dLacZ, *lac* promoter	Norrander *et al.* (1983)
pET26b(+)	T7*lac*; His(6)-tag; pelB-leader; enterokinase protease site. 5.4 kb; Km^R	Novagen
pET26dsbA	pET26b(+) derivative; contains the *dsbA* gene from *S. aureus*	This work
pPSPhoA5	plasmid carrying the *E. coli phoA* gene fused to the prepro-region of the lipase gene from *Staphylococcus hyicus*; used for efficient PhoA synthesis and secretion in *B. subtilis*; Cm^R	Darmon *et al.* (2006)
pXTC	pX derivative containing a tetracycline resistance marker instead of a chloramphenicol resistance maker; 8.4 kb, Ap^R; Tc^R	Darmon *et al.* (2006)
pXTCdsbA	pXTC carrying *dsbA* of *S. aureus* fused to the signal sequence and RBS of *mntA* of *B. subtilis* under the transcriptional control of the *xylA* promoter; Ap^R; Tc^R	This work
pHB201	*ori*-pBR322 *ori*-1060 *cat86::lacZa*; Cm^R; Em^R	Bron *et al.* (1998)
pHB-bdbCD	pHB201 vector carrying the *bdbDC* operon fused to a C-terminal his(6) sequence tag; original strain collection name pHB-DCh	This work
Strains		
S. aureus		
RN4220	Restriction-deficient derivative of NCTC 8325, cured of all known prophages	Kreiswirth *et al.* (1983)
E. coli		
DH5α	*supE44*; *hsdR17*; *recA1*; *gyrA96*; *thi-1*; *relA1*	Hanahan (1983)
TOP10	Cloning host for pTOPO vector; F-*mcr*A Δ(*mrr-hsd*RMS-*mcr*BC) Φ80*lacZ*ΔM15 Δ*lacX74 recA1 araD139 Δ(araleu) 7697 galU galK rpsL (Str^R) endA1 nupG*	Invitrogen Life technologies
B. subtilis		
168	*trpC2*	Kunst *et al.* (1997)
bdbA	*trpC2*; Δ*bdbA* (originally referred to as Δ*bdbA*)	Dorenbos *et al.* (2002)
bdbB	*trpC2*; *bdbB*::pMutin2mcs	Bolhuis *et al.* (1999)
bdbC	*trpC2 bdbC*::Km^R	Dorenbos *et al.* (2002)
bdbD	*trpC2*; *bdbD*::pMutin2pMutin2	Meima *et al.* (2002)
ΔSPβ	*trpC2*; ΔSPβ; sublancin 168 sensitive; laboratory name CBB312	Dorenbos *et al.* (2002)
bdbAD	*trpC2*; Δ*bdbA*; *bdbD*::pMutin2mcs	This work
bdbBC	*trpC2*; *bdbB*::pMutin2mcs; *bdbC*::Km^R	Dorenbos *et al.* (2002)
bdbCD	*trpC2*; *bdbCD*::Sp^R	This work
bdbABCD	*trpC2*; ΔSPβ; *bdbCD*::Sp^R	This work
XdsbA	*trpC2*; *amyE*::XTC*dsbA*	This work
ΔSPβ-XdsbA	*trpC2*; ΔSPβ; *amyE*::XTC*dsbA*	This work
bdbC-XdsbA	*trpC2*; *bdbC*::Km^R; *amyE*::XTC*dsbA*	This work
bdbD-XdsbA	*trpC2*; *bdbD*::pMutin2mcs; *amyE*::XTC*dsbA*	This work
bdbBC-X	*trpC2*; *bdbB*::pMutin2mcs; *bdbC*::Km^R; *amyE*::XTC	This work
bdbBC-XdsbA	*trpC2*; *bdbB*::pMutin2mcs; *bdbC*::Km^R; *amyE*::XTC*dsbA*	This work
bdbCD-XdsbA	*trpC2*; *bdbCD*::Sp^R; *amyE*::XTC*dsbA*	This work
bdbABCD-XdsbA	*trpC2*; ΔSPβ; *bdbCD*::Sp^R; *amyE*::XTC*dsbA*	This work

additional sequences of BdbD homologues from the high-GC Gram-positive bacteria *Frankia* sp. Ccl3, *Rubrobacter xylanophilus* (Rxy) DSM 9941, *Streptomyces coelicolor* (Sco) A3(2) and *Corynebacterium efficiens* (Cef) YS-314 were included in the analysis as outgroups to root the tree. Predictions of subcellular locations of proteins were performed with the SignalP, LipoP and TMHMM algorithms (http://www.cbs.dtu.dk/) (Juncker *et al.*, 2003; Bendtsen *et al.*, 2004).

Plasmids, bacterial strains and growth conditions

The plasmids and bacterial strains used in this study are listed in Table 4. Strains were grown with agitation at 37°C in either LB medium, S7 minimal salt medium or Paris Minimal (PM) medium. LB medium consisted of 1% tryptone, 0.5% yeast extract and 1% NaCl, pH 7.4. S7 medium consisted of 20 mM potassium phosphate (pH 7.0), 10 mM (NH$_4$)$_2$SO$_4$, 20 mM sodium glutamate (pH 7.0), 2 mM MgCl$_2$, 0.7 mM CaCl$_2$, 50 µM MnCl$_2$, 5 µM FeCl$_3$, 1 µM ZnCl$_2$, 2 µM thiamine, 2% glucose and all 20 amino acids at 2 mg ml^{-1} including or excluding cysteine. PM consisted of 10.7 mg ml^{-1} K$_2$HPO$_4$, 6 mg ml^{-1} KH$_2$PO$_4$, 1 mg ml^{-1} trisodium citrate, 0.02 mg ml^{-1} MgSO$_4$, 1% glucose, 0.1% casamino acids (Difco), 20 µg ml^{-1}L-tryptophan, 2.2 µg ml^{-1} ferric ammonium citrate and 20 mM potassium glutamate. If appropriate, media were supplemented with antibiotics at the following concentrations: ampicilin (Ap), 100 µg ml^{-1} (*E. coli*); erythromycin (Em), 100 µg ml^{-1} (*E. coli*) or 2 µg ml^{-1} (*B. subtilis*); chloramphenicol (Cm), 5 µg ml^{-1} (*B. subtilis*); tetracycline (Tc), 10 µg ml^{-1} (*B. subtilis*); spectinomycin (Sp), 100 µg ml^{-1} (*B. subtilis*); kanamycin (Km), 50 µg ml^{-1} (*E. coli*) or 20 µg ml^{-1} (*B. subtilis*). To visualize α-amylase activity (specified by the *amyE* gene), LB plates were supplemented with 1% starch.

DNA techniques

Chromosomal DNA of *B. subtilis* was isolated according to Bron and Venema (Bron and Venema, 1972). Plasmid DNA from *E. coli* was isolated using the alkaline lysis method (Sambrook *et al.*, 1989), or using the High Pure Plasmid

Isolation Kit according to the protocol supplied by the manufacturer (Roche Applied Science). Procedures for DNA purification, restriction, ligation, agarose gel electrophoresis, and transformation of competent *E. coli* cells were carried out as previously described (Sambrook *et al.*, 1989). *B. subtilis* was transformed as described by Kunst and Rapoport (Kunst and Rapoport, 1995). Polymerase chain reaction (PCR) was carried out with the Pwo DNA polymerase, using chromosomal or plasmid DNA as a template. All PCR fragments were ligated in pUC18 and used for transformation of *E. coli* DH5α, or ligated in the pTOPO® vector and used for transformation of *E. coli* TOP10 Competent Cells (Invitrogen). All constructs were checked by sequencing.

Construction of bdb-*knockout and complementation strains*

Various previously constructed *B. subtilis* 168 *bdb*-mutant strains were used to construct additional knockout and complementation strains (Table 4). *B. subtilis* bdbAD was constructed by transforming strain bdbA with genomic DNA of strain bdbD. To construct the *B. subtilis bdbCD* mutant, a 900 bp fragment upstream of the *bdbD* gene was amplified using the primers pDCd1 (TTGGTATTGGGTGAATGTGC) and pDCd2 (*CGAAAATCGCCATTCGCCAG*CAAACTC ATGTCCATCAGCA). Next, a 900 bp fragment downstream of the *bdbC* gene was amplified using the pDCd3 (*AACCCT TGCATAGGGGGATC* TCCGACACCTCATCGTTTTA) and pDCd4 (ATCTGTGCGTAAAGCTTACG) primers. The 5′ sequence (marked in italics) of the pDCd2 and the pDCd3 primers are complementary to, respectively, the Sp1 (CTG GCGAATGGCGATTTTCG) and the Sp2 (GATCCCCCTATG CAAGGGTT) primers. The Sp1 and Sp2 primers were used to amplify the spectinomycin resistance cassette (1172 bp) from plasmid pDG1726. These three PCR fragments were then purified and mixed in equal amounts (100 ng) in a PCR mixture also containing the pDCd1 and pDCd4 primers. After 10 cycles with the annealing temperature set at the optimum for the Sp1/pDCd2 and Sp2/pDCd3 combinations, the annealing temperature was increased to the optimum for the pDCd1 and pDCd4 primers, and the PCR reaction was continued for 20 cycles. The size of the final product (2972 bp) was checked on agarose gel. After purification, the PCR product was used to directly transform competent *B. subtilis* 168 cells, and the cells were selected on media containing spectinomycin. The spectinomycin-resistant colonies obtained were checked by Western blotting for the absence of BdbD production. Strain bdbABCD was constructed by transforming the ΔSPβ strain with genomic DNA of the bdbCD strain.

pXTCdsbA, carrying *dsbA* of *S. aureus* fused to the signal sequence and ribosomal binding site of *mntA* of *B. subtilis* under the transcriptional control of the *xylA* promoter (P*xylA*), was constructed as follows. In a first PCR, a fragment of 92 bp containing the ribosomal binding site and signal sequence of *mntA* of *B. subtilis* was amplified using the primers pXTC_mntA_AF (GGGGGA*CTAGT*AAGAGGAG GAGAAATATGAGACAA) and pXTC_mntA_AR (TTTTT TACCGCATCCCGTTAAAGCAAAGGTCGC). A second PCR fragment of 566 bp resulted from amplifying the *dsbA* gene of *S. aureus* using the primers pXTC_mntA_AF2 (TTAACGG

GATGCGGTAAAAAAGAATCAGCAACG) and pXTC_mntA_AR2 (GGGGG<u>GGATCCC</u>CTATTTGATTTTATCTTTTAATAAC TTC). The resulting two PCR products had an overlap of 21 nucleotides. Using this overlap, the two different fragments could be fused in 10 PCR cycles without added primers. Next, the fused product was PCR-amplified with the primers pXTC_mntAF and pXTC_mntAR2 in 20 additional PCR cycles. The resulting product of 637 bp was cloned into pTOPO. After sequence verification, the fused *dsbA* gene was excised from this plasmid with *Bam*HI and *Spe*I and ligated into the same restriction sites of plasmid pXTC, downstream of P*xylA*, resulting in plasmid pXTCdsbA.

Plasmid pXTCdsbA was used to integrate the P*xylA dsbA* construct together with the Tc resistance marker of pXTC (hereafter named XTC*dsbA* cassette), into the *amyE* locus of *B. subtilis* 168 and *B. subtilis* ΔSPβ by double cross-over recombination (Fig. 2). Selection for tetracycline resistance, and screening for an AmyE-negative phenotype on starch-containing plates enabled us to obtain strains *B. subtilis* XdsbA and *B. subtilis* ΔSPβ-XdsbA respectively. Next, the *B. subtilis* strains bdbC-XdsbA, bdbD-XdsbA and bdbCD-XdsbA, were generated by transformation of the XdsbA strain with chromosomal DNA of strains bdbC, bdbD and bdbCD, respectively, and selection of transformants with the appropriate antibiotic(s). Strain bdbABCD-XdsbA was generated by transformation of the ΔSPβ-XdsbA strain with chromosomal DNA of strain bdbCD. Finally, strain bdbBC-XdsbA was generated by transformation of the XdsbA strain first with chromosomal DNA of strain bdbB, and by subsequent transformation of the resulting bdbB-XdsbA strain with chromosomal DNA of strain bdbC. It should be noted that the deletion of *bdbC* and *bdbD* severely affects competence development (Meima *et al.*, 2002). Therefore, the introduction of the *bdbC* and *bdbD* mutations represented the final step in most strain constructions.

Plasmid pHB-bdbCD was constructed as follows. The BdbDC operon was amplified using primers pDCh1 (GGGGGG<u>CATATG</u>AAACGATGAGGTGTCGGAGT) carrying the RBS of the *bdbD* gene, and pDCh2 (GGGGGGG<u>GGATCCT</u> TA*GTGGTGGTGGTGGTGGTG*TTCAG ATTTT<u>TCGCCT</u>T TCA), carrying an Nde*I* site and a BamHI site, respectively (underlined in the primer sequences). The use of pDCh2 results in C-terminal 6His-tagging of BdbC (the sequence encoding the 6His-tag is marked in italics). The resulting PCR product of 1148 bp and the plasmid pHB201 were cleaved with the *Nde*I and *Bam*HI, and subsequently ligated. The resulting plasmid was named pHB-bdbCD. Expression of the *bdbC* and *bdbD* genes on pHB-bdbCD was verified by introduction of this plasmid in a *B. subtilis bdbCD* knockout strain and subsequent Western blotting using BdbD and 6His-tag-specific antibodies.

Purification of DsbA

For overproduction of DsbA of *S. aureus*, the *dsbA* gene was PCR-amplified and cloned in pET26 (Novagen), using restriction enzymes *Nde*I and *Xho*I. However, as the coding sequence of *dsbA* contains a *Nde*I site as well, this site was removed during the amplification procedure without changing the encoded amino acid sequence. For this purpose, first the front part of the *dsbA* gene was amplified using primers

SaDsbA-F (GGGGG<u>CATATG</u>ACTAAAAAATTACTAACATT AT) and p184p-R (CATAATCAT**A**AGGATCTTCAA). Next, this amplified product was used as the front primer in a second PCR amplification together with the reverse primer SaDsbAA-R (GGGGGAAGCTTTTCGTATTGTCCTAATA AAT). The resulting product was cloned into pUC18, yielding plasmid pUC18dsbaP184P. After verification of the sequence, the *dsbA* gene was excised from this plasmid with *Nde*I and *Xho*I and ligated into the same restriction sites of pET26b(+), downstream of the T7 promoter and upstream of an in-frame His(6)tag sequence, resulting in plasmid pET26dsbA. Subsequently, *E. coli* BL21(DE3) was transformed with this construct. To induce DsbA production, 10 ml of an overnight culture of this strain was used to inoculate 1 litre fresh LB medium. This culture was grown to an OD_{600} of 0.6–0.9 after which 1 mM IPTG final concentration was added and growth continued for another 3 h. Cells were harvested by centrifugation (15 min, 7500 r.p.m.) and resuspended in 10 vols of lysis buffer (20% sucrose, 10 mM Tris-HCl, pH 8.0). Next, cells were disrupted using a French Press (2500 PSI). Unbroken cells and cellular debris were removed by centrifugation (15 min, 6000 g, 4°C). To purify DsbA, first the membrane fraction was isolated. For this purpose the membrane fraction was collected by ultracentrifugation (100.000 g, 30 min, 4°C) and solubilized, using solubilization buffer (300 mM NaCl, 50 Mm NaPi, 10% glycerol, pH 8.0) containing 0.5% Triton X-100. This membrane fraction was loaded on an Äkta explorer (GE Healthcare) and was passed through a HisTrap column (Invitrogen) containing nickel ions. After the his-tagged DsbA was bound to the nickel ions, the concentration of elution buffer (solubilization buffer containing 300 mM imidazole) was gradually increased, leading to the release of DsbA. Eluted fractions were collected and tested for presence of DsbA by SDS-PAGE.

SDS-PAGE and Western blotting

The presence of DsbA, BdbD and PhoA in growth medium and/or cell lysates was detected by Western blotting. Cellular or secreted proteins were separated by SDS-PAGE (using precast NuPAGE gels from Invitrogen), and proteins were then semidry blotted (1.25 h at 100mA per gel) onto a nitrocellulose membrane (Protran®, Schleicher and Schuell). Subsequently, the DsbA, BdbD and PhoA proteins were detected with specific polyclonal antibodies raised in rabbits (Eurogentec). In addition, chicken antibodies against DsbA were kindly provided by Dr B. Berger-Baechi, and polyclonal antibodies against ComGC were kindly provided by Dr D. Dubnau. The detection of these antibodies was either performed with horseradish peroxidase-conjugated IgG secondary antibodies and the Super Signal® West Dura Extended Duration Substrate (Pierce) in combination with the Chemi-Genius XE Bio-Imaging system (Syngene), or with fluorescent IgG secondary antibodies (IRDye 800 CW goat anti-rabbit from LiCor Biosciences) in combination with the Odyssey Infrared Imaging System (LiCor Biosciences). In the latter case, fluorescence at 800 nm was recorded.

Proteomics

Cells of *B. subtilis* were grown at 37°C under vigorous agitation in 1 l of LB medium. After 1 h of post-exponential growth,

cells were separated from the growth medium by centrifugation. The secreted proteins in the growth medium were collected for two-dimensional gel electrophoresis (2D PAGE), gels were stained with the SYPRO Ruby protein gel stain (Molecular Probes), and protein spots were identified by matrix-assisted laser desorption/ionization – time of flight mass spectrometry (MALDI-TOF MS) as previously described (Jongbloed *et al.*, 2002). To visualize possible differences in extracellular protein composition, dual channel image analysis of stained gels was performed using the DECODON Delta 2D software (http://www.decodon.com). Each experiment was performed at least twice.

Alkaline phosphatase activity assay

The alkaline phosphatase assay with growth medium samples was performed as previously described (Darmon *et al.*, 2006). PhoA activity is calculated as $U/ml/OD_{600}$. All experiments were repeated at least three times.

Competence assay

Bacillus subtilis strains were tested for transformability by growing the cells to competence in PM medium, essentially as previously described (Kunst and Rapoport, 1995). For comparison of transformability, the various strains were grown in parallel in the presence of 2% xylose (Meima *et al.*, 2002). Chromosomal DNA of strain ΔtatAdCd (Jongbloed *et al.*, 2002), carrying a chloramphenicol-resistant marker, was used for transformation. Transformability was expressed as the percentage of chloramphenicol-resistant transformants of the total viable count. Samples for Western blotting were taken at maximum competence, essentially as described previously (Meima *et al.*, 2002).

Sublancin 168 activity assay

A halo assay for sublancin production was performed on plates with the sublancin-sensitive *B. subtilis* ΔSPβ indicator strain as previously described (Dorenbos *et al.*, 2002). It should be noted that the ΔSPβ strain lacks both the genes for production of, and immunity against sublancin 168. Briefly, 100 μl from a 100-fold diluted overnight culture of *B. subtilis* ΔSPβ was plated. After drying of the plate, 1 μl aliquots of overnight cultures of the strains to be tested for sublancin 168 production were spotted. The plates were incubated overnight at 37°C and, subsequently, growth inhibition of the indicator strain was monitored.

References

Anfinsen, C.B. (1973) Principles that govern the folding of protein chains. *Science* **181:** 223–230.

Antelmann, H., Tjalsma, H., Voigt, B., Ohlmeier, S., Bron, S., van Dijl, J.M., and Hecker, M. (2001) A proteomic view on genome-based signal peptide predictions. *Genome Res* **11:** 1484–1502.

Aslund, F., and Beckwith, J. (1999) Bridge over troubled waters: sensing stress by disulfide bond formation. *Cell* **96:** 751–753.

Bendtsen, J.D., Nielsen, H., von Heijne, G., and Brunak, S. (2004) Improved prediction of signal peptides: SignalP 3.0. *J Mol Biol* **340:** 783–795.

Bolhuis, A., Venema, G., Quax, W.J., Bron, S., and van Dijl, J.M. (1999) Functional analysis of paralogous thiol-disulfide oxidoreductases in *Bacillus subtilis. J Biol Chem* **274:** 24531–24538.

Bron, S., and Venema, G. (1972) Ultraviolet inactivation and excision-repair in *Bacillus subtilis*. I. Construction and characterization of a transformable eightfold auxotrophic strain and two ultraviolet-sensitive derivatives. *Mutat Res* **15:** 1–10.

Bron, S., Bolhuis, A., Tjalsma, H., Holsappel, S., Venema, G., and van Dijl, J.M. (1998) Protein secretion and possible roles for multiple signal peptidases for precursor processing in bacilli. *J Biotechnol* **64:** 3–13.

Chung, Y.S., Breidt, F., and Dubnau, D. (1998) Cell surface localization and processing of the ComG proteins, required for DNA binding during transformation of *Bacillus subtilis. Mol Microbiol* **29:** 905–913.

Collet, J.F., and Bardwell, J.C. (2002) Oxidative protein folding in bacteria. *Mol Microbiol* **44:** 1–8.

Darmon, E., Dorenbos, R., Meens, J., Freudl, R., Antelmann, H., Hecker, M., *et al.* (2006) A disulfide bond-containing alkaline phosphatase triggers a BdbC-dependent secretion stress response in *Bacillus subtilis. Appl Environ Microbiol* **72:** 6876–6885.

Dorenbos, R., Stein, T., Kabel, J., Bruand, C., Bolhuis, A., Bron, S., *et al.* (2002) Thiol-disulfide oxidoreductases are essential for the production of the lantibiotic sublancin 168. *J Biol Chem* **277:** 16682–16688.

Dorenbos, R., van Dijl, J.M., and Quax, W.J. (2005) Thiol disulfide oxidoreductases in bacteria. In *Recent Res. Devel. Microbiology, 9.* Pandalai, S.G. (ed.). Kerala: Research Signpost, pp. 237–269.

Dumoulin, A., Grauschopf, U., Bischoff, M., Thony-Meyer, L., and Berger-Bachi, B. (2005) Staphylococcus aureus DsbA is a membrane-bound lipoprotein with thiol-disulfide oxidoreductase activity. *Arch Microbiol* **184:** 117–128.

Erlendsson, L.S., and Hederstedt, L. (2002) Mutations in the thiol-disulfide oxidoreductases BdbC and BdbD can suppress cytochrome c deficiency of CcdA-defective *Bacillus subtilis* cells. *J Bacteriol* **184:** 1423–1429.

Erlendsson, L.S., Acheson, R.M., Hederstedt, L., and Le Brun, N.E. (2003) *Bacillus subtilis* ResA is a thiol-disulfide oxidoreductase involved in cytochrome c synthesis. *J Biol Chem* **278:** 17852–17858.

Erlendsson, L.S., Moller, M., and Hederstedt, L. (2004) *Bacillus subtilis* StoA Is a thiol-disulfide oxidoreductase important for spore cortex synthesis. *J Bacteriol* **186:** 6230–6238.

Hahn, J., Luttinger, A., and Dubnau, D. (1996) Regulatory inputs for the synthesis of ComK, the competence transcription factor of Bacillus subtilis. *Mol Microbiol* **21:** 763–775.

Hanahan, D. (1983) Studies on transformation of *Escherichia coli* with plasmids. *J Mol Biol* **166:** 557–580.

Inaba, K., Murakami, S., Suzuki, M., Nakagawa, A., Yamashita, E., Okada, K., and Ito, K. (2006) Crystal structure of the DsbB-DsbA complex reveals a mechanism of disulfide bond generation. *Cell* **127:** 789–801.

Jander, G., Martin, N.L., and Beckwith, J. (1994) Two cysteines in each periplasmic domain of the membrane protein DsbB are required for its function in protein disulfide bond formation. *EMBO J* **13:** 5121–5127.

Jongbloed, J.D., Antelmann, H., Hecker, M., Nijland, R., Bron, S., Airaksinen, U., *et al.* (2002) Selective contribution of the twin-arginine translocation pathway to protein secretion in *Bacillus subtilis. J Biol Chem* **277:** 44068–44078.

Juncker, A.S., Willenbrock, H., von Heijne, G., Brunak, S., Nielsen, H., and Krogh, A. (2003) Prediction of lipoprotein signal peptides in Gram-negative bacteria. *Protein Sci* **12:** 1652–1662.

Kadokura, H., Katzen, F., and Beckwith, J. (2003) Protein disulfide bond formation in prokaryotes. *Annu Rev Biochem* **72:** 111–135.

Kadokura, H., Tian, H., Zander, T., Bardwell, J.C., and Beckwith, J. (2004) Snapshots of DsbA in action: detection of proteins in the process of oxidative folding. *Science* **303:** 534–537.

Kobayashi, K., Ehrlich, S.D., Albertini, A., Amati, G., Andersen, K.K., Arnaud, M., *et al.* (2003) Essential *Bacillus subtilis* genes. *Proc Natl Acad Sci USA* **100:** 4678–4683.

Kreiswirth, B.N., Lofdahl, S., Betley, M.J., O'Reilly, M., Schlievert, P.M., Bergdoll, M.S., and Novick, R.P. (1983) The toxic shock syndrome exotoxin structural gene is not detectably transmitted by a prophage. *Nature* **305:** 709–712.

Kunst, F., and Rapoport, G. (1995) Salt stress is an environmental signal affecting degradative enzyme synthesis in *Bacillus subtilis. J Bacteriol* **177:** 2403–2407.

Kunst, F., Ogasawara, N., Moszer, I., Albertini, A.M., Alloni, G., Azevedo, V., *et al.* (1997) The complete genome sequence of the Gram-positive bacterium *Bacillus subtilis. Nature* **390:** 249–256.

Meima, R., Eschevins, C., Fillinger, S., Bolhuis, A., Hamoen, L.W., Dorenbos, R., *et al.* (2002) The bdbDC operon of *Bacillus subtilis* encodes thiol-disulfide oxidoreductases required for competence development. *J Biol Chem* **277:** 6994–7001.

Nakamoto, H., and Bardwell, J.C. (2004) Catalysis of disulfide bond formation and isomerization in the *Escherichia coli* periplasm. *Biochim Biophys Acta* **1694:** 111–119.

Newton, G.L., Arnold, K., Price, M.S., Sherrill, C., Delcardayre, S.B., Aharonowitz, Y., *et al.* (1996) Distribution of thiols in microorganisms: mycothiol is a major thiol in most actinomycetes. *J Bacteriol* **178:** 1990–1995.

Norrander, J., Kempe, T., and Messing, J. (1983) Construction of improved M13 vectors using oligodeoxynucleotide-directed mutagenesis. *Gene* **26:** 101–106.

Regeimbal, J., and Bardwell, J.C. (2002) DsbB catalyzes disulfide bond formation *de novo. J Biol Chem* **277:** 32706–32713.

Rietsch, A., and Beckwith, J. (1998) The genetics of disulfide bond metabolism. *Annu Rev Genet* **32:** 163–184.

Ritz, D., and Beckwith, J. (2001) Roles of thiol-redox pathways in bacteria. *Annu Rev Microbiol* **55:** 21–48.

Sambrook, J., Fritsch, E.F., and Maniatis, T. (1989) *Molecular Cloning: A Laboratory Manual.* New York: Cold Spring Harbor Laboratory Press.

Sarvas, M., Harwood, C.R., Bron, S., and van Dijl, J.M. (2004) Post-translocational folding of secretory proteins in Gram-positive bacteria. *Biochim Biophys Acta* **1694:** 311–327.

Sone, M., Kishigami, S., Yoshihisa, T., and Ito, K. (1997) Roles of disulfide bonds in bacterial alkaline phosphatase. *J Biol Chem* **272:** 6174–6178.

Stein, T. (2005) *Bacillus subtilis* antibiotics: structures, syntheses and specific functions. *Mol Microbiol* **56:** 845–857.

Tan, J.T., and Bardwell, J.C. (2004) Key players involved in bacterial disulfide-bond formation. *Chembiochem* **5:** 1479–1487.

Tjalsma, H., and van Dijl, J.M. (2005) Proteomics-based consensus prediction of protein retention in a bacterial membrane. *Proteomics* **5:** 4472–4482.

Tjalsma, H., Bolhuis, A., van Roosmalen, M.L., Wiegert, T., Schumann, W., Broekhuizen, C.P., *et al.* (1998) Functional analysis of the secretory precursor processing machinery of *Bacillus subtilis*: identification of a eubacterial homolog of archaeal and eukaryotic signal peptidases. *Genes Dev* **12:** 2318–2331.

71

5.3. Characterization of the global impact of low temperature gas plasma on vegetative microorganisms

Winter, T., Winter, J., Polak, M., Kusch, K., Mäder, U., Sietmann, R., Ehlbeck, J., van Hijum, S., Weltmann, K. D., Hecker, M., Kusch, H. (2011)

Own contribution to both manuscripts

Experimental planning, cultivation, plasma treatment of cells, proteins preparation, SDS PAGE, analysis of 2D gels and Maldi data, RNA preparation for Array analysis and analysis of array data, as well as writing of the manuscript.

Characterization of the global impact of low temperature gas plasma on vegetative microorganisms

Theresa Winter[1], Jörn Winter[2], Martin Polak[2], Kathrin Kusch[1], Ulrike Mäder[1,3], Rabea Sietmann[1], Jörg Ehlbeck[2], Sacha van Hijum[3*], Klaus-Dieter Weltmann[2], Michael Hecker[1] and Harald Kusch[1*]

[1] Institute for Microbiology, Ernst-Moritz-Arndt-University, Greifswald, Germany
[2] Leibniz Institute for Plasma Science and Technology (INP Greifswald e.V.), Greifswald, Germany
[3] Interfaculty Institute for Genetics and Functional Genomics, Department for Functional Genomics, Ernst-Moritz-Arndt-University, Greifswald, Germany

Plasma medicine and also decontamination of bacteria with physical plasmas is a promising new field of life science with huge interest especially for medical applications. Despite numerous successful applications of low temperature gas plasmas in medicine and decontamination, the fundamental nature of the interactions between plasma and microorganisms is to a large extent unknown. A detailed knowledge of these interactions is essential for the development of new as well as for the enhancement of established plasma-treatment procedures. In the present work we introduce for the first time a growth chamber system suitable for low temperature gas plasma treatment of bacteria in liquid medium. We have coupled the use of this apparatus to a combined proteomic and transcriptomic analyses to investigate the specific stress response of *Bacillus subtilis* 168 cells to treatment with argon plasma. The treatment with three different discharge voltages revealed not only effects on growth, but also clear evidence of cellular stress responses. *B. subtilis* suffered severe cell wall stress, which was made visible also by electron microscopy, DNA damages and oxidative stress as a result of exposure to plasma. These biological findings were supported by the detection of reactive plasma species by OES measurements.

1 Introduction

Low temperature gas plasma has found increasing applications in biology and medicine in the recent years [1–4], including treatment of dental cavities [5, 6], decontamination of various surfaces [7–9], and treatment of skin diseases [1, 10–13].

Gas plasmas, simply termed plasmas by physicists, can be considered to be the fourth state of matter, following by order of increasing energy, the solid state, the liquid state and the gaseous state. Strictly speaking, this fourth state is a gas made of ions and free electrons, though the plasmas employed for sterilization and other medical applications also contain uncharged particles, such as atoms, molecules and radicals [14].

Plasma can not only exist in a variety of forms, but can also be created in different ways. Plasma used in the above-mentioned applications is generated by a non-equilibrium atmospheric pressure discharge, which results in a non-thermal

*Current addresses: Sacha van Hijum, Center for Molecular and Biomolecular Informatics, NCMLS, Radboud University Nijmegen Medical Centre, P.O. Box 9101, 6500 HB Nijmegen, Netherlands; Harald Kusch, Institute of Microbiology and Genetics, Georg-August-University Göttingen, Germany

Colour Online: See the article online to view Figs. 1, 8 in colour

(cold) plasma. These gas discharges trigger a complex network of biological responses in tissues and cells [11] by generating various biologically active agents. These agents are heat, alternating electric fields, radiation (e.g. high-energy UV photons), charged particles (positive or negative ions, free electrons) and reactive neutral species (e.g. ROS, reactive nitrogen species (RNS)). The contribution of each factor strongly depends on the device setup, operating conditions (gas pressure, type and power of plasma excitation) and gas composition [11]. The effect of these various agents is also determined by whether the target material is in direct contact with the plasma or remote from it [14, 15–18].

The successful exploitation of plasma in biological settings will require an understanding of the mechanisms of interaction of gas discharges with living tissues and cells [19].

Sufficient analytical methods to investigate the effects of the interaction of plasma with microorganism have not been described so far. Therefore, we adopted functional genomic approaches to investigate these questions [11]. Proteomic and transcriptomic analyses are powerful tools for visualizing global changes in gene expression in bacterial cells after exposure to stressors such as starvation, anaerobiosis or toxic compounds. The resulting proteomic and transcriptomic signatures are defined by a set of marker proteins or genes which are up or downregulated in response to a given stress condition. The comparison of the known proteomic signatures with that generated by exposure to gas plasma enables an easier classification and interpretation of the data. The Gram positive model organism *Bacillus subtilis* was chosen, because of the extensive knowledge of its stress response mechanisms [20, 21].

We applied 2-D gel-based proteomic approaches coupled with transcriptome analysis to get a first glimpse at the complex plasma–microorganism interaction. A preliminary proteomic analysis of the effects of an argon plasma jet on mammalian cells has previously been reported by Landsberg et al. [22].

The comprehensive genome-wide analysis of the response of the microorganism to treatment with plasma in a novel growth chamber system, which we present here, is combined with an investigation of the nature of the reactive agents present in the plasma. Furthermore, the novel growth chamber system enables a reproducible plasma treatment of microorganisms in liquid cultures, here exemplified by *B. subtilis*.

2 Materials and methods

2.1 Experimental setup

An overnight culture of *B. subtilis* 168 was inoculated into Luria–Bertani broth (LB) and grown at 37°C with constant swirling to an optical density of 0.5 at 540 nm (OD_{540} 0.5). The culture was then exposed to argon plasma treatment for 15 min. Three different discharge power settings were applied to the cell suspension (0.9, 2.5 and 5 W) for growth experiments and proteomic analysis. After plasma treatment, the growth was monitored for a further 120 min and the cells were then harvested for protein preparation. As control we used a culture treated only with argon gas for 15 min at OD_{540} 0.5. Samples for microarray analyses were collected 5 min after the plasma treatment in order to visualize the immediate transcriptional response. Samples for electron microscopy were taken 5, 60 and 120 min after plasma treatment (see Section 2.6).

### 2.2 Plasma source setup and plasma diagnostic

In order to treat vegetative bacteria in liquids with low temperature plasma at atmospheric pressure a special setup is required. This setup must provide a favorable environment for the growth of bacteria and has to ensure, plasma treatment of all bacteria. Moreover, the plasma treatment must be intensive enough to induce a detectable effect in the protein pattern but must not be lethal for the bacteria. A configuration that fulfills these criteria is schematically displayed in Fig. 1.

About 45 mL bacterial suspension was placed inside a V2A-steel cup with a quadratic base area (edge length 55 mm) and a height of 30 mm. The suspension was heated to precisely 37°C using a PID-controlled Peltier element. A rotatable hollow cylinder made of 1-mm-thick V2A-steel with a diameter and a length of 48 mm was placed in the cup. Several metal bolts are mounted on the inside of the cylinder to mix the suspension. When the hollow cylinder is rotated inside the suspension, a homogenous thin film forms on its surface. The thickness of the film depends on the rotational speed ω. In this work, we generally used a constant rotation speed of ω = 1.1 rotations per second resulting in a film thickness of about 10 μm.

Both the cup and the hollow cylinder are fitted into an acrylic box. An aluminum electrode (52 mm × 52 mm × 6 mm) is mounted on a 1-mm-thick borosilicate plate as dielectric in the top cover of this box and connected to a high-voltage source. This source generates a sinusoidal high-voltage signal with a frequency of 7 kHz and peak-to-peak voltages of up to 20 kV_{pp}. The plasma power is determined from the charge–voltage Lissajous figure. An argon gas source is used to generate an air-free argon atmosphere within the box. A gas outlet permits three analytical methods to be applied to the plasma, namely temperature measurements (FOT), optical emission spectroscopy (OES) in the spectral range from 240 to 900 nm (ultra violet, visible and near infrared) and FTIR. The discharge ignited automatically, when a sufficient supply voltage was applied and a dielectric barrier discharge forms between the grounded hollow cylinder and the driven dielectric covered electrode. The plasma extension on the cylinder strongly depends on the supply voltage as Fig. 2 indicates (for additional information see Supporting Information Methods).
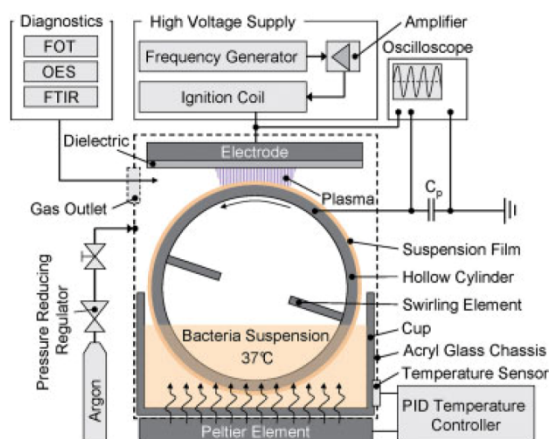
Figure 1. Experimental setup to provide vegetative growth and sufficient plasma treatment of *B. subtilis.* A dielectric barrier discharge is ignited between the dielectric covered electrode and the hollow cylinder on which a thin bacterial suspension film constitutes. In order to provide optimal growth of the bacteria the suspension is heated up to 37°C by means of a temperature regulator. In order to characterize the plasma optical emission spectroscopy (OES), Fourier transformed infrared spectroscopy (FTIR) and temperature measurements by means of a fiber optical sensor (FOT) are performed using a small slit on one side of the growth chamber.
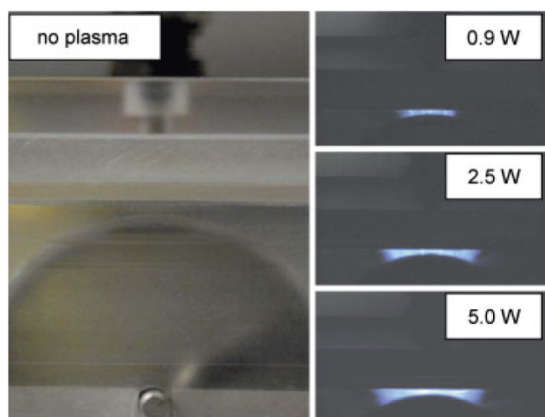
Figure 2. Argon plasma development inside the used apparatus for different discharge power settings. The plasma ignites between the dielectric and the hollow cylinder. The plasma extension on the cylinder strongly depends on the supply voltage. By increasing the power, the plasma spread on the cylinder expands and the plasma intensity rises.

2.3 Estimation of bacteria density and bacteria treatment time

To determine the bacteria number density in the thin suspension film that forms on the outside surface of the hollow cylinder, we strip off and collect the entire liquid attached to the outside cylinder surface during three full rotations. The gained suspension has a volume of (0.225 ± 0.025) mL per three full rotations or (0.075 ± 0.008) mL per single rotation, respectively. By counting a representative amount of bacteria in a counting chamber, the bacteria density on the cylinder was estimated to $(8.3 \pm 1.8) \times 10^8$ bacteria per milliliter. Consequently, an absolute amount of about $N_1 = (6.2 \pm 2.0) \times 10^7$ bacteria get plasma treated per full cylinder rotation.

Under the assumption that the bacterial concentration on the cylinder is equal to the concentration in the cup the suspension volume of 45 mL contains a total amount of $N_T = (3.7 \pm 0.8) \times 10^{10}$ bacteria. For the given plasma-treatment time of $t_p = 900$ s, the hollow cylinder performs $R = \omega \cdot t_p = 990$ rotations. Assuming a perfect mixing of the suspension every bacterium is $f_e = R_1 \cdot N_1/N_T = 1.7 \pm 0.9$ times exposed to the plasma. To estimate the total time a single bacterium is exposed to the plasma, the plasma expansion on the cylinder is measured for different supply voltages using the photographs in Fig. 2. Considering the exposition frequency f_e and the rotational speed $\omega = 1.1 \, \mathrm{s}^{-1}$ the treatment time can be calculated. The results of both, the plasma expansion on the cylinder and the total plasma-treatment time for a single bacterium, are displayed in Table S4 for different supply voltages. It is shown, that the increase of the plasma power from 0.9 to 5 W leads almost to a doubling of the plasma-treatment time.

2.4 Analytical and preparative 2-D PAGE

The cell suspension was centrifuged for 5 min at 4°C with a maximum speed $(21\,000 \times g)$ and the obtained cell pellet was washed for thrice in ice-cold TE-buffer (10 mM Tris-HCl, 1 mM EDTA, pH 8.0) and then stored at −80°C for further use. The intracellular protein extracts were obtained by cell disruption (Precellys24, Peqlab, Erlangen, Germany) and protein preparation was finished as previously described by Kohler et al. [23]. The protein concentration was determined using Roti®-Nanoquant (Carl Roth GmbH, Karlsruhe, Germany). Preparative 2-D PAGE was performed by using the immobilized pH-gradient technique [25, 26]. The protein samples (350 μg) were separated on immobilized pH gradient strips (Amersham Pharmacia Biotech, Piscataway, NJ, USA) with a pH range of 4–7. The resulting protein gels were stained with colloidal Coomassie Blue G-250G [27] and scanned with a light scanner. For identification of proteins by MALDI-TOF MS, Coomassie-stained protein spots were excised from gels using a spot cutter (Proteome Work™) with a picker head of 2 mm and transferred into 96-well microtiter plates. Digestion with trypsin and subsequent spotting of peptide solutions onto the MALDI targets were performed automatically in an Ettan Spot Handling Workstation (GE-Healthcare, Little Chalfont, United Kingdom) using a modified standard protocol. MALDI-TOF MS analyses of spotted peptide solutions were carried out on a Proteome-Analyzer 4700/4800 (Applied Biosystems, Foster

City, CA) as described previously [24]. MALDI-TOF-TOF analysis was performed for the three highest peaks of the TOF spectrum as described previously [24, 27]. Database searches were performed using the GPS explorer software version 3.6 (build 329) with the organism-specific databases. By using the MASCOT search engine version 2.1.0.4. (Matrix Science, London, UK) the combined MS and MS/MS peak lists for each protein spot were searched against a database containing protein sequences derived from the genome sequences of *B. subtilis* 168. Search parameters were as described previously [24] and an oxidation of methionine and a carboxyamidomethylation of cysteine were considered as variable modifications. The peaklists were searched with trypsin cutting fully enzymatically and allowing one missed cleavage site. For comparison of protein spot volumes, the Delta 2D software package was used (Decodon, Germany). The induction ratio of argon plasma treated cell to non-treated cells was calculated for each spot (normalized intensity of a spot on the argon plasma image/normalized intensity of the corresponding spot on the non-treated cell image). The significance of spot volume differences of 2-fold or higher was assessed by the Student's *t*-test ($\alpha < 0.01$; Delta 2D "statistics" table, TMEV plugin).

2.5 Transcriptome analysis by DNA microarray hybridization

2.5.1 Preparation of RNA

B. subtilis 168 was grown aerobically in LB medium as described above. At OD_{540} 0.5 (exponential growth phase), a discharge voltage of 2.5 W was applied for 15 min. Five minutes later, 30 mL samples were harvested by centrifugation (5 min, $9000 \times g$, 4°C) with 15 mL chilled killing buffer (20 mM Tris-HCl [pH 7.5], 5 mM $MgCl_2$, 20 mM NaN_3). The supernatant was discarded and the pellet was promptly frozen in liquid N_2. The sample was then either stored at −80°C or used immediately for RNA preparation.

The pellet was resuspended in 200 µl of ice-cold killing buffer and transferred into a pre-cooled Teflon vessel filled with liquid N_2 and containing a disruption ball. The vessel was shortly submerged into liquid N_2 and then inserted into the cell disruptor (Mikro-Desmembrator S, Sartorius) for mechanical cell disruption (2 min, shaking frequency of $3000\,min^{-1}$) [28]. The resulting cell powder was resuspended in pre-warmed (50°C) lysis solution (4 M guanidine thiocyanate, 0.025 M sodium acetate [pH 5.2], 0.5% *N*-laurylsarcosine [w/v]), transferred into Eppendorf tubes and frozen in liquid N_2. The lysate was then either stored at −80°C or immediately used for RNA extraction as previously described [29].

For transcriptome analysis, 35 µg RNA was DNase-treated using the RNase-Free DNase Set (Qiagen) and purified using the RNA Clean-Up and Concentration Micro Kit (Norgen). The quality of the RNA preparations was assessed by means of the Agilent 2100 Bioanalyzer (Agilent Technologies) according to manufacturer's instructions. For two-color hybridizations, a reference pool containing equal amounts of RNA from each sample was prepared.

2.5.2 DNA microarray analysis

Synthesis and purification of fluorescently labeled cDNA were carried out according to Charbonnier et al. [30] with minor modifications. In detail, 10 µg of total RNA was mixed with random primers (Promega) and spike-ins (Two-Color RNA Spike-In Kit, Agilent Technologies). The RNA/primer mixture was incubated at 70°C for 10 min followed by 5 min incubation on ice. Then, the following reagents were added: 10 µL of 5 × first strand buffer (Invitrogen), 5 µL of 0.1 M DTT (Invitrogen), 0.5 µL of a dNTP mix (10 mM dATP, dGTP, and dTTP, 2.5 mM dCTP), 1.25 µL of Cy3-dCTP or Cy5-dCTP (GE Healthcare) and 2 µL of SuperScript II reverse transcriptase (Invitrogen). The reaction mixture was incubated at 42°C for 60 min and then heated to 70°C for 10 min. After 5 min on ice, the RNA was degraded by incubation with two units of RNaseH (Invitrogen) at room temperature for 30 min. Labeled cDNA was then purified using the CyScribe GFX Purification Kit (GE Healthcare). The individual samples were labeled with Cy5, whereas the reference pool was labeled with Cy3. In total, 500 ng of Cy5-labeled cDNA and 500 ng of Cy3-labeled cDNA were hybridized together to the microarray following Agilent's hybridization, washing and scanning protocol (Two-Color Microarray-based Gene Expression Analysis, version 5.5).

2.5.3 Data analysis

Data were extracted and processed using the Feature Extraction software (version 9.5, Agilent Technologies). For each gene on a microarray, the error-weighted average of the log-ratio values of the individual probes was calculated using the Rosetta Resolver software (version 7.2.1, Rosetta Biosoftware). As the analysis was performed by hybridizing the individual samples against a common reference, the ratio values represent relative gene expression levels at a given time point. Further analyses were performed with the GeneSpring software (Agilent Technologies) and TMEV plugin.

2.6 Sample preparation for electron microscopy

B. subtilis 168 was cultivated as described above. One hour after plasma treatment (5 W) the cells were rapidly separated from the culture medium by filtration [31]. Microfil V filtration system and 0.45 µm pore size sterile filters were

used (Millipore) [32]. The cells on the sterile filter were washed shortly in washing solution (100 mM HEPES, 1 mM CaCl$_2$, 1 mM MgCl$_2$, 25 mM NaN$_3$) and then stored in fixation solution (1% glutaraldehyde, 4% paraformaldehyde, 0.2% picric acid, 5 mM HEPES [pH 7.4], 50 mM NaN$_3$ for 1 h at room temperature. After overnight storage at 4°C, the samples were treated with osmium tetroxide vapor for three days. After drying over sodium hydroxide disks for three wks at −20°C, the samples were mounted on aluminum stubs, sputtered with gold/palladium and examined in an EVO LS10 (Zeiss, Oberkochen, Germany).

## 3   Results

3.1   Plasma diagnostics

In order to investigate and understand the influence of plasma on microorganisms it is necessary to know what kinds of biologically active agents are produced by the discharge. Therefore, temperature measurements as well as OES and Fourier transformed infrared spectroscopy (FTIR) were performed in this work as plasma diagnostic tools.

3.2   Temperature measurements

Since the gas temperature inside the discharge chamber may have a significant effect on the microorganisms, we measured the gas temperature in the discharge region as a function of the plasma power (Supporting Information Fig. S1). For this, a fiber optical sensor (Optocon GmbH, Fotemp1) with a diameter of 0.55 mm was positioned between the dielectric and the hollow cylinder assuring that no contact to the liquid occurred. As the plasma ignites, the temperature increases about 10°C with respect to the reference condition without plasma. The variation of plasma power between 0.9 and 5 W results in temperatures of 48–55.4°C and in a temperature slope of +1.7°C/W. In contrast, additional temperature measurements of the growth broth directly after plasma treatment did not show a temperature increase but a slight temperature decrease of about 1.5°C. This effect can probably be explained by the constant influx of argon, which was not adjusted to 37°C prior to the plasma treatment.

3.3   Spectroscopic measurements (OES, FTIR)

In order to determine the composition of plasma, two spectroscopic methods (OES, FTIR) were applied. In Fig. 3, the emission spectrum of the argon discharge at a plasma power of 0.9 W is displayed over a wavelength range from 240 to 900 nm. In the near infrared spectral region (700–900 nm) strong emission of excited argon atoms are obtained. Furthermore, bands of OH(A–X) were found in
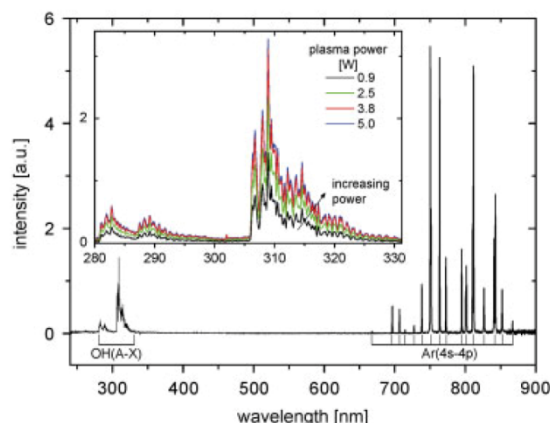
Figure 3. Overview emission spectrum of the discharge in the wavelength range from 240 to 900 nm for a plasma power of 0.9 W. For wavelength higher than 700 nm typical Ar (4s–4p) spectral lines appear. In the ultra violet spectral range only emission bands of the excited hydroxyl molecule around 280 and 308 nm occur. The embedded graph shows the power-depended emission of OH-bands in the wavelength range from 280 to 335 nm.

the UV-B spectral region (280–330 nm). These bands originate from the water vapor fractioning and show a distinct dependence on the plasma power as seen in the embedded graph of Fig. 3. Other excited species that were assumed to occur, including atomic oxygen (emission at 777 nm) or atomic hydrogen (emission at 656 nm) were not detected. Since the air initially situated inside the chamber is replaced by the argon inflow no lines of nitrogen or N$_x$O$_y$ were found.

Although the FTIR spectrometer used in this study is able to detect O$_3$, NO, NO$_2$, N$_2$O, CO, CO$_2$ and H$_2$O$_2$, none of these species were detected. This is in agreement with the OES results.

In conclusion, the biologically active agents produced by the plasma in this experimental setup are heat, excited argon species, hydroxyl radicals, UV-B radiation and high-energy particles such as ions and electrons.

3.4   Plasma treatment leads to growth arrest, depending on the discharge power

As the growth was monitored clear changes in growth were recorded after the plasma treatment and they were related to the discharge power used. All growth curves showed growth arrest during the 15 min of plasma treatment and this started immediately after initiating the argon inflow during the plasma treatment. While a 15 min plasma treatment with a discharge power of 0.9 W led to almost no growth difference compared with the control condition (15 min Argon, no plasma), both the 2.5 and the 5 W discharge led to a growth curve decline (Fig. 4). In order to show that there is

a significant difference between the growth curve of the plasma and non-plasma treated bacteria the 95% confidence interval was calculated for every plasma power setting. The strong overlap of the confidence interval between control and plasma treated cells for the lowest applied plasma power of 0.9 W (Supporting Information Fig. S2a) is replaced by a separated confidence interval of interval with rising plasma power (Supporting Information Fig. S2b and c).

3.5 Plasma treatment leads to morphological changes of cells

The cell envelope is proposed to be the primary target of plasma treatment [19, 33] with effects ranging from cell wall rupture [33] to pore formation [34–36]. To test for changes in
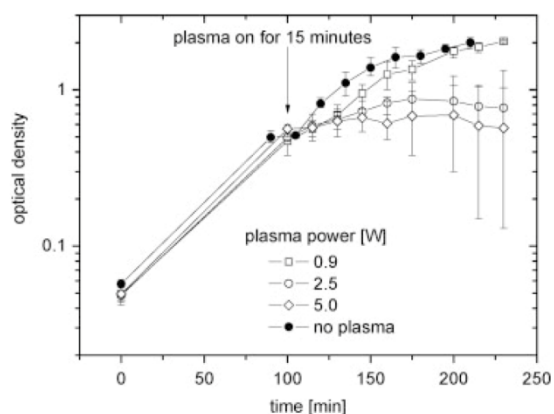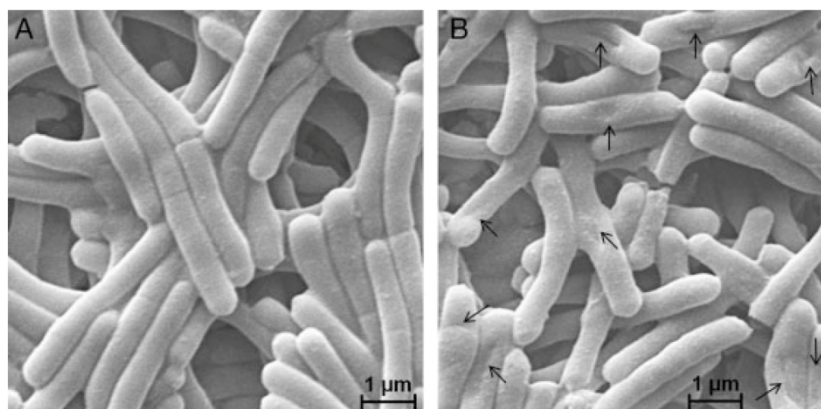

Figure 4. Effect of plasma treatment on growth of *B. subtilis*. Cells were grown aerobically in LB medium at 37°C. At an OD_{540} 0.5, different discharge power settings (0.9, 2.5, 5 W) were applied for 15 min and afterwards the growth was monitored for 120 min. Each growth curve was performed thrice and growth differences between the biological replicates are indicated by error bars.

the cell morphology due to the argon plasma treatment, samples were taken for electron microscopy analysis 5, 60 and 120 min after the plasma treatment. As a reference, non-treated cells were provided. No morphological abnormality was found in the non-plasma treated *B. subtilis* controls (Fig. 5A). The same was true for cells taken 5 min after the plasma treatment (see Supporting Information Fig. S3). However, 60 min after plasma treatment *B. subtilis* cells displayed noticeable dents on the surface indicated by arrows in Fig. 5B. These dents are still visible 120 min after plasma treatment (see Supporting Information Fig. S2D).

3.6 Plasma treatment leads to numerous changes in protein patterns
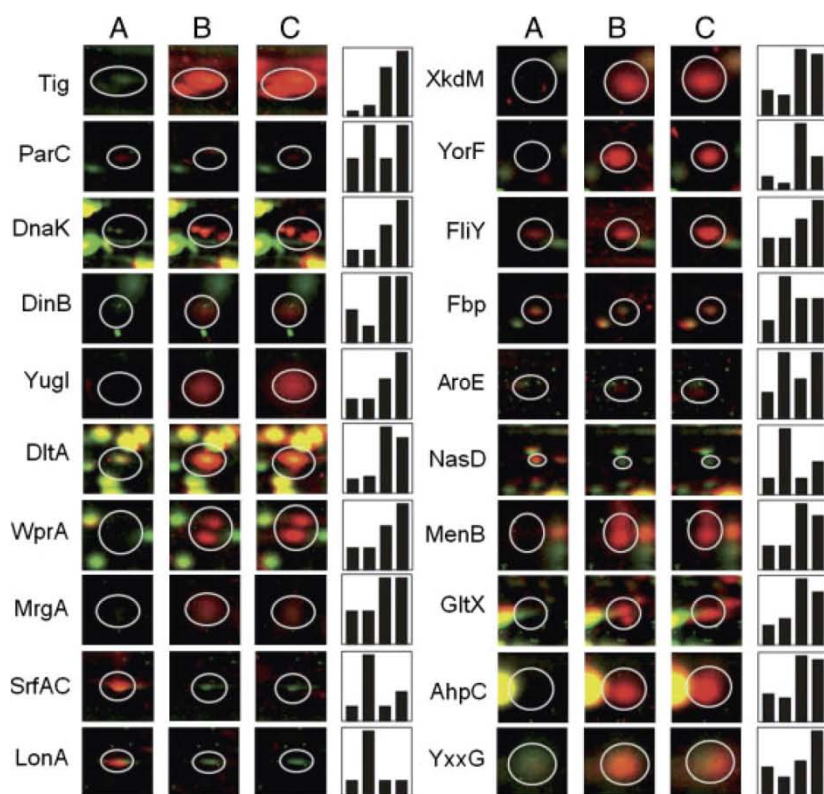
The numbers of significantly affected proteins varied considerably, depending on the discharge power employed. The lowest applied discharge power (0.9 W) yielded 13 changed proteins. In all, 45 proteins were observed at 2.5 W discharge power and 35 proteins at the highest applied power of 5 W with the proteomic approach. The actual overlay of proteins under the three applied discharge voltages is very heterogeneous. Only 1 of the 13 proteins affected at 0.9 W – RocA – is among those affected in cells treated with a plasma power of 2.5 W. RocA is also the only protein that displays an altered protein amount under all three applied discharge voltages. An overlap of three proteins between the highest (5 W) and the lowest (0.9 W) applied discharge voltage is seen. In contrast, an overlap of 21 proteins was found in the data sets of the 2.5 and 5 W treated cells (see Supporting Information Fig. S4).

In total, 70 proteins exhibit changes in abundance (ratio <0.5; >2; *p*-value 0.01) (Supporting Information Table S1, Fig. 6). In all, 32 proteins displayed an increased and 38 a decreased protein amount on the 2-D gels. The affected proteins belong to a wide range of functional categories that were derived from *Subti*wiki (http://www.subtiwiki.uni-goettingen.de). The

**Figure 5.** Putative morphological effects of plasma treatment on *B. subtilis* were investigated. Cells were grown aerobically in LB medium at 37°C. At an OD_{540} 0.5 the cells were treated with 15 min argon influx (A) or a 15 min discharge power of 5 W (B). Cells were harvested 60 min after argon plasma treatment and prepared for electron microscopy. In B, dents on the cell surface are visible (indicated by arrows).

Figure 6. The intracellular proteomes of *B. subtilis*. False-colored dual-channel image of 2-D gels of intracellular *B. subtilis* proteins (15 min argon influx) (green) and *B. subtilis* (15 min 2.5 W argon plasma treatment) (red). *B. subtilis* was grown in LB medium and treated at OD_{540} 0.5 with either 15 min argon influx (control condition) or 15 min argon plasma treatment (stress condition). 120 min after treatment, cells were harvested and proteins (350 µg) were obtained by cell disruption, followed by protein preparation. Proteins were separated on 2-D gels by using immobilized pH gradient strips with a linear pH range of 4–7. Proteins were stained with colloidal Coomassie Brilliant Blue. Protein spots present in equal amounts in conditions appear in yellow, protein spots present in higher amounts under stress conditions appear in red, and protein spots present in higher amounts under control conditions appear in green. Only proteins, which have a significantly changed protein amount (ratio <0.5; >2, *p*-value: 0.01) in the entire experiment (plasma off versus 0.9 W, versus 2.5 W and versus 5 W) have been marked (see also Supporting Information Table S1).

highest ratio of all 70 proteins can be assigned to Tig, which has a 17-fold altered protein amount. Six proteins belonging to the functional category of protein synthesis, modification and degradation display protein alteration (Tig, LonA, SecA, GltX, TufA and DnaK). Dlta and WprA, both belonging functionally to the cell wall category, show a more than 4-fold increased protein amount. MrgA, SrfAC, YugI, ParC, DinB, XkdM and YorF complete the list of proteins, which display a more than 4-fold protein amount on the 2-D gels. Eight proteins (FliY, Fbp, AroE, NasD, MenB, AhpC, YxxG) represent the group of more than 3-fold increased proteins (Fig. 7). Many of the affected proteins can be assigned to known regulons of *B. subtilis*. The best covered one is the PerR regulon, which governs the response to peroxides [37, 38]. Among the 70 proteins significantly changed in their expression as a consequence of plasma treatment, are four PerR-associated proteins (AhpC, AhpF, HemL, MrgA).

3.7 Plasma treatment leads to a rapid and global transcriptional response

Two hundred and eighty genes were found to be significantly regulated (ratio <0.5; >2; *p*-value 0.01) (Supporting Information Table S2) as a consequence of plasma treatment.

A classification according to functional groups was performed on the base of *Subti*wiki. The two most highly regulated genes were the catalase encoding *katA* gene (>200-fold upregulated) and *mrgA* (>100-fold upregulated). Both of these are transcriptionally upregulated in response to oxidative stress. The third highest upregulated gene was *yobU* (>50-fold) which so far has no known function. Eight genes were more than 20-fold induced by plasma treatment (*dhbA*, *dhbB* >30-fold, *dhbE*, *dehC*, *hmp*, *ykuN*, *ykuO*, *ykuP*) and eight genes were more than 10-fold induced (*tuaD*, *ygaK*, *dhbF*, *ahpC*, *ahpF*, *yklA*, *yolD*, *yybP*).

Interestingly, almost all significantly regulated genes belonging to the functional categories cell wall, motility and chemotaxis, coping with stress, prophages, sporulation and homeostasis were upregulated. In contrast, all genes, belonging to the functional categories metabolism of nucleotides and nucleic acids and carbon metabolism were downregulated. The largest group of regulated genes is part of the category other/unknown function (65 genes). Of these 65 genes, 36 were upregulated, the remaining 29 were down regulated. Several well known regulons were covered by the 280 significantly altered transcripts. Positively as well as negatively regulated genes of four regulons, which were best covered by the 280 genes, are displayed in Fig. 8: the LexA regulon, which acts as SOS response to DNA damage [39], the Spx regulon, containing genes that react to thiol stress

Figure 7. Details of dual-channel images of selected proteins, which were more than 3-fold induced in response to argon plasma treatment. Row A displays the comparison between argon gas and 0.9 W plasma treatment; Row B displays argon gas and 2.5 W and Row C, argon gas and 5 W. Spot analysis as in Fig. 6. The bar charts represent average spot volumes of the total spot volume (%) in the order (from left to right): control (only argon influx), argon plasma treatment with a discharge power of 0.9, 2.5 and 5 W.
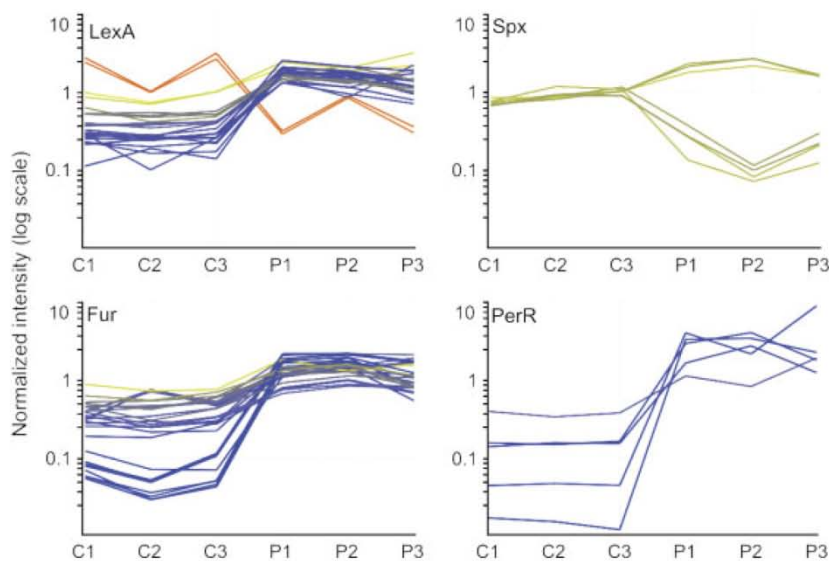
Figure 8. The four best-covered regulons are shown. Only significantly altered genes (ratio <0.5; >2; *p*-value 0.01) of the respective regulon are displayed. C1-3 represents the three control replicates and P1-3 the three plasma treatment replicates.

[38], the PerR regulon, which is the major regulator of the hydrogen peroxide stress response, and the Fur regulon, a global regulator of iron homoeostasis [40] (Supporting Information Table S3). The complete data set is accessible through GEO Series accession no. GSE27113.

4 Discussion

We have performed comprehensive proteomic and transcriptomic analysis to investigate the complex cellular response of microorganisms towards low temperature

plasma. The construction of an innovative plasma source enabled us to reproducibly cultivate *B. subtilis* 168 in liquid medium with or without plasma treatment. So far, inactivation studies of e.g. spores with the help of plasma treatment were performed mostly on solid culture media [17, 41–43]. First, it was necessary to compare the growth behavior of *B. subtilis* in flasks with the growth in the plasma apparatus. No significant growth differences were found (Supporting Information Fig. S5). In the stress experiments the 15 minutes of argon flow led to a rapid growth inhibition. This inhibition might be due to the fact that the availability of oxygen is reduced, which probably leads to anaerobic-like conditions. Nevertheless we could not detect a typical anaerobic genetic signature in our analysis. However, given the time required to exchange air for argon in the apparatus, the actual oxygen-free period may be too short for a clear anaerobic response. In line with this notion, we found no induction of the Fnr regulon which is an integral part of the system governing adaptation to low oxygen availability [44, 45]. A hint for oxygen limitation might be the induction of *nasD* (7-fold) and *hmp* (29-fold), which are known to be regulated by the ResDE two-component system. This system activates transcription of genes required for nitrate respiration in response to oxygen limitation. The nitrite reductase *nasD* and the flavohaemoglobin *hmp* are the most highly induced during nitrate respiration or by nitric oxide (NO) [46, 47]. However, as discussed later, the clear up regulation of *hmp* might rather be explained by NO stress. The slight temperature decrease of about 1.5°C of the growth broth due to the argon inflow, might also have contributed to the observed growth arrest. This temperature decrease was restored to 37°C within 10 min after the argon influx/plasma treatment and no induction of cold shock genes was detected. Together the combination of a brief oxygen deprivation and a minor temperature decrease might explain the observed growth arrest without being sufficient to leave a genetic fingerprint. In line with this explanation is the fact that no growth arrest was observed during plasma treatment with no additional gas influx (unpublished data).

To focus on the influence of plasma treatment, we chose argon gas treated cells as controls in the proteomic and transcriptomic experiments. We determined the contribution of a temperature change induced by the plasma treatment and showed that this had a negligible effect on the cells (Supporting Information Table S4).

In an analysis of the effects of plasma on microorganisms the central questions relate to the cellular targets of the treatment and to the nature of the plasma agents, which induce cellular responses.

Obviously the most exposed target of direct plasma treatment is the bacterial cell envelope. By scanning electron microscopy we showed clear morphological irregularities on the cell surface of *B. subtilis* after a 15 min argon plasma treatment (discharge power of 5 W). Since the morphological changes do not directly occur after the plasma treatment,

but are first visible 60 min after the treatment and are still observed after 120 min, we consider them to be secondary effects resulting from the deregulation of other cell mechanisms. Further indications for a destructive effect on the cell envelope were found in the proteomic and transcriptomic results. Two major cell surface proteins were found to be clearly upregulated (> 4-fold) in the proteomic results, namely DltA and WprA. In *B. subtilis* both are regulated by the two-component system YvrGHb [48] which is responsible for the regulation of cell surface maintenance. DltA is responsible for the D-alanine esterification of lipoteichoic acids and wall teichoic acids [49] and WprA is a cell wall-associated protein precursor [50]. YxxG, the second gene of the wapA-yxxG operon and another target of the YvrGHb regulon is also upregulated.

WprA is a 96 kDa cell wall-bound protein (CWBP), which is processed into two cell wall proteins, CWBP52 and CWBP23. CWBP52 is a cell wall-associated serine protease and CWBP23 has a chaperone function. Both are localized to the cell surface [50, 51]. After plasma treatment we find three WprA spots on the intracellular 2-D gels with a putative p*I* of 6 and MW of 50 kDa. This is curious since the calculated isoelectric point of the 96 kDa polypeptide is 10.1. However, the N-terminal region, corresponding to CWBP23, is acidic (p*I* 4.7), whereas the C-terminal moiety, encompassing CWBP52, is basic (p*I* 9.9). The position on the gel together with the MALDI data sequence coverage suggests that the WprA spots represent the CWBP52 polypeptide lacking the C-terminal hydrophobic region. The exact composition and origin of these post-translational modified WprA isoforms remains to be elucidated by further experiments.

The microarray data set contains a further 88 regulated cell envelope-associated genes, of which 62 were upregulated. A group of 16 genes, all of which belong to the functional category motility and chemotaxis, are regulated by the alternative Sigma factor SigD. SigD is required for expression of flagellin, motor proteins and methyl-accepting chemotaxis proteins and contributes to the expression of autolysins [52]. In total, 24 SigD-dependent genes were found to be upregulated. This consistent up regulation suggests a response to damage of flagellar structures and the efforts of the cells to rearrange the cell envelope attachments. Other examples underlining the hypothesis, that *B. subtilis* senses cell wall stress are the four upregulated SigW-dependent genes *yrhH*, *yuaF*, *yuaG* and *yuaI*. SigW belongs to the extracytoplasmic function (ECF) subfamily of the σ^{70} family of sigma factors. As the name indicates, ECF factors mainly control functions associated with the cell surface or transport and detoxification [53]. The entirety of cell wall-related processes can be assumed to result from the impact of high-energy plasma particles (e.g. ions and excited atoms) in combination with the UV-irradiation.

Behind the cell envelope barrier, a second class of possible plasma-triggered effects are damaged macromolecules such

as RNA, DNA and proteins which induce a variety of repair mechanisms.

The SOS response is an inducible DNA repair and damage tolerance system that responds to triggers such as exposure to ultraviolet light, genotoxic agents, encounter with some classes of antimicrobial agents, nutritional depletion and certain endogenous gene disruptions and is sensed by the highly conserved recombination protein RecA, which facilitates inactivation of the transcriptional repressor LexA. Two LexA-regulated proteins were detected with the proteomic approach (DinB, ParC) and 23 LexA-regulated genes with the transcriptomic approach. Three nucleotide excision repair genes, under the control of the SOS response, *uvrA*, *uvrB*, *uvrC*, were found to be upregulated. The UvrABC proteins recognize and cleave damaged DNA in a multistep ATP-dependent reaction [54]. The induction of the *uvrABC* genes in combination with *recA*, *lexA*, *dinB*, *yhaZ* and *ydgG* supports the interpretation of plasma-triggered DNA damage mainly caused by UV-radiation.

A third detectable response towards plasma treatment is an oxidative stress to OH^- radicals. Oxidative stress is sensed by specific transcriptional regulators, which activate defense mechanisms when the ROS concentration exceeds a critical level [55, 56]. In *B. subtilis*, protection against inorganic peroxides is primarily mediated by the induction of specific stress proteins, controlled by the repressor protein PerR [38, 57–60]. Induction of the PerR regulon was demonstrated with the proteomic and transcriptomic approaches by the up regulation of marker proteins such as AhpC, AhpF, MrgA, HemL, KatA and HemX. PerR is the major regulator of the hydrogen peroxide stress response and the PerR regulon includes genes coding for the antioxidant response [60]. Furthermore, 27 genes regulated by the Fur regulon were induced. Fur is a major iron-controlled transcriptional regulator in *B. subtilis* [38] and under normal conditions, Fur with Fe^{2+} as corepressor represses transcription by binding to the Fur-Box. However, during oxidative stress, Fe^{2+} is oxidized to Fe^{3+} via the Fenton reaction and this results in the generation of hydroxyl radicals [61]. Damaged iron-sulfur proteins might also have supplied free iron, which can be oxidized by Fenton chemistry to form additional hydroxyl radicals. Consequently, depletion of the corepressor Fe^{2+} abolishes Fur binding to the DNA leading to the activation of the Fur regulon which in turn enhances the iron uptake systems [38, 40, 62–64]. Another source for hydroxyl radical is the applied plasma itself, which was proven by OES measurements. Fur does directly control the transcription of at least 39 genes arranged in 20 operons [65]. In total, 27 of these genes (arranged in 14 operons) were regulated in our data set, e.g. the complete *dhbACEBF-*, the *yvyCfliDST-* and *ykuNOP*-operons were covered.

Furthermore, Spx is a global oxidative stress regulator [66]. Spx is an RNA polymerase (RNAP)-binding protein and its regulon is composed of genes, whose product function in

thiol homeostasis. Three genes, thioredoxin (*trxA*), thioredoxin reductase (*trxB*) and *nfrA* (flavin mononucleotide-dependent NADPH oxidase), known to be transcriptionally induced under conditions of thiol-specific oxidative stress were found with our data set [67]. Additionally, genes that are under negative control by Spx [68], namely *srfAB*, *srfAC*, *srfAD*, *comS*, were detected.

Reactive nitrogen species can also affect the activity of enzymes by their reaction with bound free radicals or with metal centers. Indirect effects of NO are caused by the reaction of the radical with oxygen or superoxide, resulting in the formation of a number of additional reactive nitrogen species, including nitrogen dioxide, peroxynitrite and dinitrogen trioxide. These nitrogen species differ in reactivity, stability and biological activity but result in a broad spectrum of antimicrobial activity [37, 69]. Although OES and FTIR diagnostics proved the absence of NO species, 13 of 41 known NO stress marker proteins were present in the transcriptomic data set [37]. The upregulation of *hmp* is recognizes as a central feature of NO stress adaptation in *B. subtilis* and *hmp* is 29-fold upregulated after plasma treatment. In the presence of oxygen, the Hmp enzyme acts as an NO scavenger and is responsible for the direct detoxification of NO to nitrate [70, 71]. Besides Hmp, three marker proteins for NO stress, namely YwfI, YvyD and HemH, were induced.

The comparison of the known transcriptomic signatures with so far uncharacterized stimulons like physical plasma enables an easier classification and interpretation of the data. An overview about overlapping changes in gene

	SOS	H_2O_2	Diamid	anaerob	NO	Plasma
SOS		11	0	0	0	16
H_2O_2	11		7	4	9	45
Diamid	0	7		0	4	8
anaerob	0	4	0		2	14
NO	0	9	4	2		13
Plasma	16	45	8	14	13	

Figure 9. Transcriptomic signatures of SOS response, H_2O_2-, diamide-, NO stress and anaerobiosis based on the literature. The argon plasma signature for *B. subtilis* is from this work. Numbers display the overlap of genes, which were regulated in the respective experiment.

expression between transcriptomic signatures for various stress experiments from the literature [37, 72–75] with the newly investigated argon plasma stress is displayed in Fig. 9. This comparison underlines the similarity to signatures involved in oxidative stress response.

This growth chamber apparatus may in future experiments easily be adapted to cultivate and analyze other pro- or eukaryotic species. An interesting task will be the comparison of soil adapted microorganisms to those colonizing or infecting the human host with regard to the plasma stress response. Another future line of investigation will be the modification of plasma parameters and their effects on the microbial proteome and transcriptome. This opens up the opportunity to systematically investigate the microbe–plasma interaction in greater detail.

5   References

[1] Fridman, G., Friedman, G., Gutsol, A., Shekhter, A. B. et al., Applied plasma medicine. *Plasma Process. Polymers* 2008, *5*, 503–533.

[2] Weltmann, K. D., Kindel, E., von Woedtke, T., Hahnel, M. et al., Atmospheric-pressure plasma sources: prospective tools for plasma medicine. *Pure Appl. Chem.* 2010, *82*, 1223–1237.

[3] Weltmann, K. D., von Woedtke, T., Brandenburg, R., Ehlbeck, J., Biomedical applications of atmospheric pressure plasma. *Chem. Listy* 2008, *102*, 1450–1451.

[4] Morfill, G. E., Kong, M. G., Zimmermann, J. L., Focus on plasma medicine. *New J. Phys.* 2009, *11*.

[5] Sladek, R. E. J., Stoffels, E., Walraven, R., Tielbeek, P. J. A., Koolhoven, R. A., Plasma treatment of dental cavities: a feasibility study. *IEEE Trans. Plasma Sc.* 2004, *32*, 1540–1543.

[6] Bussiahn, R., Brandenburg, R., Gerling, T., Kindel, E. et al., The hairline plasma: An intermittent negative dc-corona discharge at atmospheric pressure for plasma medical applications. *Appl. Phys. Lett.* 2010, *96*, 143701.

[7] Ben Gadri, R., Roth, J. R., Montie, T. C., Kelly-Wintenberg, K. et al., Sterilization and plasma processing of room temperature surfaces with a one atmosphere uniform glow discharge plasma (OAUGDP). *Surf. Coat. Technol.* 2000, *131*, 528–542.

[8] Brandenburg, R., Krohmann, U., Stieber, M., Weltmann, K. D. et al., Antimicrobial treatment of heat sensitive products by atmospheric pressure plasma sources. *Plasma Assisted Decontamination of Biological and Chemical Agents*, Springer 2008, 51–63.

[9] Cheng, C., Liu, P., Xu, L., Zhang, L. Y. et al., Development of a new atmospheric pressure cold plasma jet generator and application in sterilization. *Chin. Phys.* 2006, *15*, 1544–1548.

[10] Daeschlein, G., von Woedtke, T., Kindel, E., Brandenburg, R. et al., Antimicrobial activity of an atmospheric pressure plasma jet agian relevant wound pathogens in vitro on a simulated wound environment. *Plasma Process. Polymers* 2010, *7*, 224–230.

[11] Ehlbeck, J., Schnabel, U., Polak, M., Winter, J. et al., Low temperature atmospheric pressure plasma sources for microbial decontamination. *J. Phys. D – Appl. Phys.* 2011, *44*, 013002.

[12] Fridman, G., Peddinghaus, M., Ayan, H., Fridman, A. et al., Blood coagulation and living tissue sterilization by floating-electrode dielectric barrier discharge in air. *Plasma Chem. Plasma Process.* 2006, *26*, 425–442.

[13] Shekhter, A. B., Serezhenkov, V. A., Rudenko, T. G., Pekshev, A. V., Vanin, A. F., Beneficial effect of gaseous nitric oxide on the healing of skin wounds. *Nitric Oxide – Biol. Chem.* 2005, *12*, 210–219.

[14] Moisan, M., Barbeau, J., Moreau, S., Pelletier, J. et al., Low-temperature sterilization using gas plasmas: a review of the experiments and an analysis of the inactivation mechanisms. *Int. J. Pharm.* 2001, *226*, 1–21.

[15] Boudam, M. K., Moisan, M., Saoudi, B., Popovici, C. et al., Bacterial spore inactivation by atmospheric-pressure plasmas in the presence or absence of UV photons as obtained with the same gas mixture. *J. Phys. D – Appl. Phys.* 2006, *39*, 3494–3507.

[16] Laroussi, M., Low temperature plasma-based sterilization: Overview and state-of-the-art. *Plasma Process. Polymers* 2005, *2*, 391–400.

[17] Roth, S., Feichtinger, J., Hertel, C., Characterization of *Bacillus subtilis* spore inactivation in low-pressure, low-temperature gas plasma sterilization processes. *J. Appl. Microbiol.* 2010, *108*, 521–531.

[18] Laroussi, M., Leipold, F., Evaluation of the roles of reactive species, heat, and UV radiation in the inactivation of bacterial cells by air plasmas at atmospheric pressure. *Int. J. Mass Spectrom.* 2004, *233*, 81–86.

[19] Dobrynin, D., Fridman, G., Friedman, G., Fridman, A., Physical and biological mechanisms of direct plasma interaction with living tissue. *New J. Phys.* 2009, *11*, 0115020.

[20] Antelmann, H., Hecker, M., Zuber, P., Proteomic signatures uncover thiol-specific electrophile resistance mechanisms in *Bacillus subtilis*. *Expert Rev. Proteomics* 2008, *5*, 77–90.

[21] Hecker, M., Volker, U., Towards a comprehensive understanding of *Bacillus subtilis* cell physiology by physiological proteomics. *Proteomics* 2004, *4*, 3727–3750.

[22] Landsberg, K., Scharf, C., Darm, K., Wende, K. et al., The use of proteomics to investigate plasma–cell interaction. *Plasma Med.* 2010, *1*, 55–63.

[23] Kohler, C., Wolff, S., Albrecht, D., Fuchs, S. et al., Proteome analyses of Staphylococcus aureus in growing and non-growing cells: a physiological approach. *Int. J. Med. Microbiol.* 2005, *295*, 547–565.

[24] Eymann, C., Dreisbach, A., Albrecht, D., Bernhardt, J. et al., A comprehensive proteome map of growing *Bacillus subtilis* cells. *Proteomics* 2004, *4*, 2849–2876.

[25] Bernhardt, J., Buttner, K., Scharf, C., Hecker, M., Dual channel imaging of two-dimensional electropherograms in *Bacillus subtilis*. *Electrophoresis* 1999, *20*, 2225–2240.

[26] Candiano, G., Bruschi, M., Musante, L., Santucci, L. et al., Blue silver: a very sensitive colloidal Coomassie G-250 staining for proteome analysis. *Electrophoresis* 2004, *25*, 1327–1333.

[27] Wolff, S., Antelmann, H., Albrecht, D., Becher, D. et al., Towards the entire proteome of the model bacterium *Bacillus subtilis* by gel-based and gel-free approaches. *J. Chromatogr. B, Analyt. Technol. Biomed. Life Sci.* 2007, *849*, 129–140.

[28] Eymann, C., Homuth, G., Scharf, C., Hecker, M., *Bacillus subtilis* functional genomics: global characterization of the stringent response by proteome and transcriptome analysis. *J. Bacteriol.* 2002, *184*, 2500–2520.

[29] Homuth, G., Masuda, S., Mogk, A., Kobayashi, Y., Schumann, W., The dnaK operon of *Bacillus subtilis* is heptacistronic. *J. Bacteriol.* 1997, *179*, 1153–1164.

[30] Charbonnier, Y., Gettler, B., Francois, P., Bento, M. et al., A generic approach for the design of whole-genome oligoarrays, validated for genomotyping, deletion mapping and gene expression analysis on *Staphylococcus aureus*. *BMC Genomics* 2005, *6*, 95.

[31] Meyer, H., Liebeke, M., Lalk, M., A protocol for the investigation of the intracellular *Staphylococcus aureus* metabolome. *Anal. Biochem.* 2010, *401*, 250–259.

[32] Saez, M. J., Lagunas, R., Determination of intermediary metabolites in yeast. Critical examination of the effect of sampling conditions and recommendations for obtaining true levels. *Mol. Cell. Biochem.* 1976, *13*, 73–78.

[33] Pompl, R., Jamitzky, F., Shimizu, T., Steffes, B. et al., The effect of low-temperature plasma on bacteria as observed by repeated AFM imaging. *New J. Phys.* 2009, *11*, 115023.

[34] Coulombe, S., Leveille, V., Yonson, S., Leask, R. L., Miniature atmospheric pressure glow discharge torch (APGD-t) for local biomedical applications. *Pure Appl. Chem.* 2006, *78*, 1147–1156.

[35] Leveille, V., Coulombe, S., Design and preliminary characterization of a miniature pulsed RF APGD torch with downstream injection of the source of reactive species. *Plasma Sources Sci. Technol.* 2005, *14*, 467–476.

[36] Weaver, J. C., Electroporation of cells and tissues. *IEEE Trans. Plasma Sci.* 2000, *28*, 24–33.

[37] Hochgrafe, F., Wolf, C., Fuchs, S., Liebeke, M. et al., Nitric oxide stress induces different responses but mediates comparable protein thiol protection in *Bacillus subtilis* and *Staphylococcus aureus*. *J. Bacteriol.* 2008, *190*, 4997–5008.

[38] Zuber, P., Management of oxidative stress in Bacillus. *Ann. Rev. Microbiol.* 2009, *63*, 575–597.

[39] Kelley, W. L., Lex marks the spot: the virulent side of SOS and a closer look at the LexA regulon. *Mol. Microbiol.* 2006, *62*, 1228–1238.

[40] Giedroc, D. P., Hydrogen peroxide sensing in *Bacillus subtilis*: it is all about the (metallo)regulator. *Mol. Microbiol.* 2009, *73*, 1–4.

[41] Boudam, M. K., Moisan, M., Synergy effect of heat and UV photons on bacterial-spore inactivation in an N-2-O-2 plasma-afterglow sterilizer. *J. Phys. D – Appl. Phys.* 2010, *43*, 295202.

[42] Deng, X. T., Shi, J. J., Kong, M. G., Physical mechanisms of inactivation of *Bacillus subtilis* spores using cold atmospheric plasmas. *IEEE Trans. Plasma Sci.* 2006, *34*, 1310–1316.

[43] Mahfoudh, A., Moisan, M., Seguin, J., Barbeau, J. et al., Inactivation of Vegetative and Sporulated Bacteria by Dry Gaseous Ozone. *Ozone-Science & Eng.* 2010, *32*, 180–198.

[44] Nakano, M. M., Zuber, P., Anaerobic growth of a ''strict aerobe'' (*Bacillus subtilis*). *Ann. Rev. Microbiol.* 1998, *52*, 165–190.

[45] Reents, H., Munch, R., Dammeyer, T., Jahn, D., Hartig, E., The Fnr regulon of *Bacillus subtilis*. *J. Bacteriol.* 2006, *188*, 1103–1112.

[46] Kommineni, S., Yukl, E., Hayashi, T., Delepine, J. et al., Nitric oxide-sensitive and -insensitive interaction of *Bacillus subtilis* NsrR with a ResDE-controlled promoter. *Mol. Microbiol.* 2010, *78*, 1280–1293.

[47] Spiro, S., Regulators of bacterial responses to nitric oxide. *FEMS Microbiol. Rev.* 2007, *31*, 193–211.

[48] Serizawa, M., Kodama, K., Yamamoto, H., Kobayashi, K. et al., Functional analysis of the YvrGHb two-component system of *Bacillus subtilis*: identification of the regulated genes by DNA microarray and northern blot analyses. *Biosci. Biotechnol. Biochem.* 2005, *69*, 2155–2169.

[49] Perego, M., Glaser, P., Minutello, A., Strauch, M. A. et al., Incorporation of D-alanine into lipoteichoic acid and wall teichoic acid in *Bacillus subtilis*. *Identification of genes and regulation. J. Biol. Chem.* 1995, *270*, 15598–15606.

[50] Antelmann, H., Yamamoto, H., Sekiguchi, J., Hecker, M., Stabilization of cell wall proteins in *Bacillus subtilis*: a proteomic approach. *Proteomics* 2002, *2*, 591–602.

[51] Margot, P., Karamata, D., The wprA gene of *Bacillus subtilis* 168, expressed during exponential growth, encodes a cell-wall-associated protease. *Microbiology* 1996, *142*, 3437–3444.

[52] Chen, L., Helmann, J. D., The *Bacillus subtilis* sigma D-dependent operon encoding the flagellar proteins FliD, FliS, and FliT. *J. Bacteriol.* 1994, *176*, 3093–3101.

[53] Cao, M., Kobel, P. A., Morshedi, M. M., Wu, M. F. et al., Defining the *Bacillus subtilis* sigma(W) regulon: a comparative analysis of promoter consensus search, run-off transcription/macroarray analysis (ROMA), and transcriptional profiling approaches. *J. Mol. Biol.* 2002, *316*, 443–457.

[54] Truglio, J. J., Croteau, D. L., Van Houten, B., Kisker, C., Prokaryotic nucleotide excision repair: the UvrABC system. *Chem. Rev.* 2006, *106*, 233–252.

[55] Farr, S. B., Kogoma, T., Oxidative stress responses in *Escherichia coli* and *Salmonella typhimurium*. *Microbiol. Rev.* 1991, *55*, 561–585.

[56] Pomposiello, P. J., Demple, B., Global adjustment of microbial physiology during free radical stress. *Adv. Microb. Physiol.* 2002, *46*, 319–341.

[57] Bsat, N., Herbig, A., Casillas-Martinez, L., Setlow, P., Helmann, J. D., *Bacillus subtilis* contains multiple Fur homologues: identification of the iron uptake (Fur) and peroxide regulon (PerR) repressors. *Mol. Microbiol.* 1998, *29*, 189–198.

[58] Chen, L., Keramati, L., Helmann, J. D., Coordinate regulation of *Bacillus subtilis* peroxide stress genes by hydrogen peroxide and metal ions. *Proc. Natl. Acad. Sci. USA* 1995, *92*, 8190–8194.

[59] Bsat, N., Chen, L., Helmann, J. D., Mutation of the *Bacillus subtilis* alkyl hydroperoxide reductase (ahpCF) operon reveals compensatory interactions among hydrogen peroxide stress genes. *J. Bacteriol.* 1996, *178*, 6579–6586.

[60] Duarte, V., Latour, J. M., PerR vs OhrR: selective peroxide sensing in *Bacillus subtilis*. *Mol. Biosyst.* 2010, *6*, 316–323.

[61] Py, B., Barras, F., Building Fe-S proteins: bacterial strategies. *Nat. Rev. Microbiol.* 2010, *8*, 436–446.

[62] Varghese, S., Wu, A., Park, S., Imlay, K. R., Imlay, J. A., Submicromolar hydrogen peroxide disrupts the ability of Fur protein to control free-iron levels in *Escherichia coli*. *Mol. Microbiol.* 2007, *64*, 822–830.

[63] Zheng, M., Doan, B., Schneider, T. D., Storz, G., OxyR and SoxRS regulation of fur. *J. Bacteriol.* 1999, *181*, 4639–4643.

[64] Lee, J. W., Helmann, J. D., Functional specialization within the Fur family of metalloregulators. *Biometals* 2007, *20*, 485–499.

[65] Baichoo, N., Wang, T., Ye, R., Helmann, J. D., Global analysis of the *Bacillus subtilis* Fur regulon and the iron starvation stimulon. *Mol. Microbiol.* 2002, *45*, 1613–1629.

[66] You, C., Sekowska, A., Francetic, O., Martin-Verstraete, I. et al., Spx mediates oxidative stress regulation of the methionine sulfoxide reductases operon in *Bacillus subtilis*. *BMC Microbiol.* 2008, *8*, 128.

[67] Tam le, T., Antelmann, H., Eymann, C., Albrecht, D. et al., Proteome signatures for stress and starvation in *Bacillus subtilis* as revealed by a 2-D gel image color coding approach. *Proteomics* 2006, *6*, 4565–4585.

[68] Nakano, S., Erwin, K. N., Ralle, M., Zuber, P., Redox-sensitive transcriptional control by a thiol/disulphide switch in the global regulator, Spx. *Mol. Microbiol.* 2005, *55*, 498–510.

[69] Fang, F. C., Antimicrobial reactive oxygen and nitrogen species: concepts and controversies. *Nat. Rev. Microbiol.* 2004, *2*, 820–832.

[70] Hausladen, A., Gow, A. J., Stamler, J. S., Nitrosative stress: metabolic pathway involving the flavohemoglobin. *Proc. Natl. Acad. Sci. USA* 1998, *95*, 14100–14105.

[71] Poole, R. K., Nitric oxide and nitrosative stress tolerance in bacteria. *Biochem. Soc. Trans.* 2005, *33*, 176–180.

[72] Au, N., Kuester-Schoeck, E., Mandava, V., Bothwell, L. E. et al., Genetic composition of the *Bacillus subtilis* SOS system. *J. Bacteriol.* 2005, *187*, 7655–7666.

[73] Mostertz, J., Scharf, C., Hecker, M., Homuth, G., Transcriptome and proteome analysis of *Bacillus subtilis* gene expression in response to superoxide and peroxide stress. *Microbiology* 2004, *150*, 497–512.

[74] Ye, R. W., Tao, W., Bedzyk, L., Young, T. et al., Global gene expression profiles of *Bacillus subtilis* grown under anaerobic conditions. *J. Bacteriol.* 2000, *182*, 4458–4465.

[75] Leichert, L. I., Scharf, C., Hecker, M., Global characterization of disulfide stress in *Bacillus subtilis*. *J. Bacteriol.* 2003, *185*, 1967–1975.

5.4. Common versus noble- *Bacillus subtilis* differentially responds to air and argon gas plasma

Winter, T., Bernhardt, J., Winter, J., Mäder, U., Schlüter, R., Weltmann, K. D., Hecker, M., Kusch, H.

submitted to *PLoS ONE*

Common versus noble- *Bacillus subtilis* differentially responds to air and argon gas plasma

Theresa Winter[1], Jörg Bernhardt[1,4], Jörn Winter[2,3], Ulrike Mäder[1,5], Rabea Schlüter, Klaus-Dieter Weltmann[2], Michael Hecker[1], Harald Kusch[6]

[1]Institute for Microbiology, Ernst-Moritz-Arndt-University, Greifswald, Germany

[2]Leibniz Institute for Plasma Science and Technology (INP Greifswald e.V.), Felix-Hausdorff-Str. 2, 17489 Greifswald, Germany

[3]Center for Innovation Competence *plasmatis*, Felix-Hausdorff-Str. 2, 17489 Greifswald, Germany

[4]DECODON GmbH, Biotechnikum Greifswald, Walther-Rathenau-Straße 49 a, 17489 Greifswald, Germany

[5]Interfaculty Institute for Genetics and Functional Genomics, Department for Functional Genomics, Ernst-Moritz-Arndt-University, 17489 Greifswald, Germany

[6]Institute for Microbiology and Genetics, Georg-August-University Göttingen, Germany

Corresponding Author information: Theresa Winter, Institute for Microbiology, Ernst-Moritz-Arndt-University Greifswald, 17489, Greifswald, Germany, Tel. +49-3834-864214, fax: +49-3834-864202, e-mail: theresa.winter@uni-greifswald.de

Running title: low temperature plasma impact on growing bacteria

Abtract

The study of low temperature gas plasmas is not only a physicist´s specific topic anymore. Especially since low temperature plasma is not only applied for decontamination and sterilization but also in the medical field in terms of wound and skin treatment [1,2,3]. For the improvement of already established but also for new plasma techniques, in-depth knowledge on the interactions between plasma and microorganism is essential.

Here we present a follow up investigation on the effects of argon plasma on growing *Bacillus subtilis* 168. A growth chamber system suitable for low temperature gas plasma treatment of bacteria in liquid medium enabled a first glimpse on the complex cellular response. In order to gain further knowledge, a second kind of plasma treatment was applied. Combined proteomic and transcriptomic analyses were used to investigate the specific stress response of *B. subtilis* cells to treatment with not only argon but also air plasma.

Besides an overlap of cellular responses due to both- argon and air plasma treatment (DNA damage and oxidative stress), a variety of gas dependent cellular responses such as growth retardation and morphological changes were observed. Only argon plasma treatments lead to a phosphate starvation response whereas air plasma induced the tryptophane operon implying damage by photooxidation.

Biological findings such as oxidative stress responses were supported by the detection of reactive plasma species by OES and FTIR measurements.

Introduction

The study of low temperature gas plasma and its interaction with biological samples has been in the focus of research for many years [4,5,6,7,8].

Plasma is, following by order of increasing energy (solid state, liquid state and gaseous state), the fourth state of matter. It is a partially ionized gas that provides a variety of biological active agents at the same time dependent on the adjusted parameters like gas composition, flow rate, moisture, temperature and excitation properties. These agents are heat, radiation (UV and V-UV), electromagnetic fields, charged particles as well as neutrals and radicals. The superposition of these components gives plasma extraordinary properties but at the same time complicates the understanding of its interaction with biological material. Despite the research effort in recent years in the characterization of plasma-cell interactions, the detailed mode of action is still to a great extent unknown [6,9,10]. This applies for prokaryotic cells, as they cover potential pathogens for humans such as *Staphylococcus aureus* or *Staphylococcus epidermidis* causing a variety of harmful diseases. Furthermore, eukaryotic cells and tissues respectively are of interest in the field of plasma applications, as the human skin can also come in direct contact with plasma, e.g. during wound treatment. The effect of plasma on cells and on their structures and compounds such as cell membranes, DNA, lipids, proteins and others are the key for understanding the plasma´s mode of action.

While bactericidal effects are undisputed, the actual mode of action of plasma at the molecular level is mainly unstudied [11]. But this knowledge is essential for the successful exploitation of plasma in biological settings and for the safe application of plasma devices on tissue.

In order to investigate the effect of plasma on the molecular level in bacterial cells, we adopted well established functional genomics approaches. Proteome and transcriptome analyses are powerful tools to uncover global changes in gene expression in bacterial cells after exposure to stress inducing stimuli such as starvation, heat, anaerobiosis, toxic compounds and for this study – plasma [12]. The resulting proteomic and transcriptomic signatures have been defined by a set of marker proteins or genes those expression is altered in response to a given stress condition [13,14]. Because of extensive knowledge of its stress responses, *B. subtilis* has been selected as a model for the comparison of already known stress signatures with those generated by the exposure to plasma stress.

A first investigation about the effects of argon plasma to *B. subtilis* proved the expected complex cellular response and made, for the first time, a detailed and comprehensive understanding on the transcriptomic and proteomic level possible [12]. In order to expand our knowledge, air plasma and its effects on *B. subtilis* was investigated. The completely different properties of air plasma (e.g. reactive species, heat, radiation) compared to argon plasma seemed an adequate way to gain further understanding about the impact of plasma composition and its direct effect on the cells. The experimental design was identical to the previous study in order to assure reproducibility and comparability. The newly introduced growth chamber system was demonstrated to allow a reproducible plasma treatment of microorganisms in liquid cultures.

A 2-D gel based proteomic approach was complemented with transcriptome analysis. The biological findings were supported by plasma diagnostics enabling an investigation of the reactive species present in argon and air plasma.

Results

Plasma diagnostics

Temperature measurements

Since temperature can have a significant effect on *B. subtilis* cells, the gas temperature in the discharge region was measured for both gases, argon and air (Fig. 1) by using an fiber optical sensor (Optocon GmbH, Fotemp1,diameter: 0.55 mm). The sensor was positioned between the dielectric and the hollow cylinder with no contact to the liquid. In order to avoid long term drifts of the growth medium's temperature the heating of the liquid was controlled by a PID regulator and monitored by a standard thermometer.

For argon plasma, plasma power between 0.9 W and 5 W results in temperatures of 48°C to 55.4°C. In contrast the growth broth temperature measured subsequently to plasma treatment showed a slight temperature decrease of about 1.5°C. This effect can be explained by the constant influx of room tempered argon gas during the plasma treatment.

A steeper temperature increase was observed for air plasma compared to argon gas. Here, the variation of plasma power between 2.0 W and 7.4 W results in a temperature increase from 60°C to 92.5°C. This higher temperature is due to the

higher applied power and the lack of a cooling gas flux through the chamber, since the air plasma is ignited in stationary air atmosphere. Despite the increase of temperature of the plasma gas the temperature of the growth broth remained unchanged.

Results of emission (OES) and absorption (FTIR) measurements

In Fig. 2 the optical emission spectra of the generated argon and air plasma are displayed for discharge power settings of 5.0 W and 4.9 W, respectively. In argon plasma dominant atomic lines of excited argon are obtained together with bands of the excited hydroxyl radical (OH $A^2\Sigma^+ \rightarrow X^2\Pi$). In air plasma the 2nd positive system of nitrogen (N_2 $C^3\Pi_u \rightarrow B^3\Pi_g$) contributes the strongest emission component. Furthermore, spectral lines produced by atomic oxygen O(3p-3s) were detected at 777.2 nm, 777.4 nm and 777.5 nm (not spectrally resolved here). In contrast to argon plasma no bands of excited OH are detectable. In both plasma gas settings radiation in the UV-A region (320-400 nm) and in the UV-B region (280-320 nm) is generated. The intensity of the produced radiation is directly linked to the applied power. By increasing the power the radiation intensity increases, too (data not shown here).

Fig. 3 shows the FTIR spectra obtained for argon and air plasma. In contrast to the argon plasma, where no infrared active species were detected in the considered spectral range, air plasma produces detectable concentrations of ozone (O_3), nitrous oxide (N_2O) and dinitrogen pentoxide (N_2O_5). These species are the result of miscellaneous reactions of molecular or atomic oxygen and nitrogen in combination with nitrogen oxide species [15]. Since the FTIR spectrometer only allows analysis of the exhaust gas outside the chamber it is very likely that other nitrogen oxide molecules like nitric oxide (NO), nitrogen dioxide (NO_2) and the nitrate radical (NO_3) are present inside the discharge region.

Growth retardation depends on plasma treatment and discharge power.

Monitoring growth for 120 minutes after plasma treatment reveals differences depending on the used gas and the applied discharge power. In the argon plasma experiment, three different power settings were applied for 15 min (0.9 W; 2.5 W; 5 W). Growth of control (15 min treatment with argon gas) as well as the plasma treated samples retard during the 15 min treatment. But only argon plasma ignited

with power settings of 2.5 W and 5 W caused clear growth curve declines. 0.9 W discharge power resulted in a growth curve similar to the control condition (see Fig. 4).

In contrast, air plasma inhibited growth only at the highest discharge power (7.4 W). Cells treated with discharge power settings of 2.0 W, 3.5 W and 4.9 W grow at similar rate as the control samples (no plasma treatment) (see Fig. 4).

Plasma treatment leads to morphological changes of cells.

The cell envelope represents the boundary between the organized inner compartment of the cell and the environment. Consequently, it is the primary target for reactive species, which derive from plasma treatment- such as heat, alternating electric fields, charged particles, radiation and reactive neutral species [6,16,17]. Either the structural integrity or specific functions of the cell wall can be targeted and affected. In order to visualize morphological changes due to plasma treatment, samples which had been exposed to argon and air plasma were prepared for electron microscopy. As a reference, non treated cells were provided. Interestingly, plasma treated *B. subtilis* cells displayed plasma specific changes in their cell morphology. Argon plasma causes the formation of dents of the cell surface. They initially appeared 60 min after plasma treatment (see Fig. 5; B-C). Air plasma treated cells become speckled 60 min after plasma treatment and another 60 min later, fibres appear between cells (see Fig. 5; X-Z).

Protein patterns differ due to plasma composition and power

Three different stress conditions were investigated: (i) argon plasma compared to only argon gas, (ii) air plasma compared to untreated cell and (iii) argon gas compared to normal atmospheric air and no plasma treatment. The used gas admixtures as well as the applied plasma power had an influence on the number of affected proteins. In total, the amount of 65 proteins was significantly changed (ratio <0.5 ;>2 ; p-value 0.01) due to argon plasma stress, 84 proteins after air plasma stress and 8 due to pure argon gas. The latter was investigated, in order to evaluate the impact of pure argon gas compared to atmospheric air conditions.

39 of the 65 changed proteins under argon plasma stress displayed a decreased and 26 proteins an increased amount on the 2D gels. The two most highly induced proteins under argon plasma treatment are DltA and OdhB (> 5 fold).

Only 16 of 84 proteins show an increased protein amount due to air plasma treatment. DnaK, LonA, MenD, MrgA, SrfAC, XkdK and XkdM display the highest alterations of more than 4fold in due course of the air plasma treatment.

Seven proteins with decreased protein amounts were assigned to pure argon gas treatment and one with an increased protein amount- namely TufA (2.5 fold). The complete list of proteins, their ratios and functional grouping according to SubtiWiki can be found in Tab. S1.

In general increased plasma power does not lead to an increased number of affected proteins. In the argon plasma experiment, the lowest applied discharge power (0.9 W) resulted in 15 changed proteins. Most proteins- namely 56 proteins were observed at 2.5 W discharge power and 37 proteins at the highest applied power of 5 W. In contrast to argon gas ignited plasma, the lowest applied air plasma power (2 W) resulted in altered amounts of 50 proteins. The increased plasma powers (3.5 W, 4.9 W) lead to 19 and 21 changed proteins, respectively. The highest applied air plasma power of 7.4 W resulted in 69 altered proteins.

To visualize the different protein changes of all three experiments, a color-coded 2D image was created (Fig. 6.). Data of all three investigated discharge voltages for argon plasma and four discharge voltages for air plasma, as well as all control conditions are displayed in Figure 6.

The differences between all three experiments are multilayered , revealing that the overlap between the individual conditions differs considerably. Only two proteins display changes under all three conditions- the naphthoate synthase MenB and the elongation factor TufA. Due to pure argon gas and argon plasma two proteins exhibit changes (IolD, YrbE); four proteins due to pure argon gas and air plasma (CitB, FtsY, KatE, YfhM) and 21 proteins alter in their amount due to argon and air plasma (e.g. RocA, DnaK, AhpF, MrgA).

Plasma treatment leads to a fast and global transcriptional response

Application of argon gas without ignited plasma revealed 774 affected genes. However in the argon plasma experiment 219 genes were specifically regulated. Altered expression of 614 genes was restricted to the air plasma experiment (ratio <0.5;>2;p-value 0.01) (see supplement). The two most regulated genes under argon plasma stress were catalase *katA* (>200-fold up regulated) and *mrgA* (>100-fold up regulated) protecting cells against oxidative stress. Under air plasma stress, five

genes, which are part of the biosynthesis of tryptophan (Trp) are up to 200fold up regulated - namely *trpC, trpF* (both >200fold), *trpB, trpD* and *trpE.* Furthermore *hxlA, hxlB*, flavohemoglobin *hmp* and the catalase *katA* are also more than 100 fold induced. The two most induced genes under argon plasma stress are also highly induced under air plasma stress (*katA* (>190fold); *mrgA* (27fold)). Vice versa, of the highly induced air plasma genes, only *hmp* (29fold induced) is found to be also regulated in the argon plasma experiment. *TrpB,C,D,E,F* and *hlxA, hlxB* are less than 2fold induced or did not pass the ratio threshold in the argon plasma experiments in contrast to air plasma. The complete gene list, their ratios and functional grouping according to SubtiWiki can be found in Tab. S2.

Visualization via Voronoi treemaps

To support the analysis of gene expression data at the transcriptome level, we used a structured representation of gene regulatory information derived from *SubtiWiki* [18]. *SubtiWiki* classifies genes in an acyclic multihierarchical tree graph according e.g. to their regulation. For a well-arranged visualization, Voronoi treemaps were adapted for an intuitive display of large omics data sets with their relative expression data and regulatory classification [19,20] derived from the argon gas only, argon plasma and air plasma experiment. Expression data were visualized in the treemaps using a color gradient: For illustration of mRNA expression level, colors of the range orange (lower than average), yellow (equal to average) and blue (higher than average) were applied to Voronoi cells. The isolated examination of elements of interest makes differences in the transcription pattern between the three experiments clearly visible. As displayed in Figure 7, both plasma treatments as well as pure argon gas resulted in a very heterogeneous pattern, especially with respect to regulons associated with cell envelope stress. Only pure argon gas resulted in the induction of the extracytoplasmic function (ECF) σ factors σ^M, σ^W and σ^X, whereas σ^D is clearly induced under argon plasma stress and σ^Y shows an induction under both plasma stresses. A more homogenous pattern can be observed for other stress regulons. The general stress response regulon controlled by σ^B, the LexA-dependent SOS response regulon, the thiol specific oxidative stress regulon Spx and the oxidative/electrophile stress regulon MhqR are induced under all three conditions but the level of induction differs. In contrast, the oxidative stress regulons Fur and PerR are clearly induced under plasma stress only but not by pure argon gas.

Discussion

In an initial study we analysed the cellular response of argon plasma treated *B. subtilis* cells with a proteomic and transcriptomic approach in a newly developed growth chamber system [12]. By applying the identical experimental setup only changing argon gas by atmospheric air, we here addressed the question if the cellular plasma stress response is general or gas specific.

Argon gas- an unexpected impact on *B. subtilis*

In order to reveal the actual response to argon plasma it was necessary to identify genes, which were significantly altered only by argon gas. The comparison of the two control conditions, argon gas and air- resulted in 774 altered genes. This finding reveals that the impact of argon gas is higher than previously envisioned. The noble gas Argon is inert and does not react chemically with any element at normal temperature and pressure. Despite their chemical indifference, noble gases are known to be biologically active. Next to argon, xenon and helium have shown sedative, hypnotic and analgesic properties. Even neuroprotective effects have been proven [21,22,23].

As air is completely replaced by a constant influx of argon gas, an anaerobic stress response and related physiological effects such as growth retardation were expected. Among the 774 altered genes are 26 genes of the ResD and Rex regulon, which govern the absence of oxygen [24,25,26]. Their presence is proof of an anaerobic condition during the argon experiments. Alongside, growth retardation as under the argon plasma treatment was also observed during argon gas only conditions. Striking is the induction of the σ^W, σ^M and σ^X regulons due to pure argon gas treatment. All three are extracytoplasmic function (ECF) σ factors related to cell envelope homeostasis and antibiotic resistance. They are induced by various stresses which affect the cell envelope such as cell wall antibiotics, alkaline shock, heat and ethanol [27,28]. Despite the clear cell envelope stress response, argon gas alone did not lead to a morphological disruption of the cell envelope detectable by electron microscopy.

Furthermore, 86 σ^B regulated genes are induced due to pure argon gas. The SigB-dependent general stress response with its more than 150 regulon members is induced by a whole collection of diverse stimuli that includes extreme temperatures, ethanol- butanol and osmotic stress, energy stress such as starvation for glucose, phosphate, and oxygen as well as cell wall stress imposed by the addition of

antibiotics such as vancomycin and bacitracin [29]. The expression of the SigB regulon provides *B. subtilis* cells with a non-specific, multiple stress resistance against a wide range of stresses [30,31].

Effects of oxygen availability and temperature on *B. subtlis* during plasma treatment

Interestingly, growth behaviour of argon and atmospheric air plasma treatment differed to the point that a rapid growth inhibition was observed during the 15 min argon plasma treatment but not during air plasma treatment, respectively. The argon gas influx might have lead to an insufficient oxygen supply resulting in a discontinued growth. Temperature changes might be a second reason for the growth arrest. Despite the elevated temperature in the small discharge region of the plasma gas, no temperature increase of the growth medium could be determined. Notably, during the argon plasma experiment, a slight temperature decrease of about 1.5°C of the culture due to the non tempered argon inflow was measured but was restored to 37°C within 10 min after argon influx. This minor temperature shift did not reasonably influence the bacterial transcriptome. Also no heat shock genes were found to be induced under argon plasma stress despite of the elevated temperature in the discharge region of 55°C. Contrarily, air plasma treatment leads to a clear induction of heat shock genes despite the same short exposition time of the cells in the discharge region as in the argon plasma experiment. But as the temperature in the discharge region increases here up to 90°C, class I heat shock genes, as *groES* (4,8 fold) and *groEL* (3,7 fold) are induced and so are all class III heat shock genes of the CtsR regulon (e.g. *clpE* 20.3 fold, *clpC* 7.5 fold, *mcsA* 5.3 fold, *ctsR* 4.4 fold) [32].

Morphological responses after plasma treatment

The cell envelope is obviously the most exposed target of plasma treatment. The type of irregularities apparently differs between the two applied plasma treatments. In case of argon plasma clear dents appeared firstly 60 min after plasma treatment and did not alter in due course of time [12]. Moreau et al. (2007) found similar morphological effects despite a different plasma source and a different organism [33]. Contrarily, by applying air plasma to the cells, we detected a speckled bacterial surface after 60 min and spider web like filaments after 120 min. Speculating on the basis of the findings by electron microscopy these filaments may resemble chromatin

structures or so called neutrophil extracellular traps (NETs)[34]. These NETs are released during a form of pathogen-induced cell death and can trap and kill various bacterial, fungal and protozoal pathogens. Their release is one of the first lines of defense against pathogens and was recently named NETosis [35]. Further investigations are needed to reveal the composition of these air plasma triggered filaments.

The cell wall- primary target of plasma

The differences between the applied plasma stresses regarding cell wall biosynthesis also became evident on the transcriptional level. Argon plasma induced many genes associated with functions of cell wall synthesis and degradation which does not apply for air plasma, respectively. Argon plasma induced genes of the PhoP regulon. PhoP and PhoR form a two component system responding to phosphate starvation. Its activation enables cells to use limiting phosphate resources more efficiently or to make accessible alternative phosphate sources. One response of phosphate starved cells is the substitution of at least part of the wall teichoic acid with teichuronic acid, a phosphate free anionic polymer [36].

PhoP regulon genes include two major vegetative alkaline phosphatase (APase) structural genes, *phoA* and *phoB [37]* and a gene encoding an APase-alkaline phosphodiesterase (APDase), *phoD* [38], which has a putative role in cell wall teichoic acid turnover, the phosphate transport operon *pstSACBABB [39]* and the *tuaABCDEFGH* operon. The latter is responsible for the synthesis of teichuronic acid, which replaces the teichoic acid in the cell walls of phosphate-starved cells [40]. Transcription of *tagAB* and *tagDEF* was shown to be repressed by PhoP-P [41]. In contrast to air plasma the complete *tuaABCDEFGH and pstSACBABB* operons are induced due to argon plasma treatment (see Fig. 8A, adopted from [42]). The high-affinity phosphate uptake operon *pstSACBABB* is even higher induced due to argon gas only which supports the assumption of a cell envelope stress due to argon gas as discussed above. The disturbed cell envelope might have reduced the available phosphate and triggered the cell´s requirement for this essential substrate, leading to the recovery of inorganic phosphate from organic sources such as teichoic and nucleic acids. As phosphate is not only a component of DNA, RNA, phospholipids but also part of the principal nucleotide cofactors required for energy transfer and

catalysis in the cells, argon plasma and its reactive species lead to noticeable disturbance in the phosphate balance.

Radiation and its effect on biomolecules

Behind the cell envelope barrier, many other possible targets for reactive plasma species are present- such as RNA, DNA and proteins. Damage of these biomolecules induce a variety of repair mechanisms. Once again, clear differences between the two applied plasma treatments became obvious on the transcriptional level. In contrast to argon plasma, air plasma induced genes related to amino acid metabolism. Intriguing is the induction of the complete tryptophan (Trp) operon *trpEDCGBA* by air plasma stress (see Fig. 8B).

Photooxidation and the resulting damage of aromatic amino acids might be the primary reason for the extensive induction of the *trp* operon. When proteins are exposed to light, the peptide backbone or the side chains of amino acids such as cysteine but also of aromatic amino acids like- tryptophan (Trp), tyrosine (Tyr) and phenylalanine (Phe), can undergo photooxidation. Photodegradation can lead to changes in primary, secondary and tertiary structures of proteins. Mainly photooxidation begins with the absorption of light resulting in excitation of an electron to higher energy singlet state. Are these proteins in an aqueous solution, the wavelengths for peptide backbone absorption range from 280-305 nm for Trp, 260-290 nm for Tyr, 240-270 nm for Phe, and 250-300 nm for cystine. The processes that follow excitation to the higher energy state e.g. relaxation to ground state, formation of triplet state and reaction with oxygen to form peroxy radicals [43], are influenced by the pH of the solution, by temperature, polarity, nearby side chain and protein structure.

The absorption wavelength of Trp and cysteine correlates with the OH (A-X) (v'=1, v''=0) emission bands at around 285 nm and the emission bands of the second positive system of nitrogen $C^3\Pi_u \rightarrow B^3\Pi_g$ (v'=4, v''=2) at around 295 nm measured in our experiment by means of OES. Hence, both plasma gas settings produce UV photons with sufficient energy for photoexcitation of Trp and cysteine. As oxygen is only present during the air plasma experiment, only here oxygen is available as a possible reaction partner for excited molecules and consequently only due to air plasma clear photooxidative damages can be detected.

Another hint for damaged aromatic compounds might be the induction of MhqR. MhqR was shown to be induced by aromatic compounds such as catechol and 2-methylhydroquinone (2-MHQ) [44]. The latter are quinones, which are endogenously produced electrophiles and part of the respiratory chain. Quinones have two modes of action, an oxidative and a reduced electrophilic mode which can react to semi-quinone anions which in turn reduce molecular oxygen to ROS such as superoxide anions [45]. Air plasma treatment might have lead to an artificially elevated intracellular level of such electophiles possibly leading to the induction of all seven MhqR regulon genes (*mhqA*, *mhqED*, *mhqNOP* and *azoR2*).

Radiation associated DNA damage

UV radiation is a known genotoxic agent and induces several lesions within DNA [46]. Exposure to UV radiation leads to photochemical products such as cyclobutane pyrimidine dimers, pyrimidine–pyrimidinone photoproducts and photohydrates. As UV radiation is mostly one major reactive element produced by plasma a clear induction of the DNA repair mechanisms for argon and air plasma treatments were expected.

The SOS response is known to be triggered by the exposure to UV light. Two major protein players regulate the SOS response: RecA and LexA. RecA inactivates the transcriptional respressor LexA [47,48]. The immediate SOS response which can be detected by microarray analysis is very pronounced. 25 LexA dependent genes are induced due to argon plasma treatment and 32 genes due to air plasma treatment, respectively. Also the nucleotide excision repair genes *uvrA, uvrB, uvrC* controlled by the SOS response are clearly induced by both plasma treatments. The same accounts for *yneA* which delays cell division until DNA repair is completed [49]. No LexA regulated proteins were found with the proteomic approach. A possible reason for that may be the time span of 120 min being sufficient to allow the repair of DNA damage.

Superoxide response

Supported by the induction of characteristic regulons, *B. subtilis* cells suffer from oxidative stress when treated with argon as well as air plasma. Generally speaking, both applied plasma treatments generate ROS but only air plasma generates RNS. As proven by plasma diagnostics, the reactive oxygen species differ between the two applied plasma stresses. Whereas argon plasma treatment led only to the formation

of hydroxyl radicals, in air plasma nitrogen, atomic oxygen, O_3, N_2O and N_2O_5 are detectable.

Reactive metal centers of redox- active proteins are the target of ROS and RNS. Enzymes bearing an exposed $[4Fe\text{-}4S]^+$ cluster can suffer oxidation to $[3Fe\text{-}4S]^+$. The released iron is reduced, in turn, by reaction with cysteine or reduced flavin to Fe2+, which participates with H_2O_2 in Fenton chemistry, yielding highly reactive hydroxyl radicals [50,51].

Air plasma induces 11 genes of the CymR regulon, which controls the sulfur metabolism. Sulfur is a crucial atom in cysteine and methionine, as well as in several coenzymes and cofactors such as thiamine, biotin, or coenzyme A (CoA). Among these compounds, cysteine is important- as mentioned above- for the biogenesis of enzymes containing [Fe-S] clusters and for protein folding and assembly via formation of disulfide bonds. Moreover, cysteine-derived proteins such as thioredoxin play a central role in protection against oxidative stress. CymR has been described as a repressor of the cysteine biosynthesis [52]. The same destructive photooxidative effects of light can be assumed for the cysteines as for Trp.

The protection against reactive oxygen species is mediated by detoxification- and repair enzymes. Their synthesis is typically regulated by redox-sensing transcription factors such as the bacterial peroxide-sensors PerR [53]. Expression of marker genes of the PerR regulon such as *ahpC*, *ahpF*, *mrgA* and *katA* was found to be significantly altered with the proteomic and transcriptomic approaches under argon and air plasma stress. 13 of known 15 genes were found to be regulated in the array data sets due to argon plasma and 11 genes due to air plasma, respectively. Furthermore, 38 of 45 known Fur regulated genes were induced due to argon plasma stress and 29 due to air plasma stress. Fur is a major iron-controlled transcriptional regulator in *B. subtilis*. Under normal conditions, Fur with Fe^{2+} as co-repressor blocks transcription by binding to the Fur-Box. But during oxidative stress, Fe^{2+} is oxidized to Fe^{3+} via the Fenton reaction and the Fur-Box becomes accessible [50,51].

A third oxidative stress response regulator- namely Spx was found to be significantly induced also, but to different extents in our plasma experiments. Spx is a regulatory protein of genes involved in thiol homeostasis if cells encounter oxidative protein stress by non-native disulphide bond formation [54,55]. 12 of 17 known Spx activated genes were found due to air plasma but only 3 genes due to argon plasma treatment. All three were already found to be altered by argon gas only. Additionally, five genes,

which are under negative control by Spx [56], namely *srfAA, srfAB, srfAC, srfAD* and *comS* were detected due to both plasma experiments.

Conclusion and outlook

Figure 9 summarizes the complex cellular response to either argon or air plasma stress. The simple replacement of argon gas by atmospheric air led to a broad spectrum of similar but also plasma specific stress responses. We were able to demonstrate that both plasma stresses provoked an oxidative-, as well as a SOS stress response. Argon plasma specific responses were besides morphological deformations, the induction of the phosphate starvation response regulon PhoP. Air plasma displayed different morphological changes and specifically induces heat shock genes as well as the trp and cymR genes as a responses to photooxidative damage.

Clearly, the use of plasmas in medicine might open up new vistas of treatment. On the practical side many question have to be answered such as: (i) what type of plasmas should be 'designed' for which purpose; (ii) what can plasmas 'do' that current medical treatment cannot; (iii) where are plasmas a more economical alternative to current applications and standards [57]. Before plasma can safely be used in everyday application in hospitals for wound and skin treatment, it is of major importance to further evaluate the interaction of living pro- and eukaryotic cells with plasma. When these fundamental questions are well investigated and understood, a safe, successful and most important widely accepted implementation in the field of life science will be achieved.

Materials and methods

Experimental setup

Bacterial cultures of *B. subtilis* 168 were inoculated with an overnight culture to an optical density of 0.5 at 540 nm (OD_{540} 0.5) into Luria-Bertani broth (LB) followed by incubation with constant swirling at 37°C. Bacterial growth was monitored by measuring the OD at 540 nm. At OD_{540} 0.5, plasma treatment was set for 15 min. Plasma was ignited either in Argon gas or Air. Different discharge power settings were applied (see Tab.1) to the cell suspension for growth experiments and the proteomic approach.

After plasma treatment, the growth was monitored for further 120 min and then the cells were harvested for protein preparation. As reference condition, the cell suspension was treated only with argon gas or air for 15 min at OD_{540} 0.5. The sample taking time point for mircroarray analysis was set 5 min after the 15 min plasma treatment at OD_{540} 0.5 and for electron microscopy was set 0 min, 60 min and 120 min after plasma treatment. All experiments were performed at least three times.

Plasma source setup and plasma diagnostic

In order to treat vegetative bacteria in liquids with physical plasma at atmospheric pressure a special setup is required. This setup must provide a favorable environment for the growth of bacteria and assure that all bacteria get plasma-treated. Moreover, the plasma-treatment must be intensive enough to induce a detectable effect in the protein pattern but must not be lethal for the used bacteria. Detailed description of the setup, which fulfills these criteria and diagnostics (temperature measurements (FOT), optical emission spectroscopy (OES) and Fourier transformed infrared spectroscopy (FTIR) are publish by Winter et al. [12]. In the setup presented in Winter et. al. argon was introduced into the discharge chamber by a constant argon gas influx of 1 standard liter per minute. When using air as discharge gas the discharge chamber was once filled with ambient air by opening the chamber for a sufficient time. Subsequently the plasma was ignited in the stationary air atmosphere.

Analytical and preparative two-dimensional (2-D) PAGE

The proteins were prepared for the 2-D page as previously described by Kohler et al. [58]. The protein concentration was determined using Roti®-Nanoquant (Carl Roth GmbH & Co, Karlsruhe, Germany). Preparative 2-D PAGE was performed by using the immobilized pH gradient technique [59,60]. The protein samples (350 µg) were separated on immobilized pH gradient strips (Amersham Pharmacia Biotech, Piscataway, NJ) with a pH range of 4-7. The resulting protein gels were stained with colloidal Coomassie Blue G-250G [61] and scanned with a light scanner. For detailed description of proteins identification by MALDI-TOF MS and MALDI-TOF-TOF analysis see [59,62]. Database searches were performed using the GPS explorer

software version 3.6 (build 329) with the organism-specific databases. By using the MASCOT search engine version 2.1.0.4. (Matrix Science, London, UK) the combined MS and MS/MS peak lists for each protein spot were searched against a database containing protein sequences derived from the genome sequences of *B. subtilis* 168. Search parameters were as described previously [59] and an oxidation of methionine and a carboxyamidomethylation of cysteine were considered as variable modifications. The peaklists were searched with trypsin cutting fully enzymatically and allowing one missed cleavage site. For comparison of protein spot volumes, the Delta 2D software package was used (Decodon GmbH Germany). The induction ratio of argon or air plasma treated cells to non treated cells was calculated for each spot (normalized intensity of a spot on the plasma stress image/normalized intensity of the corresponding spot on the non treated cell image). The significance of spot volume differences of two-fold or higher was assessed by the Student´s *t* test (α<0.01; Delta 2D "statistics" table, TMEV plugin).

Transcriptome analysis by DNA microarray hybridization

B. subtilis 168 was grown aerobically in LB medium as described above. At OD_{540} 0.5 (exponential growth phase), a discharge voltage of 2.5 W (argon experiment) and a 7.4 W discharge voltage (air experiment) was applied for 15 minutes. Five minutes later, 30 ml samples were harvested by centrifugation (5 min, 9000 x *g*, 4°C) with 15 ml chilled killing buffer (20 mM Tris-HCl [pH 7.5], 5 mM $MgCl_2$, 20 mM NaN_3). The supernatant was discarded and the pellet promptly frozen in liquid N_2. The sample was then either stored at -80°C or immediately used for RNA preparation as previously decribted by [63,64].

For transcriptome analysis, 35 µg RNA were DNase-treated using the RNase-Free DNase Set (Qiagen) and purified using the RNA Clean-Up and Concentration Micro Kit (Norgen). The quality of the RNA preparations was assessed by means of the Agilent 2100 Bioanalyzer (Agilent Technologies) according to the manufacturer's instructions. For two-color hybridizations, a reference pool containing equal amounts of RNA from each sample was prepared. Detailed description of DNA microarray analysis and data analysis are already published in [12].

Sample preparation for Electron microscopy

B. subtilis 168 was cultivated as described above. 60 min after plasma treatment (argon experiment- 5 W, air experiment- 7.4 W) the cells were rapidly separated from the culture medium by filtration [65]. Microfil V filtration system and 0.45 µm pore size sterile filters were used (Millipore) [66]. The cells on the sterile filter were washed shortly in washing solution (100 mM Hepes, 1 mM $CaCl_2$, 1 mM $MgCl_2$, 25 mM NaN_3) and then stored in fixation solution (1 % glutaraldehyde, 4 % paraformaldehyde, 0.2 % picric acid, 5 mM HEPES [pH 7.4], 50 mM NaN_3 for 1 hour at room temperature. After overnight storage at 4°C, the samples were treated with osmium tetroxide vapour for three days. After drying over sodium hydroxide disks for three weeks at -20°C, the samples were mounted on aluminium stubs, sputtered with gold/palladium and examined in an EVO LS10 (Zeiss, Oberkochen, Germany) as previously described in [12].

Acknowledgments

Figure legends

Fig. 1: Temperature in the plasma region for argon and air discharges in dependence of the applied power.

Fig. 2: Optical emission spectra of argon and air plasma for power settings of 5.0 W and 4.9 W, respectively. The spectra are normalized to the maximal intensity value.

Fig. 3: FTIR spectra of the exhaust argon and air plasma gas.

Fig. 4: Effect of plasma treatment on growth of *B. subtilis* in dependence of gas and power settings. Cells were grown aerobically in LB medium at 37 °C. At an OD_{540} 0.5, three different discharge power settings (0.9 W, 2.5 W, 5 W) were applied for 15 min in the argon plasma experiment and four different discharge power settings (2.0 W, 3.5 W, 4.9 W, 7.4 W) were applied for 15 min in the air plasma experiment. Afterwards the growth was monitored for 120 min. Each growth curve was performed three times and growth differences between the biological replicates are indicated by error bars.

Fig. 5: Putative morphological effects of plasma treatment on *B. subtilis* were investigated. Cells were grown aerobically in LB medium at 37 °C and plasma treated at an OD_{540} 0.5. (A) As a control untreated *B. subtilis* cells are displayed. (B-C) Dents on the surface of 15 min argon plasma treated cells (5 W) are indicated by arrows. (X) After 60 min, speckles appear on the surface of air plasma treated (7.4 W) cell and after 120 min fibers become visible (Y-Z).

Fig. 6: Color-coded proteome map of *B. subtilis* summarizing the samples exposed to pure argon gas, argon plasma and air plasma. All protein patterns of *B. subtilis* were combined to generate a fused stress proteome map of *B. subtilis* using the union image fusion approach of the Delta2D software. All spots induced specifically after one condition or generally also by the other conditions are indicated according their induction profile by using the appropriate color code (upper right image).

Fig. 7: (left) Gene expression of argon plasma and (right) air plasma treated *B. subtilis* compared with untreated cells. Each cell in the graph displays a single gene locus that belongs to other hierarchically/regulatory related elements in parent convex-shaped categories. These are again summarized in higher-level regulatory categories. Functionally related elements seem in close neighbourhood to each other. Treemap design is based on hierarchically structured regulatory data (black borders: regulon/thin black borders within the regulons: operon/smallest cells: gene). + /− depict regulons being induced (+) or repressed (−) depending on the regulator assigned to the area. To visualize differences in expression level compared with the average level colour coding was applied as following: blue—decreased level (dec.), yellow—same level as average (avg.), orange—increased level (inc.).

Fig. 8: Assignment of genes/operons and their transcriptional regulation by PhoP (A) and tryptophan biosynthesis in *B. subtilis* (B). Transcriptomic data for the respective enzymes are presented (induction ratios as logarithm to the base 2 are shown). Ratios of control condition (argon gas vs. air), argon plasma and air plasma are displayed. Red boxes denote ratios when the respective transcript was significantly induced und the respective stress condition and yellow boxes indicate ratios which failed the statistical tests (ratio <0.5;>2;p-value 0.01).

Fig. 9: Schematic cells and their morphological and molecular changes after (A) argon and (B) air plasma treatment.

Figures

Fig.1:
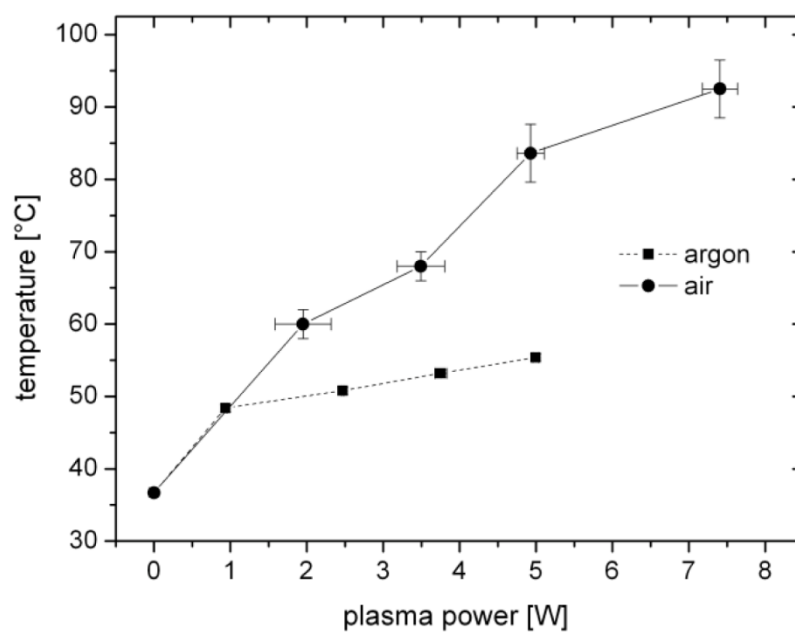
Fig.2:
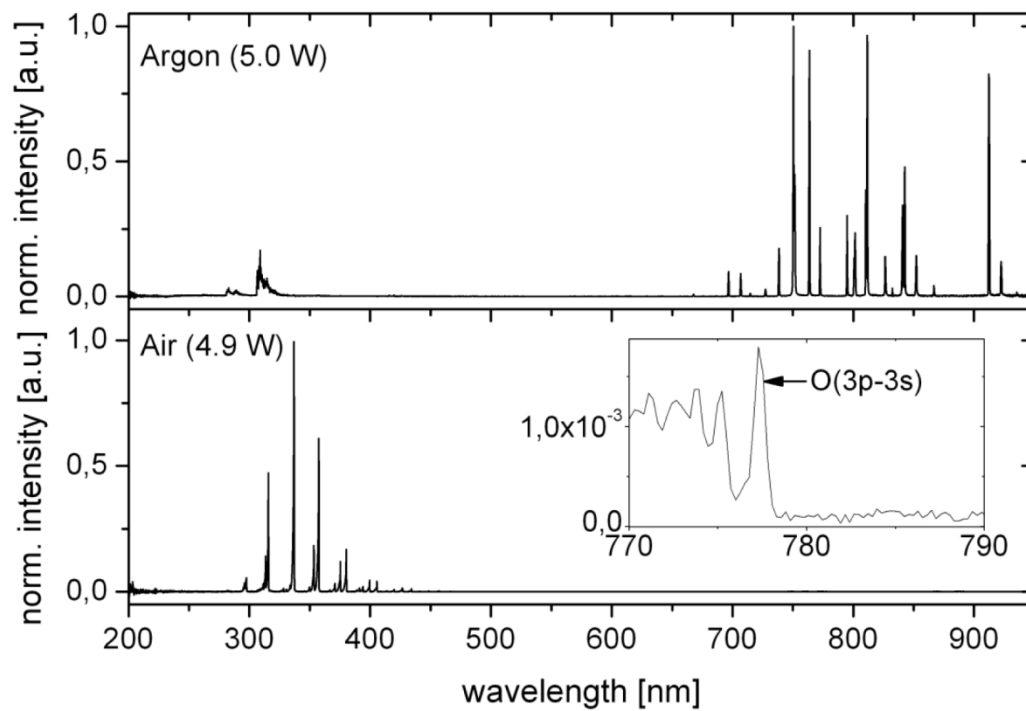
Fig.3:
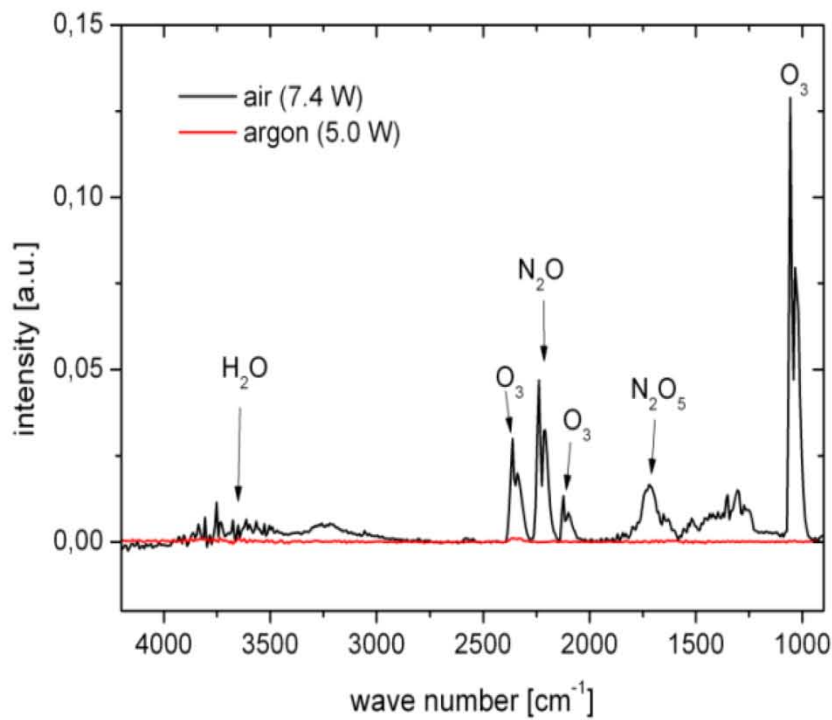
Fig.4:
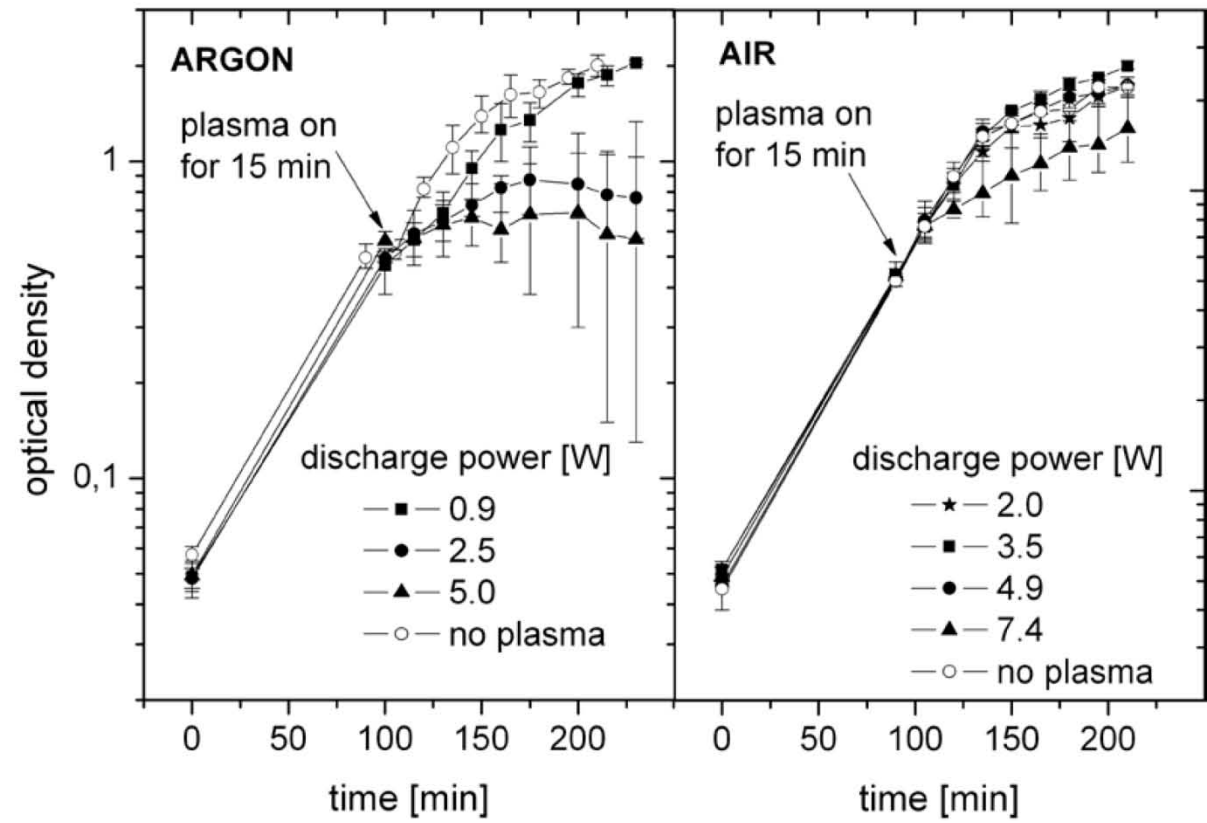
Fig.5:
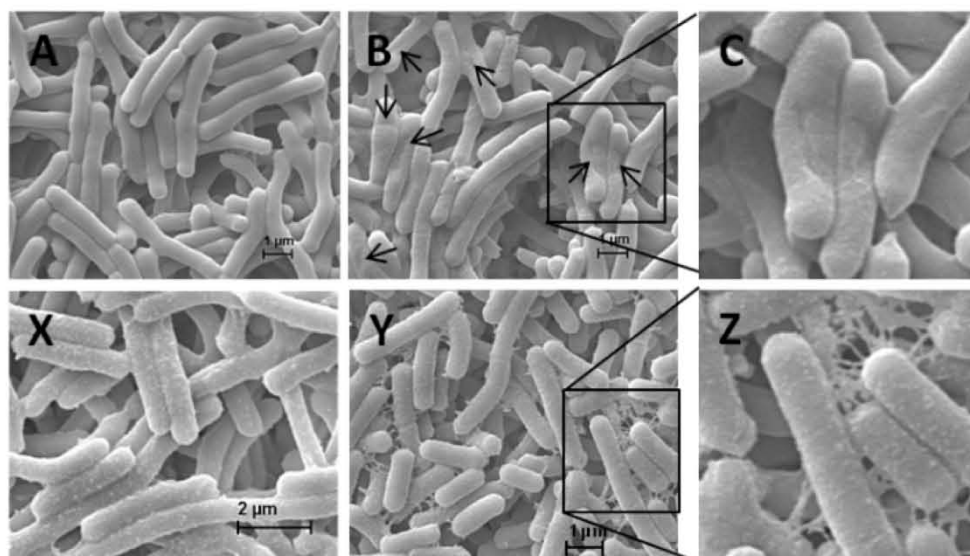
Fig.6:
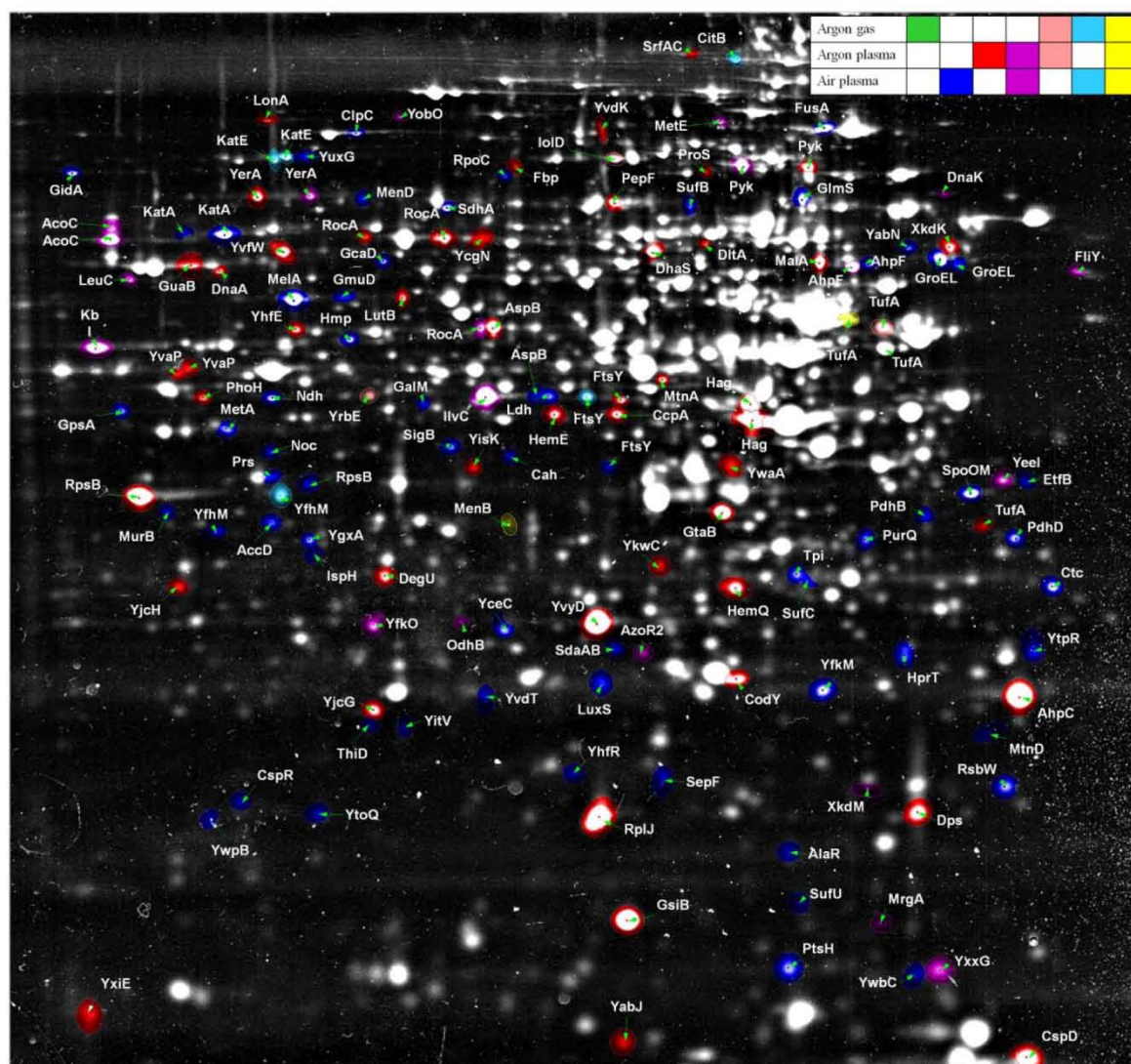
Fig.7:
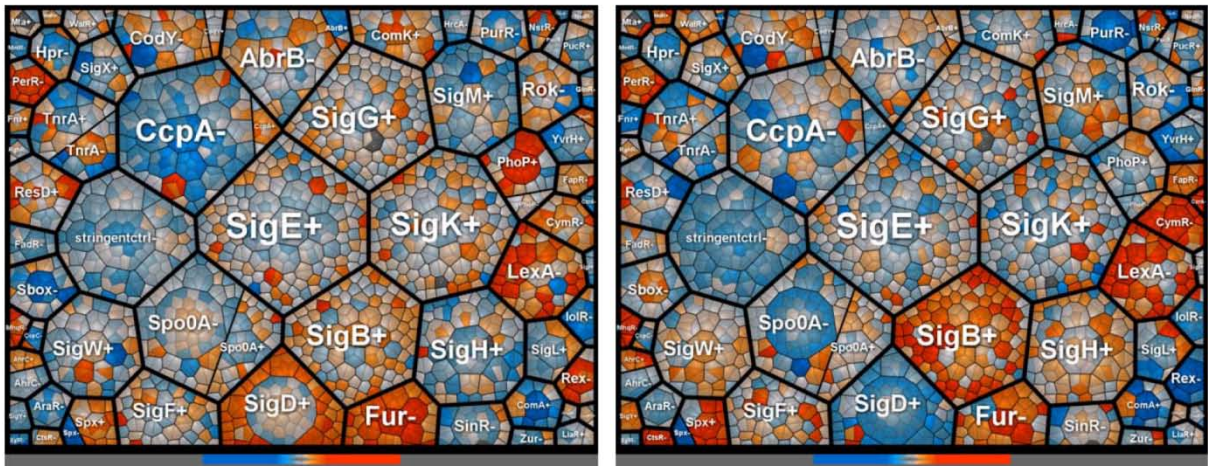
Fig. 8:
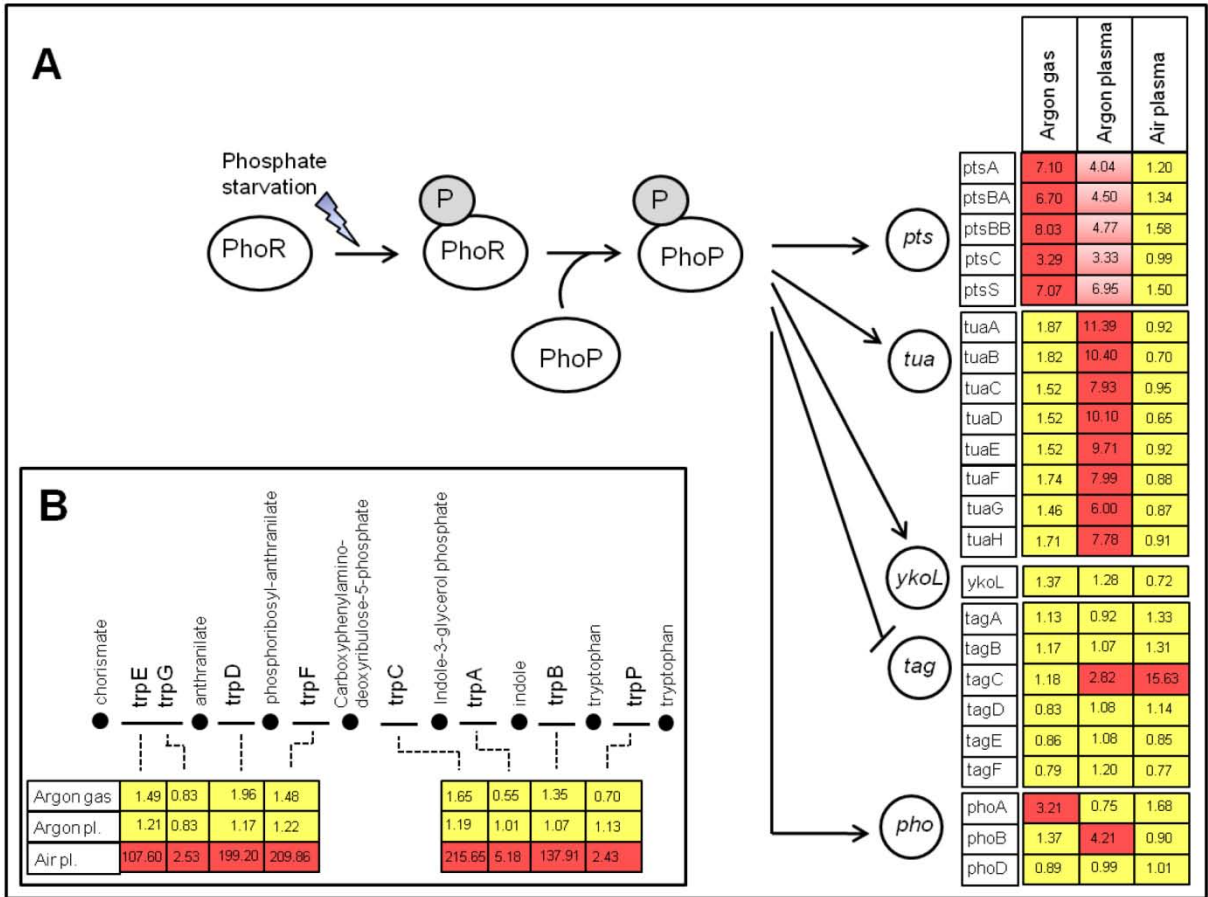
Fig.9:
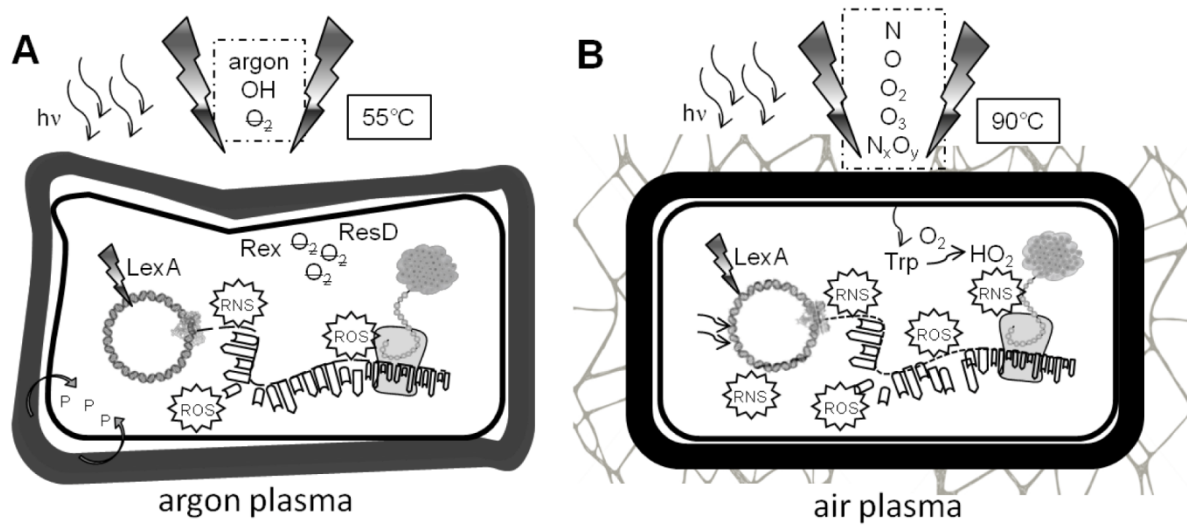
Tables

Tab. 1: Discharge power settings for Argon and Air plasma

Argon		Air	
Supply voltage [kV]	Plasma power [W]	Supply voltage [kV]	Plasma power [W]
7.3	0.9	16.2	2.0
10.5	2.5	18.1	3.5
13.2	5	19.0	4.9
		20.3	7.4

References

1. Daeschlein G, von Woedtke T, Kindel E, Brandenburg R, Weltmann KD, et al. (2010) Antimicrobial Activity of an Atmospheric Pressure Plasma Jet Agian Relevant Wound Pathogens in vitro on a Simulated Wound Environment. Plasma Processes and Polymers 7: 224-230.
2. Fridman G, Peddinghaus M, Ayan H, Fridman A, Balasubramanian M, et al. (2006) Blood coagulation and living tissue sterilization by floating-electrode dielectric barrier discharge in air. Plasma Chemistry and Plasma Processing 26: 425-442.
3. Shekhter AB, Serezhenkov VA, Rudenko TG, Pekshev AV, Vanin AF (2005) Beneficial effect of gaseous nitric oxide on the healing of skin wounds. Nitric Oxide-Biology and Chemistry 12: 210-219.
4. Ehlbeck J, Schnabel U, Polak M, Winter J, von Woedtke T, et al. (2011) Low temperature atmospheric pressure plasma sources for microbial decontamination. Journal of Physics D-Applied Physics 44.
5. Fridman G, Friedman G, Gutsol A, Shekhter AB, Vasilets VN, et al. (2008) Applied plasma medicine. Plasma Processes and Polymers 5: 503-533.
6. Kong MG, Kroesen G, Morfill G, Nosenko T, Shimizu T, et al. (2009) Plasma medicine: an introductory review. New Journal of Physics 11: -.
7. Laroussi M (2005) Low temperature plasma-based sterilization: Overview and state-of-the-art. Plasma Processes and Polymers 2: 391-400.
8. Moisan M, Barbeau J, Moreau S, Pelletier J, Tabrizian M, et al. (2001) Low-temperature sterilization using gas plasmas: a review of the experiments and an analysis of the inactivation mechanisms. International Journal of Pharmaceutics 226: 1-21.
9. Cooper M, Fridman G, Fridman A, Joshi SG (2010) Biological responses of Bacillus stratosphericus to floating electrode-dielectric barrier discharge plasma treatment. J Appl Microbiol 109: 2039-2048.
10. Kalghatgi S, Kelly CM, Cerchar E, Torabi B, Alekseev O, et al. (2011) Effects of non-thermal plasma on mammalian cells. PLoS One 6: e16270.
11. Heinlin J, Morfill G, Landthaler M, Stolz W, Isbary G, et al. (2010) Plasma medicine: possible applications in dermatology. J Dtsch Dermatol Ges 8: 968-976.
12. Winter T, Winter J, Polak M, Kusch K, Mader U, et al. (2011) Characterization of the global impact of low temperature gas plasma on vegetative microorganisms. Proteomics 11: 3518-3530.
13. Antelmann H, Hecker M, Zuber P (2008) Proteomic signatures uncover thiol-specific electrophile resistance mechanisms in Bacillus subtilis. Expert Rev Proteomics 5: 77-90.
14. Hecker M, Volker U (2004) Towards a comprehensive understanding of Bacillus subtilis cell physiology by physiological proteomics. Proteomics 4: 3727-3750.
15. Polak M, Winter J, Schnabel U, Ehlbeck J, Weltmann KD (2011) Innovative plasma generation in flexible biopsy channels for inner-tube decontamination and medical applications. Plasma Processes and Polymers accepted.
16. Dobrynin D, Fridman G, Friedman G, Fridman A (2009) Physical and biological mechanisms of direct plasma interaction with living tissue. New Journal of Physics 11: -.
17. Pompl R, Jamitzky F, Shimizu T, Steffes B, Bunk W, et al. (2009) The effect of low-temperature plasma on bacteria as observed by repeated AFM imaging. New Journal of Physics 11: -.
18. Lammers CR, Florez LA, Schmeisky AG, Roppel SF, Mader U, et al. (2010) Connecting parts with processes: SubtiWiki and SubtiPathways integrate gene and pathway annotation for Bacillus subtilis. Microbiology 156: 849-859.

19. Otto A, Bernhardt J, Meyer H, Schaffer M, Herbst FA, et al. (2010) Systems-wide temporal proteomic profiling in glucose-starved Bacillus subtilis. Nat Commun 1: 137.

20. Becher D, Hempel K, Sievers S, Zuhlke D, Pane-Farre J, et al. (2009) A proteomic view of an important human pathogen--towards the quantification of the entire Staphylococcus aureus proteome. PLoS One 4: e8176.

21. Loetscher PD, Rossaint J, Rossaint R, Weis J, Fries M, et al. (2009) Argon: neuroprotection in in vitro models of cerebral ischemia and traumatic brain injury. Crit Care 13: R206.

22. Ruzicka J, Benes J, Bolek L, Markvartova V (2007) Biological effects of noble gases. Physiol Res 56 Suppl 1: S39-44.

23. Yarin YM, Amarjargal N, Fuchs J, Haupt H, Mazurek B, et al. (2005) Argon protects hypoxia-, cisplatin- and gentamycin-exposed hair cells in the newborn rat's organ of Corti. Hear Res 201: 1-9.

24. Nakano MM, Zuber P (1998) Anaerobic growth of a "strict aerobe" (Bacillus subtilis). Annu Rev Microbiol 52: 165-190.

25. Reents H, Munch R, Dammeyer T, Jahn D, Hartig E (2006) The Fnr regulon of Bacillus subtilis. J Bacteriol 188: 1103-1112.

26. Wang E, Bauer MC, Rogstam A, Linse S, Logan DT, et al. (2008) Structure and functional properties of the Bacillus subtilis transcriptional repressor Rex. Mol Microbiol 69: 466-478.

27. Eiamphungporn W, Helmann JD (2008) The Bacillus subtilis sigma(M) regulon and its contribution to cell envelope stress responses. Mol Microbiol 67: 830-848.

28. Mascher T, Hachmann AB, Helmann JD (2007) Regulatory overlap and functional redundancy among Bacillus subtilis extracytoplasmic function sigma factors. J Bacteriol 189: 6919-6927.

29. Hecker M, Pane-Farre J, Volker U (2007) SigB-dependent general stress response in Bacillus subtilis and related gram-positive bacteria. Annu Rev Microbiol 61: 215-236.

30. Gaidenko TA, Price CW (1998) General stress transcription factor sigmaB and sporulation transcription factor sigmaH each contribute to survival of Bacillus subtilis under extreme growth conditions. J Bacteriol 180: 3730-3733.

31. Volker U, Maul B, Hecker M (1999) Expression of the sigmaB-dependent general stress regulon confers multiple stress resistance in Bacillus subtilis. J Bacteriol 181: 3942-3948.

32. Schumann W (2003) The Bacillus subtilis heat shock stimulon. Cell Stress Chaperones 8: 207-217.

33. Moreau M, Feuilloley MGJ, Veron W, Meylheuc T, Chevalier S, et al. (2007) Gliding arc discharge in the potato pathogen Erwinia carotovora subsp atroseptica: Mechanism of lethal action and effect on membrane-associated molecules. Applied and Environmental Microbiology 73: 5904-5910.

34. Brinkmann V, Reichard U, Goosmann C, Fauler B, Uhlemann Y, et al. (2004) Neutrophil extracellular traps kill bacteria. Science 303: 1532-1535.

35. Remijsen Q, Kuijpers TW, Wirawan E, Lippens S, Vandenabeele P, et al. (2011) Dying for a cause: NETosis, mechanisms behind an antimicrobial cell death modality. Cell Death Differ 18: 581-588.

36. Lahooti M, Harwood CR (1999) Transcriptional analysis of the Bacillus subtilis teichuronic acid operon. Microbiology 145 (Pt 12): 3409-3417.

37. Bookstein C, Edwards CW, Kapp NV, Hulett FM (1990) The Bacillus subtilis 168 alkaline phosphatase III gene: impact of a phoAIII mutation on total alkaline phosphatase synthesis. J Bacteriol 172: 3730-3737.

38. Eder S, Shi L, Jensen K, Yamane K, Hulett FM (1996) A Bacillus subtilis secreted phosphodiesterase/alkaline phosphatase is the product of a Pho regulon gene, phoD. Microbiology 142 (Pt 8): 2041-2047.

39. Eymann C, Mach H, Harwood CR, Hecker M (1996) Phosphate-starvation-inducible proteins in Bacillus subtilis: a two-dimensional gel electrophoresis study. Microbiology 142 (Pt 11): 3163-3170.

40. Liu W, Hulett FM (1998) Comparison of PhoP binding to the tuaA promoter with PhoP binding to other Pho-regulon promoters establishes a Bacillus subtilis Pho core binding site. Microbiology 144 (Pt 5): 1443-1450.

41. Liu W, Eder S, Hulett FM (1998) Analysis of Bacillus subtilis tagAB and tagDEF expression during phosphate starvation identifies a repressor role for PhoP-P. J Bacteriol 180: 753-758.

42. Schau M, Eldakak A, Hulett FM (2004) Terminal oxidases are essential to bypass the requirement for ResD for full Pho induction in Bacillus subtilis. J Bacteriol 186: 8424-8432.

43. Kerwin BA, Remmele RL, Jr. (2007) Protect from light: photodegradation and protein biologics. J Pharm Sci 96: 1468-1479.

44. Towe S, Leelakriangsak M, Kobayashi K, Van Duy N, Hecker M, et al. (2007) The MarR-type repressor MhqR (YkvE) regulates multiple dioxygenases/glyoxalases and an azoreductase which confer resistance to 2-methylhydroquinone and catechol in Bacillus subtilis. Mol Microbiol 66: 40-54.

45. Liebeke M, Pother DC, van Duy N, Albrecht D, Becher D, et al. (2008) Depletion of thiol-containing proteins in response to quinones in Bacillus subtilis. Mol Microbiol 69: 1513-1529.

46. Ravanat JL, Douki T, Cadet J (2001) Direct and indirect effects of UV radiation on DNA and its components. J Photochem Photobiol B 63: 88-102.

47. Au N, Kuester-Schoeck E, Mandava V, Bothwell LE, Canny SP, et al. (2005) Genetic composition of the Bacillus subtilis SOS system. J Bacteriol 187: 7655-7666.

48. Kelley WL (2006) Lex marks the spot: the virulent side of SOS and a closer look at the LexA regulon. Mol Microbiol 62: 1228-1238.

49. Mo AH, Burkholder WF (2010) YneA, an SOS-induced inhibitor of cell division in Bacillus subtilis, is regulated posttranslationally and requires the transmembrane region for activity. J Bacteriol 192: 3159-3173.

50. Py B, Barras F (2010) Building Fe-S proteins: bacterial strategies. Nat Rev Microbiol 8: 436-446.

51. Zuber P (2009) Management of oxidative stress in Bacillus. Annu Rev Microbiol 63: 575-597.

52. Even S, Burguiere P, Auger S, Soutourina O, Danchin A, et al. (2006) Global control of cysteine metabolism by CymR in Bacillus subtilis. J Bacteriol 188: 2184-2197.

53. Faulkner MJ, Helmann JD (2011) Peroxide stress elicits adaptive changes in bacterial metal ion homeostasis. Antioxid Redox Signal 15: 175-189.

54. Nakano S, Kuster-Schock E, Grossman AD, Zuber P (2003) Spx-dependent global transcriptional control is induced by thiol-specific oxidative stress in Bacillus subtilis. Proc Natl Acad Sci U S A 100: 13603-13608.

55. Zuber P (2004) Spx-RNA polymerase interaction and global transcriptional control during oxidative stress. J Bacteriol 186: 1911-1918.

56. Nakano S, Erwin KN, Ralle M, Zuber P (2005) Redox-sensitive transcriptional control by a thiol/disulphide switch in the global regulator, Spx. Mol Microbiol 55: 498-510.

57. Morfill GE, Kong MG, Zimmermann JL (2009) Focus on Plasma Medicine. New Journal of Physics 11.

58. Kohler C, Wolff S, Albrecht D, Fuchs S, Becher D, et al. (2005) Proteome analyses of Staphylococcus aureus in growing and non-growing cells: a physiological approach. Int J Med Microbiol 295: 547-565.

59. Eymann C, Dreisbach A, Albrecht D, Bernhardt J, Becher D, et al. (2004) A comprehensive proteome map of growing Bacillus subtilis cells. Proteomics 4: 2849-2876.

60. Bernhardt J, Buttner K, Scharf C, Hecker M (1999) Dual channel imaging of two-dimensional electropherograms in Bacillus subtilis. Electrophoresis 20: 2225-2240.

61. Candiano G, Bruschi M, Musante L, Santucci L, Ghiggeri GM, et al. (2004) Blue silver: a very sensitive colloidal Coomassie G-250 staining for proteome analysis. Electrophoresis 25: 1327-1333.

62. Wolff S, Antelmann H, Albrecht D, Becher D, Bernhardt J, et al. (2007) Towards the entire proteome of the model bacterium Bacillus subtilis by gel-based and gel-free approaches. J Chromatogr B Analyt Technol Biomed Life Sci 849: 129-140.

63. Eymann C, Homuth G, Scharf C, Hecker M (2002) Bacillus subtilis functional genomics: global characterization of the stringent response by proteome and transcriptome analysis. J Bacteriol 184: 2500-2520.

64. Homuth G, Masuda S, Mogk A, Kobayashi Y, Schumann W (1997) The dnaK operon of Bacillus subtilis is heptacistronic. J Bacteriol 179: 1153-1164.

65. Meyer H, Liebeke M, Lalk M (2010) A protocol for the investigation of the intracellular Staphylococcus aureus metabolome. Anal Biochem 401: 250-259.

66. Saez MJ, Lagunas R (1976) Determination of intermediary metabolites in yeast. Critical examination of the effect of sampling conditions and recommendations for obtaining true levels. Mol Cell Biochem 13: 73-78.

Eidesstattliche Erklärung

Hiermit erkläre ich, dass diese Arbeit bisher von mir weder an der Mathematisch-Naturwissenschaftlichen Fakultät der Ernst-Moritz-Arndt-Universität Greifswald noch an einer anderen wissenschaftlichen Einrichtung zum Zwecke der Promotion eingereicht wurde.

Ferner erkläre ich, dass ich diese Arbeit selbständig verfasst und keine anderen als die darin angegebenen Hilfsmittel benutzt habe.

Lebenslauf

Persönliche Daten:

Name:	Theresa Winter, geb. Söth
Geburtstag:	20.12.1979
Geburtsort:	Bad Muskau
Familienstand:	verheiratet, zwei Kinder

Schulausbildung:

1986 - 1990:	Grundschule Weißkeißel
1990 - 1992:	Mittelschule „Geschwister Scholl" Krauschwitz
1992 - 1998:	Städtisches Gymnasium Weißwasser
04.07.1998:	Allgemeine Hochschulreife

Studium:

2000-2005:	Biologie (Diplom) an der Ernst-Moritz-Arndt Universität Greifswald
05.12. 2005:	Diplomprüfung, Institut für Botanik; Thema der Diplomarbeit: „Reproduktionsbiologische und populationsgenetische Untersuchung von *Myosotis praecox*"

Promotion:

09/ 2006 – 01/2011	wissenschaftlicher Mitarbeiter an der Universität Greifswald, Institut für Mikrobiologie
seit Januar 2011	Stipendiat im Graduiertenkolleg GRK 840

Danksagung